THE

ASTROPHYSICAL JOURNAL

An International Review of Spectroscopy and Astronomical Physics

FOUNDED IN 1895 BY GEORGE E. HALE AND JAMES E. KEELER

VOLUME 91

JANUARY–JUNE, 1940

THE UNIVERSITY OF CHICAGO PRESS
CHICAGO, ILLINOIS

THE CAMBRIDGE UNIVERSITY PRESS, LONDON
THE MARUZEN COMPANY LIMITED, TOKYO
THE COMMERCIAL PRESS LIMITED, SHANGHAI

PUBLISHED JANUARY, MARCH, APRIL, MAY,
JUNE 1940

COMPOSED AND PRINTED BY THE UNIVERSITY OF CHICAGO PRESS
CHICAGO, ILLINOIS, U.S.A.

CONTENTS

NUMBER 1

NUMBER 2

NUMBER 3

THE ASTROPHYSICAL JOURNAL

AN INTERNATIONAL REVIEW OF SPECTROSCOPY AND ASTRONOMICAL PHYSICS

VOLUME 91 JANUARY 1940 NUMBER 1

ATMOSPHERIC ABSORPTION OF INFRARED SOLAR RADIATION AT THE LOWELL OBSERVATORY

II. THE SPECTRAL INTERVAL: 5.5–8 μ

ARTHUR ADEL AND C. O. LAMPLAND

ABSTRACT

The intensity variations in the telluric spectrum between the limits 5.5 and 8 μ are great. They are here empirically specified as functions of the atmospheric water-vapor content.

This is the second in a series of papers describing the degree of absorption suffered by incoming infrared radiations as a consequence of the absorption spectrum of the earth's atmosphere. The first paper[1] in the series dealt with the continuous absorption due to the pure rotation spectrum of the water-vapor molecule. The present communication concerns itself with the variations in transmission of the discrete absorption bands which occupy the spectral interval from 5.5 to 8 μ. Additional analyses will eventually cover in similar fashion the remainder of the infrared telluric spectrum to the limit of atmospheric transmission near 14 μ.

It seems useful at this time to review very briefly the investigations on atmospheric transmission and related problems in progress at Flagstaff during the last three years. These include a series of papers,[2] begun earlier than the current one and continuing through the present, whose purpose it is to discuss the positions, structures, and identifications of the absorption bands in the infrared spectrum

[1] A. Adel, *Ap. J.*, **89**, 1, 1939. [2] Consult this *Journal* and the *Physical Review*.

of solar radiation arriving at the earth's surface. The primary purpose of all these studies is the determination of essential data required for the more complete evaluation and interpretation of astronomical radiometric observational material, especially the planetary measurements now in progress, as well as the data accumulated in years past. The importance of trustworthy atmospheric transmissions for the evaluation of planetary-radiation data is apparent. In observations of bodies outside the earth our own atmosphere intervenes as a selectively and imperfectly transparent medium, displaying considerable variation in its behavior. That portion of sunlight reflected by the planets is quite freely transmitted, but the planet's emission spectrum of long wave lengths is severely depleted. For example, from considerations of the intensity of the incident solar radiation and the albedo of Venus or from considerations of the planet's temperature,[3] it is to be expected that a considerable fraction of its planetary radiation would be emitted in the spectral range 5.5–8 μ. As a matter of fact, only a small percentage of planetary radiation appears to be found in this spectral band, a result attributable to the water-vapor absorption in the earth's atmosphere.

While the application of the infrared analysis of the atmosphere to the Observatory's radiometric program is of immediate importance, its significance is enhanced by its application to other fields as well. It is an important means of observing atmospheric constituents present in minute amount, for example, ozone and the oxides of nitrogen. Further, it provides necessary data bearing on problems of long-standing interest to meteorologists.

In that portion of the telluric spectrum confined between the limits 5.5 and 8 μ, daily fluctuation and great seasonal variation of intensity occur. The principal features of this spectral interval are the great water-vapor band with a long base of zero transmission and the banded absorption due to the oxides of nitrogen, probably nitrous oxide (N_2O) and nitrogen pentoxide (N_2O_5).[4] The nitrogen oxides band is contained in the long-wave-length or diverging wall

[3] A. Adel, *Ap. J.*, **86**, 337, 1937.

[4] A. Adel, "Note on the Atmospheric Oxides of Nitrogen," *ibid.*, **90**, 627, 1939.

of the water-vapor band. The position of the diverging wall oscillates between wide limits, being specifically determined by the amount of water vapor present in the atmosphere. In this manner it not only affects the actual contour of the water band, but it markedly affects the apparent form of the nitrogen oxides band. In further description of the region it must be added that when the atmospheric water vapor falls below 3 or 4 mm of liquid equivalent, a small amount of solar energy penetrates the entire atmospheric column in the vicinity of 6.3 μ. And it appears there as a small island of energy in an otherwise completely absorbed region. This is a consequence of the structure of the 6.3 μ water-vapor band, which may be popularly described as a doublet.

The six graphs of solar intensity (at the earth's surface) against wave length, which are contained in Figure 1, are arranged to exhibit the progressive change in the region 5.5–8 μ corresponding to diminishing water-vapor content of the atmosphere. The plots also cover the spectral interval from 8 to 11 μ, the region to be discussed in the next paper in this series. These automatically recorded curves of the relative intensity distribution in sunlight at the earth's surface were obtained with a rock-salt-prism spectrometer. The liquid water equivalent of the atmospheric water vapor was approximately 10 mm for curve No. 1 and approximately 1 mm for curve No. 6. Under each curve is given the wave-length scale graduated in 0.1's μ on the dispersion of rock salt. It is especially instructive to examine the progress of intensities at 6.3 and at 7.5 μ. However, a correct appreciation of the variations can be secured only by reducing the curves of Figures 1 and 2 to curves of transmission. The curve of the continuous absorption coefficient in this spectral region is known, as is the gray-body temperature of the sun (7000° K).[1] It is, accordingly, possible to accomplish the reduction to curves of percentage transmission.

Figure 2 displays the transmissions obtained from a set of curves similar to those of Figure 1 but better adapted to the present purpose. The plot is on the scale of normal dispersion. The dispersion axis for a given curve lies opposite the letter corresponding to that curve. Each vertical division is equal to 1 per cent on the

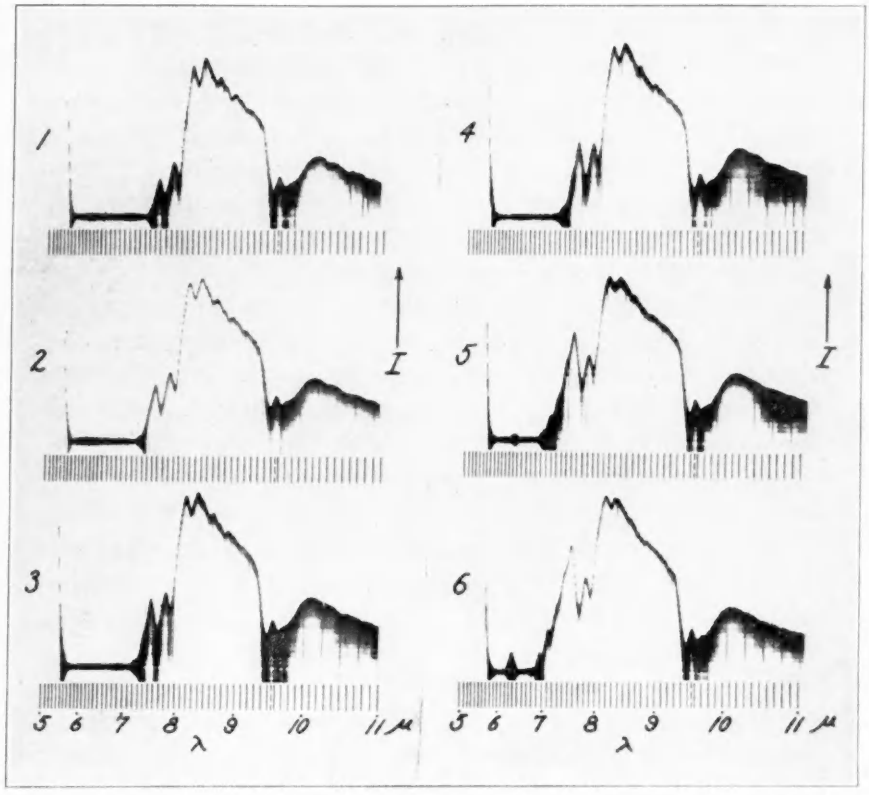

FIG. 1.—Solar intensity as a function of wave length. Curves 1–6 correspond to diminishing water-vapor content of the atmosphere.

scale of 100 per cent. The liquid water equivalent of the atmospheric water vapor corresponding to curves *A–F* is:

A: 10.2 mm; *B:* 6.0 mm; *C:* 4.7 mm; *D:* 3.1 mm; *E:* 2.1 mm; *F:* 1.1 mm
A: 10.0 mm; *B:* 5.9 mm; *C:* 4.6 mm; *D:* 3.0 mm; *E:* 2.1 mm; *F:* 1.0 mm

The upper row refers to the region about 6.3 μ, the latter having always been observed at a slightly smaller zenith distance than the

TABLE 1

VARIATIONS IN THE TELLURIC SPECTRUM

λ (μ)	20.5 Mm (Percentage)	*A*	*B*	*C*	*D*	*E*	*F*
5.5	0.0	1.0	2.0	3.0	7.0	10.0	11.6
5.6	0.0	0.8	0.8	0.9	2.3	4.0	5.2
5.7	0.0	0.0	0.2	0.3	0.4	1.0	1.1
5.8	0.0	0.0	0.0	0.1	0.0	0.2	0.3
5.9	0.0	0.0	0.0	0.0	0.0	0.0	0.0
6.0	0.0	0.0	0.0	0.0	0.0	0.0	0.0
6.1	0.0	0.0	0.0	0.0	0.0	0.0	0.0
6.2	0.0	0.0	0.0	0.0	0.1	0.0	1.2
6.3	0.0	0.0	0.0	0.0	0.3	0.7	2.4
6.4	0.0	0.0	0.0	0.0	0.3	0.3	1.2
6.5	0.0	0.0	0.0	0.0	0.0	0.0	0.0
6.6	0.0	0.0	0.0	0.0	0.0	0.0	0.0
6.7	0.0	0.0	0.0	0.0	0.0	0.0	0.0
6.8	0.0	0.0	0.0	0.0	0.0	0.0	0.7
6.9	0.0	0.0	0.0	0.0	0.2	1.2	3.1
7.0	0.0	0.0	0.0	0.0	1.6	3.5	6.3
7.1	0.0	0.0	0.0	0.9	3.6	7.1	11.3
7.2	0.0	0.0	1.2	2.1	6.2	11.5	17.0
7.3	0.0	0.8	4.4	5.9	10.8	18.4	24.0
7.4	0.0	4.3	10.9	14.0	20.6	27.2	34.2
7.5	2.2	10.5	19.5	22.7	29.6	31.4	42.0
7.6	1.8	8.0	15.2	17.0	24.5	28.8	29.0
7.7	5.4	13.3	17.4	19.6	19.7	24.4	26.6
7.8	9.0	19.9	25.7	26.6	27.3	32.4	36.3
7.9	9.4	18.7	26.4	26.7	27.4	32.8	38.8
8.0	25.6	44.6	47.8	54.8	52.4	60.7	63.1

former. F. E. Fowle's spectroscopic method was employed in all determinations of atmospheric water-vapor content. Curve *G*, which is the transmission of an amount of water vapor equivalent to 0.8 mm of liquid water, was determined by Fowle.[5] In the comparison of curve *G* with curves *A–E* it must be remembered that Fowle em-

[5] *Smithsonian Miscellaneous Collections*, **68**, No. 8, 1917.

ployed a laboratory source of radiation as opposed to the sun and a laboratory concentration of water vapor as opposed to the earth's atmosphere. The nitrogen oxides band is, consequently, missing from curve *G*. The nitrogen oxides band appears to be essentially un-

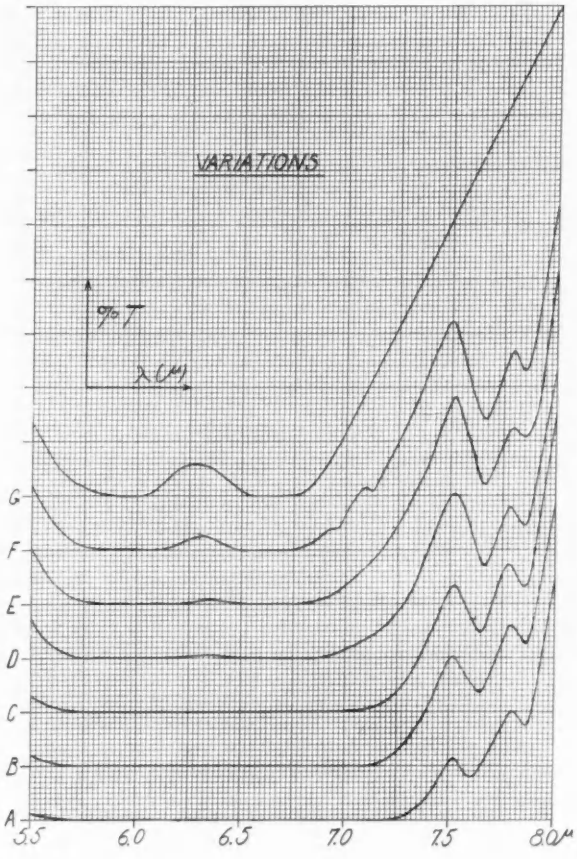

FIG. 2

affected by the presence of water vapor, for reconstruction of the band walls reveals constant percentage absorption for the band in spite of the tenfold variation in the amount of water vapor.

In Table 1 the transmissions given by curves *A*–*F* are listed at intervals of $\frac{1}{10}\,\mu$. The table also includes the transmission of the

region as determined by an atmospheric water-vapor content equivalent to 2 cm of liquid.

The significant features of Figure 2 are graphically summarized in Figure 3. The curves labeled 6.3, 7.5, and 7.66 μ describe the variations in transmission of the maximum at the center of the great

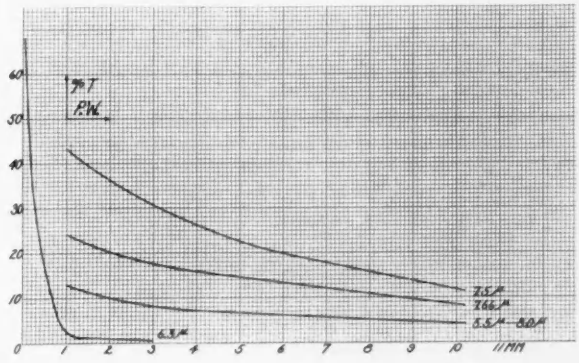

FIG. 3

water band, the maximum of the short-wave-length lobe of the nitrogen oxides band, and the minimum of the succeeding trough, respectively. The precise wave lengths of these features vary somewhat, of course, with the atmospheric water-vapor content. The prolongation of the 6.3 μ-curve below 1 mm of liquid water equivalent was made possible by the incorporation of three laboratory measurements by Fowle.[5] The fourth curve describes the transmission of the entire region.

LOWELL OBSERVATORY
FLAGSTAFF, ARIZONA

INTEGRATED PHOTOGRAPHIC MAGNITUDES OF SIXTY-EIGHT GLOBULAR CLUSTERS*

WILLIAM H. CHRISTIE

ABSTRACT

The photographic magnitudes of sixty-eight globular clusters have been determined with a schraffierkassette attached to the 10-inch Cooke refractor. The scale was established by polar comparisons for an average of nine stars in each field.

The cluster magnitudes have been compared by Seares with other determinations by Holetschek, Vorontsov-Velyaminov, Bernheimer, Vyssotsky and Williams, Stebbins and Whitford, and Shapley.

The magnitudes of the sixty-eight globular clusters given in this paper were obtained with a schraffierkassette[1] attached to the 10-inch Cooke refractor. In order to integrate completely the light of a cluster, the throw of the schraffierkassette must be at least twice the diameter of the object. Shapley's diameters have been used as a guide and have proved to be accurate enough for the purpose. Series of exposures with squares of various size have been made on several clusters, and the run of the measured magnitudes indicates that complete integration has usually been accomplished.

The images of the clusters have been compared with those of near-by stars, an average of nine comparison stars having been used for each cluster. The magnitudes of the reference stars were determined by direct schraffierkassette comparisons of the cluster fields with stars in the polar region, correction for differential extinction being made as usual. To avoid confusion and overlapping of images, the exposures to the pole and to the field, except for a few of the brighter clusters, were made on separate plates taken from the same box and developed together. The data for the polar stars were obtained from *Magnitudes and Colors of Stars North of 80°*,[2] supplement-

* *Contributions from the Mount Wilson Observatory, Carnegie Institution of Washington*, No. 620.

[1] *Mt. W. Contr.*, No. 476; *Ap. J.*, **78**, 313, 1933.

[2] Seares, Ross, and Joyner, mimeograph edition, Pasadena, 1935.

ed, for the fainter stars, by the international magnitudes of the North Polar Sequence.

Measures of blue and red stars in the polar area show that, when the schraffierkassette is used with the 10-inch Cooke refractor, the color correction required to reduce the results to the international system is negligible. The integrating action of this combination nullifies the large correction originating in the chromatic and other aberrations of the objective which affect focal images obtained with the 10-inch refractor.

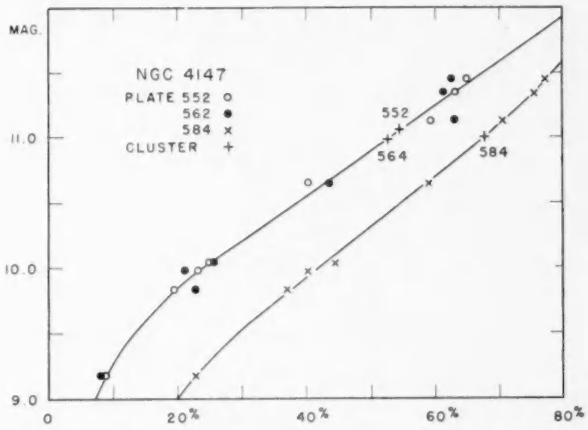

FIG. 1.—Typical reduction-curves used in the determination of the magnitude of a cluster.

The plates were measured with the Ross thermoelectric photometer. Settings were made on several points surrounding the image of each comparison star or cluster. The mean of the corresponding deflections of the galvanometer was adopted as that for the clear film in the vicinity of the object to be measured, the zero of the galvanometer being read with no light falling on the cell. The deflection obtained from settings on the star or cluster was then expressed as a percentage of that adopted for the clear film. The "clear film," especially in crowded Milky Way regions, may, of course, include the images of numerous faint stars; but since the images of surrounding stars are also superimposed upon the clusters, it is believed that the effect of extraneous stars is negligible. The star density in the vicin-

ity of a cluster may, however, differ from that of the polar region; and it is possible that small systematic errors have been introduced

TABLE 1

INTEGRATED MAGNITUDES OF 68 GLOBULAR CLUSTERS

NGC	Pg. Mag.	No.	A.D. Clusters	PC	A.D. Comp. Stars	NGC	Pg. Mag.	No.	A.D. Clusters	PC	A.D. Comp. Stars
288	8.96	2	0^m08	2	0.03	6342	11.35	2	0^m12	1	.....
1851	7.72	8	.02	4	.06	6356	9.68	3	.03	3	.....
1904	8.39	4	.08	4	.09	6402	9.44	4	.14	5	0.08
2298	10.48	4	.10	4	.15	6426	12.33	3	.10	5	.12
2419	11.51	8	.17	6	.16	6440	12.05	2	.04	3	09
4147	11.01	7	.03	4	.06	6441	8.93	3	.04	5	.11
4590	9.12	8	.15	4	.18	6517	12.90	2	.18	3	.13
5024	8.68	8	.07	5	.12	6522	10.40	6	.07	4	.13
5139*	5.1	4	.3	....	.....	6528	11.04	6	.11	4	.13
5272	7.21	2	.02	2	.03	6539	12.39	2	.12	3	.16
5466	10.39	1	.....	3	.04	6553	10.20	4	.29	7	.31
5694	10.87	2	.05	2	.05	6569	10.63	6	.06	4	.11
5824	10.08	4	.15	4	.12	6624	9.53	8	.11	4	.05
5897	9.61	1	.....	4	.05	6626	8.48	8	.22	10	.24
5904	7.04	2	.06	4	.05	6637	8.94	9	.08	4	.06
5986	8.72	2	.07	2	.08	6638	10.24	4	.34	7	.44
6093	8.39	7	.08	6	.14	6652	9.86	9	.04	4	.05
6121	7.41	3	.08	4	.02	6656	6.48	1	.....	5	.08
6144	10.85	2	.00	2	.16	6681	8.95	9	.10	4	.09
6171	10.10	4	.12	4	.07	6712	9.98	3	.02	2	.04
6205	6.78	8	.09	5	.09	6715	8.74	7	.23	2	.02
6218	7.95	2	.05	3	.10	6723	7.75	1	.....	3	.05
6229	10.26	2	.02	3	.04	6760	11.25	3	.10	2	.10
6235	11.52	1	.....	1	.....	6779	9.55	4	.10	2	.05
6254	7.64	2	.02	3	.07	6809	7.08	1	.....	5	.11
6266	8.16	5	.08	4	.05	6864	9.50	4	.03	5	.07
6273	8.29	5	.10	4	.06	6934	10.01	3	.23	3	.05
6284	10.61	4	.06	4	.08	6981	10.24	5	.17	4	.05
6287	11.24	4	.08	4	.07	7006	11.45	4	.03	4	.06
6293	9.38	6	.09	4	.06	7078	7.33	8	.07	3	.07
6304	9.82	4	.07	2	.05	7089	7.30	2	.02	4	.08
6316	10.10	4	.08	2	.06	7099	8.58	7	.07	3	.04
6325	12.66	3	.18	3	.18	7492	12.33	3	0.12	5	0.12
6333	8.92	3	.10	3	.....	.....	.....	.....	.....	.....	.....
6341	7.30	2	0.01	2	0.06	.....	.....	.....	.....	.....	.....

* ω Centauri. Magnitude from comparison with H.D. stars in field.

through the polar comparisons, since it is unlikely that the deflection for a cluster or star, relative to that for the clear film, is wholly

free from the influence of this background fog. The matter requires further attention.

The galvanometer deflections for the comparison stars (expressed as percentages of the deflection for the clear film) were plotted against their magnitudes. The magnitude of the cluster was then read from the smooth curve drawn through these points. Three typical reduction-curves for NGC 4147 are shown in Figure 1.

The magnitudes for the comparison stars used for ω Centauri (NGC 5139) were taken from the *Henry Draper Catalogue*, since polar comparisons for stars having zenith distances ranging from 75° to 85° and polar distances of from 130° to 140° are unreliable. The comparison stars were corrected for differential atmospheric extinction by reducing them to the altitude of the cluster.

The mean integrated magnitudes of the clusters, on the international photographic scale, are given in the second column of Table 1. The number of measures included in the mean, the average deviation of the measures from the mean, the number of polar comparisons, and their average deviation appear successively in the remaining columns of the table.

The average error (0.8 of the mean error) for a single determination of a cluster magnitude, exclusive of the zero-point error in the comparison stars, was obtained from the average deviation (AD) in the fourth column of Table 1 by the formula

$$\mathrm{AE} = \mathrm{AD}\sqrt{\frac{n}{n-1}},$$

where n is the number of individual determinations. The averages of these values for successive magnitude intervals, for both clusters and comparison stars, are as given in the accompanying table.

	Apparent Photographic Magnitude					
	7.5	8.5	9.5	10.5	11.5	12.5
Clusters						
AE (No.)	±0.05 (9)	±0.11 (13)	±0.10 (11)	±0.14 (15)	±0.11 (7)	±0.16 (6)
Stars						
AE (No.)	±0.08 (51)	±0.10 (55)	±0.08 (36)	±0.14 (57)	±0.12 (24)	±0.15 (22)

For any object in a globular cluster

$$M = m - a + 5 - 5 \log \rho ,$$

where a is the absorption expressed in magnitudes and ρ the true distance. A similar expression involving the integrated absolute and apparent magnitudes (M_c, m_c) of the cluster, combined with the formula for M, gives for M_c, free from the influence of any absorption,

$$M_c = m_c - (m - M) .$$

This formula may be used to obtain the M_c of clusters for which the distance modulus, $m - M$, has been determined photometrically.

TABLE 2

FREQUENCY DISTRIBUTION OF ABSOLUTE MAGNITUDES

M_c	No.	M_c	No.
−9.9 to −9.5	1	−6.9 to −6.5	8
9.4 to 9.0	0	6.4 to 6.0	0
8.9 to 8.5	2	5.9 to 5.5	3
8.4 to 8.0	8	5.4 to 5.0	4
7.9 to 7.5	11	−4.9 to −4.5	1
−7.4 to −7.0	10		

There are 48 such cases in Shapley's list. One approximate value of $m - M$ (NGC 104) has been rejected, and one by Baade (NGC 2419)[3] has been added. For 39 of these, integrated photographic magnitudes are given in Table 1. For the others, Shapley's integrated cluster magnitudes, reduced to the international photographic system by Table 5, have been used. The resulting frequency-curve for M_c (for clusters brighter than a limiting apparent magnitude of about 12.0) is shown in Table 2 and in Figure 2.

The asymmetry of the curve and the suggested secondary maximum are noteworthy. According to the present data, maximum frequency occurs close to $M_c = -7.7$. None of the values falls between −5.9 and −6.5. The faintest cluster included is NGC 7492 (−4.7), and the brightest, ω Centauri (−9.5). The distance modulus of

[3] *Mt. W. Contr.*, No. 529; *Ap. J.*, **82**, 396, 1935.

the latter was taken from the recent study of the cluster by W. Charles Martin.[4]

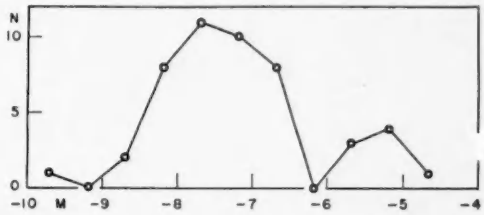

FIG. 2.—Frequency distribution of absolute photographic magnitudes among the globular clusters.

I am indebted to Dr. Seares for the following discussion of the results of this investigation.

COMPARISON WITH OTHER MEASURES

Comparison of the present measurements with other observations requires, in general, a knowledge of the colors of the clusters. The only extensive series of color indices available is that of Stebbins and Whitford,[5] made with a photoelectric cell. These data reveal a conspicuous relationship between the observed color C_2 and the amount of obscuration as indicated by counts of extragalactic nebulae. Color excess in many instances is therefore certainly an important fraction of C_2. This conclusion has been criticized[6] on the ground that, if the color excess be calculated in the usual way with the aid of the spectral types of the clusters, most of its dependence on galactic latitude disappears; all the so-called K and M types are within the zone of avoidance. There is reason to believe, however, that the types assigned to clusters are in many instances essentially color classes, the type having been determined by the intensity distribution of the continuous spectrum rather than by spectral lines, which are mostly invisible. The criticism therefore fails unless more dependable evidence can be found for the preferential occurrence of late-type clusters (if such exist) in low latitudes.

[4] *Leiden Annalen*, **17**, Part 2, 38, 1938.

[5] *Mt. W. Contr.*, No. 547; *Ap. J.*, **84**, 132, 1936.

[6] Wilhelm Becker, *Fortschritte der Astronomie*, **1**, 50, 1938.

The departure from black-body radiation often accompanying color excess at once raises a question as to whether the values of C_2 can be satisfactorily reduced to the international system by the customary mean formula[7]

$$C_p = 2.62\,(C_2 + 0.21). \qquad (1)$$

This formula has been calibrated on the standard stars of the Polar Sequence, which, as a matter of fact, are themselves affected by a moderate amount of selective absorption and should be applicable to similar regions in other parts of the sky; but whether it can be used for heavily obscured clusters in the zone of avoidance is still an open question. To begin with, the emitted radiation is composite in type; and even if the corresponding effective color-temperature curve were certainly linear, a superadded absorption varying as $1/\lambda^n$ would transform the curve into a nonlinear relationship unless n were equal to unity. The reduction of C_2 to the wave-length interval corresponding to standard photographic and photovisual magnitudes by means of (1) might therefore in certain cases give values of C_p differing systematically from C, the color index obtained directly from standard magnitudes.

In any event, equation (1) should apply, approximately at least, to clusters in regions of normal nebular density, even in low galactic latitudes. For example, ten such objects of known spectral type (or color class, as the case may be), when compared with the correlated series for unobscured main-sequence stars,[8] namely,

Spectrum.....	Ao	A5	Fo	F5	Go
Int. C.....	−0.14	−0.02	+0.10	+0.22	+0.37

give a mean color excess E of only +0.06. Again, four other clusters in slightly obscured regions give $E = +0.15$. Since these quantities are in nowise unusual, the values of C_p from (1) here appear to be systematically correct.

The test may be pushed somewhat farther by comparing the values of C_p with the excellent color indices (C_{VW}) for 15 clusters meas-

[7] Stebbins and Whitford, *Mt. W. Contr.*, No. 586; *Ap. J.*, **87**, 237, 1938, eq. (7).

[8] Unpublished data.

ured by Vyssotsky and Williams.[9] The regression-curve for a grouping according to C_p, which, because of the small accidental error affecting C_p, must be close to the true relationship, may be expressed in the form

$$C_p = 0.94\,(C_{VW} - 0.18)\,. \tag{2}$$

We then have the following data:

	Ao	Ko	Ko–Ao
C_{VW}.....	0.00	1.15	1.15
C_p.....	−0.17	0.91	1.08
Int. C.....	−0.14	0.98	1.12

(3)

in which the first line is from the paper by Vyssotsky and Williams and the second has been calculated from (2). The agreement of the latter with the international values in the third line is all that can be expected from the scanty data used. Here again the values of C_p seem to be systematically correct. Nevertheless, any general statement to this effect must be expressed with some reservation because only five of the clusters underlying the data in (3) are within the zone of avoidance, and none is fainter than about the eighth magnitude. The most heavily obscured objects are therefore not included in the comparison.

Another possible influence of absorption is a modification of the relative color equation normally to be expected in the magnitudes obtained by two different methods. The mean effective wave lengths of both series may be changed, but one more than the other. A comparison of the photographic results in Table 1 with the photoelectric measures (Pe) of Stebbins and Whitford[5] affords an example for which there seems to be no other explanation. For the Polar Sequence the relationship is [10]

$$\mathrm{IPg} - \mathrm{Pe} = -0.12 + 0.20C\,, \tag{4}$$

but for the two series of cluster magnitudes this formula does not necessarily hold. Since diaphragms with angular apertures of 64″ or 128″ at most were used in measuring Pe, the number of clusters that

[9] *Ap. J.*, **77**, 301, 1933.

[10] Seares, *Mt. W. Contr.*, No. 587; *Ap. J.*, **87**, 257, 1938, eq. (16).

can be utilized for a comparison is small. The 22 objects for which the integration appears to be sufficiently complete suggest a small negative color coefficient; they certainly do not admit of the rather large positive value of formula (4).

We proceed now to further details of the comparison with Pe. Disregarding color equation altogether, we find the mean difference

$$\text{Pg} - \text{Pe} = -0.13 \qquad (22 \text{ clusters; AD} = \pm 0.15)\,. \tag{5}$$

The rejection of five questionable cases leaves the apparent color relation unchanged and gives

$$\text{Pg} - \text{Pe} = -0.11 \qquad (17 \text{ clusters; AD} = \pm 0.08)\,. \tag{6}$$

Collected according to values of Pe, the group means for the two selections are (number of clusters in parentheses):

Pe	9.2	10.3	11.2	12.3
Pg − Pe.....	−0.05 (4)	−0.11 (6)	−0.22 (6)	−0.12 (6)
	−0.05 (4)	−0.08 (4)	−0.17 (5)	−0.11 (4)

(7)

These differences indicate that there is no serious discordance in scale between the photoelectric and the present series of measures. The zero-point differences shown by (5) and (6) agree with (4), which checks the zero point of the photographic values in Table 1.

Comparisons with the photographic magnitudes of Vorontsov-Velyaminov,[11] of Vyssotsky and Williams,[9] and of Shapley[12] are shown in Tables 3, 4, and 5. Any relative color equation in these three series is concealed by the scatter in the differences, and for Shapley at least it is certainly small.

Since Vorontsov-Velyaminov's results are based ultimately on the Harvard visual scale, the differences in Table 3 should agree with the corrections which reduce this scale to the international system, as, in fact, they do within a few hundredths of a magnitude.[13]

One seriously discordant difference (NGC 6809, −0.32 mag.) has been excluded from the comparison with Vyssotsky and Williams.

[11] *A. N.*, **236**, 1, 1929.

[12] "Star Clusters," *Harvard Obs. Mono.*, No. 2, 1930.

[13] Seares, *Mt. W. Contr.*, No. 288; *Ap. J.*, **61**, 284, 1925.

In Table 4 the mean values in the first and second columns correspond to data in Sh Pg intervals of 1.5 mag. and are the basis of the regression-curve in Table 5 (residuals in third column, Table 4), which may be useful for statistical studies involving clusters meas-

TABLE 3

VORONTSOV-VELYAMINOV, AND VYSSOTSKY AND WILLIAMS

VV Pg	Pg−VV	AD	No.	VW Pg	Pg−VW	AD	No.
8.0	+0.17	±0.31	10	6.8	+0.33	±0.12	8
9.1	.25	.22	7	7.9	+0.32	±0.20	6
10.2	+0.19	±0.27	7	.....	.....	.....	.....

TABLE 4

SHAPLEY

Sh Pg	Pg−Sh	O−C	AD	No.
4.0	+2.90	+0.02	±0.12	5
5.6	2.08	− .10	.17	9
7.2	1.65	+ .11	.20	14
8.8	0.86	− .07	.27	14
10.2	0.54	+ .05	.29	14
11.7	+0.08	0.00	±0.47	10

TABLE 5

SHAPLEY, REGRESSION-CURVE

Sh Pg	Pg−Sh	Sh Pg	Pg−Sh
3.5	+3.10	8.5	+1.04
4.5	2.65	9.5	+0.71
5.5	2.22	10.5	+0.40
6.5	1.81	11.5	+0.11
7.5	+1.42	12.5	−0.15

ured by Shapley that do not occur in the present list. All the clusters of Table 1 are included in the comparison except NGC 5694, which is not in Shapley's list, and NGC 5139 (ω Centauri). The approximate difference for the latter, Pg − Sh = +2 mag., disagrees with the well-defined regression-curve.

The magnitudes of globular clusters and of other NGC objects

that probably have been used more than any others are the visual estimates of Holetschek.[14] The mean differences Pv − Hl in Table 6 were obtained by first reducing the photographic magnitudes of Table 1 to the international photovisual system by forming Pv = Pg − C_p, the color index C_p being that from equation (1). Since the uncertainty in the group means is 0.1 or 0.2 mag, these means may be regarded as constant. In other words, within the uncertainty corresponding to the exceptionally large average deviations, Holetschek's scale apparently differs from the international photovisual scale only by a zero-point correction of +0.40 mag.

TABLE 6

HOLETSCHEK

Hl Vis	Pv−Hl	AD	No.
6.4	+0.33	±0.34	8
7.3	.50	.32	7
8.4	.52	.48	8
9.3	.25	.70	7
10.0	+0.40	±0.65	8
All	+0.40	±0.50	38

Some of Holetschek's clusters have been reobserved by Bernheimer.[15] For these the mean difference is

$$\text{Pg} - \text{Be Vis} = +0.16 \qquad (16 \text{ clusters; AD} = \pm 0.42)\,. \qquad (8)$$

If the differences for Holetschek and for Bernheimer be separated into two groups according as the clusters are situated in regions of normal or of low nebular density (in effect, a segregation according to small and to large values of C_p), there appears in both cases for the faint stars what seems to be a large color equation of indeterminate amount. The coefficient probably depends on the magnitude. For Holetschek we have, in the mean, something like

$$\text{Pg} - C_p - \text{Hl} = +0.6 - 0.3\,C_p\,. \qquad (9)$$

[14] *Annalen der wiener Sternwarte*, **20**, 1907.

[15] *Lund Obs. Circ.*, No. 5, 1932.

If real, the color term may originate either in C_p, through the failure of equation (1), or in Hl (and in Be). Because of the large uncertainty affecting the v al estimates, the term is relatively unimportant for the compari s in (8) and in Table 6 and has been disregarded. It is mentio d here to focus attention in future investigations on the behavio C_p when the obscuration is heavy.

In conclusion I w to express to Dr. Seares my sincere appreciation of his interest nd advice throughout this investigation. To Dr. Baade and Dr. H bble I also owe thanks for many helpful discussions.

CARNEGIE INSTITUTION OF WASHINGTON
MOUNT WILSON C ERVATORY
July 19

THE COLORS OF 1332 B STARS*

JOEL STEBBINS,[1] C. M. HUFFER, AND A. E. WHITFORD

ABSTRACT

The colors of 1332 stars of spectral types B, O, cB, and cA have been measured with a photoelectric cell at Madison or at Mount Wilson. The list includes nearly all O–B5 stars north of $-15°$ declination and brighter than visual magnitude 7.5, and, in addition, nearly all O–B2 stars north of $-40°$ of whatever magnitude to the limit of the *Henry Draper Catalogue*.

The effective wave lengths of the cell with the two filters used and for an equal-energy source are 4260 and 4770 A. The scale of the colors is close to two-thirds of the international scale. The probable error of a color index is ± 0.02 to ± 0.03 mag. for Madison, and ± 0.01 to ± 0.02 mag. for Mount Wilson.

The color excesses of B stars are correlated with the intensities of interstellar lines. The space reddening is greater toward the center than toward the anticenter of the galaxy. Even the brightest regions of the Milky Way are partially obscured. The absorption in the galaxy is not uniform but spotted and irregular.

The present paper is an extension of the previous study of the colors of 733 B stars[2] measured at Madison with a photoelectric photometer. The new program includes about 600 additional B stars measured with the 15-inch refractor at Madison and with the 60- and 100-inch reflectors at Mount Wilson. The present paper gives the data and measures of individual stars, and some general conclusions on space reddening were presented at the symposium at the dedication of the McDonald Observatory.[3]

Observing list.—The first list, which will be designated as the "733 stars," included nearly all O–B5 stars north of $-15°$ declination and brighter than visual magnitude 7.5. The extended list now adds nearly all O–B2 stars north of $-40°$ of whatever magnitude to the limit of the *Henry Draper Catalogue*. To these were added miscellaneous cB, cA, and faint Be stars distributed along the Milky Way, which were furnished by Mr. Merrill, and additional B3, B5, and B stars in several selected regions. Because the B stars tend to occur

* *Contributions from the Mount Wilson Observatory, Carnegie Institution of Washington*, No. 621.

[1] Research associate of the Mount Wilson Observatory, Carnegie Institution of Washington.

[2] *Pub. Washburn Obs.*, **15**, Part 5, 1934.

[3] *Mt. W. Contr.*, No. 617; *Ap. J.* **90**, 209, 1939.

in groups and also because the *Henry Draper Catalogue* is not complete much beyond magnitude 8.0, the stars of our list are by no means uniformly distributed along the Milky Way. The stars are grouped according to magnitude and spectrum in Table 1. The magnitude groups are 0.00–0.99, 1.00–1.99, and so on. The stars fainter than 10.0 are negligible in number. The stars from B6 to B9 are nearly all carried over from the 733 list. Of the two A stars which crept in, one has interstellar D lines and the other was classified as B3 in the *Henry Draper Catalogue*.

TABLE 1

DISTRIBUTION OF STARS BY MAGNITUDE AND SPECTRUM

Mag.	cB	cA	O	Bo	B1	B2	B3	B4	B5	B6	B7	B8	B9	B	A	Composite	Total
0	1	...	...	...	...	...	...	...	...	...	...	...	...	...	...	.....	1
1	2	1	...	...	...	2	...	...	1	...	...	...	...	...	...	.....	6
2	2	...	1	5	2	2	...	...	1	...	...	...	...	...	...	.....	13
3	2	...	1	2	3	6	4	1	5	...	1	4	1	...	...	1	31
4	8	4	6	4	5	8	37	3	21	1	1	4	2	...	1	.....	105
5	4	6	15	7	4	17	67	1	23	3	12	15	5	...	...	.....	159
6	13	5	17	26	9	39	93	6	80	2	5	12	2	1	...	1	311
7	13	3	29	42	15	46	71	1	69	1	2	1	2	9	1	.....	305
8	2	1	1	52	11	63	33	1	36	1	...	3	1	19	...	.....	224
9	...	...	1	30	2	29	23	1	31	...	...	2	2	22	...	.....	163
10	...	...	...	2	...	2	...	...	4	...	...	...	...	5	...	.....	13
11	...	...	...	...	...	...	...	...	...	...	...	...	...	1	...	.....	1
Total	47	20	71	170	51	214	328	14	271	8	21	41	15	57	2	2	1332

The photometer.—The colors were measured with a photoelectric cell and two filters, giving essentially the color system of the 733 stars. The effective wave lengths for an equal-energy source are 4260 and 4770 A. Most of the measures, which extended over the years 1930–1938, were made with four potassium cells—two at Madison and two at Mount Wilson. The color scale, about two-thirds that of the international scale for color index, varied little from cell to cell or from telescope to telescope; but the zero point for colors had to be carefully determined for each change of instrumental conditions—for instance, when the large mirrors were resilvered, or especially when they were aluminized. The zero point was continually controlled by measures of standard B stars or by A stars in the North Polar Sequence.

The measures of the 733 stars at Madison and the earlier measures at Mount Wilson were made with a Kunz potassium cell and a Lindemann electrometer. From 1933 all measures were made with a Kunz cell and a thermionic amplifier perfected by Whitford. For bright stars, down to fourth or fifth magnitude with the 15-inch, the amplifier has no special advantage over the electrometer; but for seventh or eighth magnitude with the 15-inch or for tenth or eleventh magnitude with the 60-inch the amplifier is easily one or two magnitudes more sensitive than the electrometer. Stars of magnitude 9.0 or fainter would be called difficult with the 15-inch, but the color of any star in the *Henry Draper Catalogue* is easily measured with the 60-inch.

TABLE 2

NORMAL COLORS

Class	Color Index	Class	Color Index
O	−0.23	A0	−0.10
B0	− .22	A5	+ .03
B1	− .21	F0	+ .09
B2	− .20	F5	+ .18
B3	− .19	G0	+ .33
B4	− .18	G5	+ .49
B5	− .17	K0	+ .64
B6	− .16	K5	+0.90
B7	− .14	.....	.....
B8	− .13	.....	.....
B9	−0.12	.....	.....

Atmospheric extinction.—The colors were reduced to outside the atmosphere by applying the correction $0.05 f \sec z$, where the factor f varies from about 1.5 to 2.0, depending upon the estimated quality of the night. At Mount Wilson we adopted $f = 1.6$ for practically all measures. The quality of the California sky makes it difficult to distinguish between different nights; on the Madison standard they are usually perfect. The outstanding errors due to extinction are certainly quite small. Most of the conclusions on space reddening depend upon differences in color of stars not widely separated in the sky, and the extinction comes in only as a differential effect.

Normal colors.—As the new results are mostly for faint B stars which are affected by interstellar absorption, we have very little

material for improvement of the system of normal colors. That previously obtained is therefore repeated in Table 2.

The color index on the present scale is denoted as C_1, to distinguish it from the color C_2, measured with the lighter filters used on nebulae and clusters. Various determinations have been made of the relation of these colors to the international color C. From the scales for giant stars in unobscured regions Seares[4] has used gKo − Ao equal to 1.12 and 0.74 for C and C_1, respectively. Hence, neglecting the zero points, $C/C_1 = 1.12/0.74 = 1.51$. From 11 white stars of the North Polar Sequence with C ranging from −0.08 to +0.49 we find $C/C_1 = 1.49 \pm 0.02$. However, the relation between the two systems is not strictly linear; and when 6 red stars of the Sequence are included in the solution, we get $C/C_1 = 1.44 \pm 0.01$. We see no better procedure than to use the round figure $C/C_1 = 1.50$ for the range of the colors of the B stars. Therefore, our color excess E_1, derived by subtracting the normal color in Table 2 from the observed color of a star, should be multiplied by 1.50 to get E on the international scale.

The observations.—The observations at Madison extended from 1930 to 1937; at Mount Wilson, from 1931 to 1938. A count of the number of observations gives the following:

	Madison	Mt. Wilson	Both	Total
Stars	852	366	114	1332
Observations	2470	835	.....	3305

The average number of observations per star is about 2.5; but for 165 stars there is only one observation each, made usually at Mount Wilson. During some seasons the photometer was used mostly for faint clusters and nebulae, and the B stars were taken incidentally. However, barring a misidentification, a single observation with a large reflector gives a color that no amount of measuring with a small telescope will improve.

All the measures are brought together in Table 3. The original results for 733 stars have been improved in many cases by additional

[4] *Mt. Wilson Contr.*, No. 587, p. 20; *Ap. J.*, **87**, 276, 1938.

observations, and the combined material has been made as nearly homogeneous as possible.

The first three columns contain the number, right ascension, and declination taken from the *Henry Draper Catalogue*. An asterisk following the HD number refers to a note at the end of the table. The MWC numbers are from the catalogue of Merrill and Burwell.[5]

The magnitude *m* in the fourth column is always visual. When given to two decimals, it is the regular Harvard photometric magnitude. If given to one decimal, it is the visual magnitude computed from the photoelectric measures with the Harvard magnitudes of near-by stars used as standards. When followed by a colon (:) the magnitude is simply the *DM* visual magnitude given in the *Henry Draper Catalogue*. We have found that the probable error of such a *DM* magnitude is about ± 0.3. A magnitude from the photoelectric measures has a probable error of about ± 0.1, depending upon the standards used.

The spectral type in the fifth column is the Victoria classification[6] when that was available. The classifications for the c and Be stars were furnished by Merrill. Spectra in italics are from the *Henry Draper Catalogue*.

The galactic co-ordinates *l* and *b* in the sixth and seventh columns were taken from the Lund Tables and are referred to the pole at R.A. 12^h40^m, Decl. $+28°$ (1900). The previous co-ordinates of the 733 stars were on the Vatican system; but these have all been revised, and the new values have been checked, either differentially or by duplicate computation. The interpolations were made to the nearest tenth of a degree, without special effort to get the last digit absolutely correct.

The eighth, ninth, and tenth columns contain the color index C_1 measured at Madison and at Mount Wilson and the mean. In forming the means, double weight was ordinarily given to Mount Wilson observations.

In the eleventh column the number of observations refers to the number of nights; different measures of a star on the same night were always combined into a single observation.

[5] *Mt. Wilson Contr.*, No. 471; *Ap. J.*, **78**, 87, 1933.

[6] *Pub. Dominion Ap. Obs.*, **5**, No. 2, 1931; No. 3, 1933.

The color excess E, in the twelfth column, was formed by subtracting the normal color index of Table 2 from the mean observed color index. In forming this excess the stars of rough classification B were assumed to be of class B3. The uncertainty in the classification would ordinarily make a difference of only two or three hundredths in the color excess. The reduction to the international system is given by $E = 1.50E_1$.

In the thirteenth column the distance modulus $m_0 - M$ was formed from the corrected magnitude

$$m_0 = m - 7E_1 ,$$

and the assumed absolute magnitude M from Table 4. The reasons for taking the total visual absorption $A_V = 7E_1$ are given in the previous paper.[2]

Precision of the measures.—The best test of the precision of the measures is given by the stars observed at both Madison and Mount Wilson. From 114 differences M − W between the eighth and ninth columns of Table 3, including all the bad ones, we have

$$\text{M} - \text{W} = +0.0045 \pm 0.0030 \text{ (p.e.)} .$$

The probable error of one difference is ±0.032, which with weights 1 and 2 could be distributed as ±0.026 for M and ±0.018 for W. Other internal evidence gives the Mount Wilson measures greater precision. For instance, from 74 stars observed in two different years we have

$$\text{W}_{37} - \text{W}_{36} = -0.0042 \pm 0.0023 .$$

The probable error of one difference is ±0.020; of one observation, ±0.014; and of the mean of two, ±0.010. The errors are mostly systematic by seasons and nights. We can assume that the probable error of a color index in Table 3 is ±0.02 to ±0.03 for Madison and ±0.01 to ±0.02 for Mount Wilson.

Absolute magnitudes.—Most determinations of the absolute magnitudes of B stars have been made before the effect of interstellar absorption was recognized. In the previous paper we took the results of Plaskett and Pearce and of Strömberg derived from the

TABLE 3

COLORS OF B STARS

HD	R.A. 1900	DECL. 1900	m	SPEC.	l	b	C_1			No.	E_1	m_0-M
							M	W	Mean			
73	$0^h\ 0^m.5$	+42° 50′	8.5	*B2*	82°.4	−18°.6	−0.19	−0.21	−0.20	2, 1	0.00	11.5
108	0 0.9	+63 7	7.36	O6fq	85.6	+ 1.4	.00	.....	.00	4	+ .23	10.2
593	0 5.3	+59 6	6.70	B2s	85.5	− 2.6	− .14	.....	− .14	2	+ .06	9.2
698	0 6.3	+57 39	7.08	cB8eα	85.5	− 4.1	.00	.....	.00	2	+ .13	11.7
829	0 7.6	+37 9	6.57	B3s	82.9	−24.4	− .15	.....	− .15	2	+ .04	8.5
886	0 8.1	+14 38	2.87	B2ss	78.7	−46.7	− .19	.....	− .19	3	+ .01	5.8
1334	0 12.5	+58 30	7.9	B5	86.4	− 3.3	− .13	.....	− .13	2	+ .04	9.2
1337	0 12.5	+50 53	6.12	O8n	85.6	−10.9	− .20	.....	− .20	2	+ .03	10.4
1383	0 12.9	+61 10	7.8	Bo	86.7	− 0.7	− .02	.....	− .02	4	+ .20	10.3
1544	0 14.6	+61 31	8.5	B2n	87.0	− 0.3	− .06	.....	− .06	4	+ .14	10.5
MWC5	0 14.8	+61 54	9.0	B(o)e	87.0	0.0	.00	.....	.00	3	+ .22	11.4
1743	0 16.6	+61 38	8.7	Bo	87.2	− 0.2	− .03	.....	− .03	2	+ .19	11.3
1810	0 17.4	+61 41	8.4	B3n	87.3	− 0.2	− .05	.....	− .05	2	+ .14	9.6
1976	0 18.9	+51 28	5.36	B4n	86.7	−10.4	− .16	.....	− .16	4	+ .02	7.1
2083	0 20.0	+71 15	6.94	Bo	88.4	+ 9.3	− .12	.....	− .12	2	+ .10	10.1
2329	0 22.1	+58 0	7.24	B3	87.6	− 3.9	− .04	.....	− .04	4	+ .15	8.4
2451	0 23.2	+61 57	8.9	B1	88.0	0.0	− .12	.....	− .12	5	+ .09	11.9
2654	0 25.1	+61 48	7.31	B3	88.2	− 0.1	− .08	.....	− .08	4	+ .11	8.7
2729	0 25.7	+65 58	6.14	B7n	88.6	+ 4.0	− .12	.....	− .12	2	+ .02	7.1
2789	0 26.3	+66 36	8.3	B2ne	88.6	+ 4.6	+ .08	+ .03	+ .05	2, 1	+ .25	9.5
2905	0 27.3	+62 23	4.24	cBoeα	88.5	+ 0.5	− .09	.....	− .09	3	+ .13	8.8
3191	0 30.1	+60 55	8.7	B3n	88.8	− 1.1	.....	+ .04	+ .04	2	+ .23	9.3
3240	0 30.5	+53 38	5.14	B8	88.7	− 8.3	− .19	.....	− .19	3	− .06	6.4
3360	0 31.4	+53 21	3.72	B2s	88.7	− 8.6	− .22	.....	− .22	7	− .02	6.9
3366	0 31.5	+72 21	7.06	B3s	89.3	+10.3	− .08	.....	− .08	2	+ .11	8.5
3369	0 31.5	+33 10	4.44	B3	87.9	−28.8	− .18	.....	− .18	2	+ .01	6.6
3379	0 31.6	+14 41	5.86	B3	87.0	−47.3	− .21	.....	− .21	2	− .02	8.2
3901	0 36.5	+49 58	4.85	B3	89.4	−12.0	− .16	.....	− .16	3	+ .03	6.8
3940	0 36.9	+63 45	7.40	*B5*	89.7	+ 1.8	+ .23	.....	+ .23	3	+ .40	6.2
3950	0 37.0	+51 48	6.93	Bo	89.4	−10.2	− .08	.....	− .08	2	+ .14	9.9
4142	0 38.8	+47 19	5.55	B5n	89.8	−14.7	− .19	.....	− .19	3	− .02	7.3
4180	0 39.2	+47 44	4.70	B4neβ	89.9	−14.3	− .14	.....	− .14	2	+ .04	6.3
4717	0 44.2	+62 37	8.2	cA1	90.5	+ 0.9	.....	+ .18	+ .18	2	+ .26	11.9
4727	0 44.3	+40 32	4.42	B5s	90.9	−21.5	− .13	.....	− .18	2	− .01	6.1
4768	0 44.6	+59 7	7.9	cB3	90.6	− 2.9	+ .06	.....	+ .06	2	+ .25	11.6
4841	0 45.4	+63 14	7.07	cB5	90.6	+ 1.2	+ .14	.....	+ .14	3	+ .31	10.4
5005	0 47.0	+56 5	7.9	O6	91.0	− 5.9	− .12	.....	− .12	2	+ .11	11.6
5394	0 50.7	+60 11	2.25	Bone	91.3	− 1.8	− .11	.....	− .11	2	+ .11	5.4
5458	0 51.3	+62 1	9.1	B2n	91.3	0.0	.....	− .03	− .03	1	+ .17	10.9
5551	0 52.2	+63 11	7.7	B1	91.4	+ 1.2	+ .13	.....	+ .13	2	+ .34	8.9
5689	0 53.5	+63 5	9.3	Bon	91.5	+ 1.1	.....	− .04	− .04	1	+ .18	11.9
6048	0 56.7	+59 36	8.9	B9	92.1	− 2.3	.....	− .03	− .03	1	+ .09	8.7
6084	0 57.0	+51 16	6.81	B5	92.7	−10.6	− .10	.....	− .10	2	+ .07	7.9
6118	0 57.3	+31 16	5.46	B9s	94.3	−30.6	− .14	.....	− .14	2	− .02	6.0
6148	0 57.5	+47 20	8.1	*B5*	93.1	−14.6	− .11	.....	− .11	2	+ .06	9.3
6182	0 57.8	+61 18	8.4	B1	92.1	− 0.6	+ .08	+ .06	+ .07	3, 1	+ .28	10.0
6226	0 58.2	+47 6	6.70	B5	93.2	−14.8	− .15	.....	− .15	2	+ .02	8.2
6300	0 58.9	+50 29	9.50	B4	93.1	−11.4	− .16	.....	− .16	2	+ .02	8.3
6343	0 59.4	+65 26	7.10	B5eβ	92.0	+ 3.5	.....	− .03	− .03	1	+ .14	7.7
6417	1 0.0	+57 14	7.10	B5	92.7	− 4.7	− .10	.....	− .10	2	+ .07	8.2
6675	1 2.4	+69 10	7.1	*Bo*	92.0	+ 7.3	− .06	.....	− .06	4	+ .16	9.9
7103	1 6.2	+61 21	8.4	*B*	93.1	− 0.5	.....	+0.15	+ .15	1	+ .34	.....
7157	1 6.8	+61 10	6.29	B9	93.2	− 0.7	− .08	.....	− .08	2	+ .04	6.4
7252	1 7.7	+60 21	7.26	B2	93.4	− 1.5	− .10	.....	− .0	2	+ .10	9.6
7636	1 11.2	+57 6	7.6:	B2ne	94.2	− 4.6	−0.10	.....	−0.10	2	+0.10	9.9

TABLE 3—*Continued*

HD	R.A. 1900	Decl. 1900	m	Spec.	l	b	C_1 M	C_1 W	C_1 Mean	No.	E_1	m_0-M
7694	1^h11^m7	+54° 54′	7.41	B3	94°6	− 6°8	−0.18	.....	−0.18	2	+0.01	9.5
7902	1 13.6	+57 40	7.2	cB5ea	94.5	− 4.0	+ .03	.....	+ .03	2	+ .20	11 3
8209	1 16.4	+43 4	6.62	B5n	97.0	−18.4	− 15	.....	− .15	2	+ .02	8.1
8768*	1 21.4	+62 45	9.0	*B*	94.7	+ 1.1	+ .02	.....	+ .02	3	+ .21	.....
8965	1 23.3	+59 44	7.26	B2	95.4	− 2.0	− .04	.....	− .04	2	+ .16	9.1
9105	1 24.6	+62 51	7.46	cB5(e)	95.1	+ 1.3	+ .16	.....	+ .16	3	+ .33	10.7
9311	1 26.6	+60 10	7.26	B5s	96.0	− 1.3	+ .07	.....	+ .07	4	+ .24	7.0
MWC14	1 27.9	+63 7	8.7	B(8)eβ	95.4	+ 1.6	.....	+0.23	+ .23	3	+ .36	7.2
10125	1 33.9	+63 40	8.5	*B*	96.0	+ 2.3	− .03	.....	− .03	2	+ .16	.....
10260	1 35.3	+60 32	6.63	*B8*	96.7	− 0.7	− .11	− .14	− .13	2, 2	.00	7.4
10516	1 37.4	+50 11	4.19	Bone	99.3	−10.8	− .13	.....	− .13	3	+ .09	7.5
10898	1 41.9	+57 58	7.4	*Bo*	98.2	− 3.1	+ .02	− .03	− .01	2, 1	+ .21	9.8
MWC18	1 42.7	+60 33	9.3	B(3)ne	97.6	− 0.5	.....	+ .06	+ .06	2	+ .25	9.7
11241	1 45.4	+54 39	5.49	B3	99.4	− 6.2	− .22	− .30	− .25	4, 1	− .06	8.1
E232552	1 45.9	+54 50	8.2	B(2)ne	99.5	− 6.0	+ .03	.00	+ .01	3, 1	+ .21	9.7
11415	1 47.2	+63 11	3.44	B5s	97.5	+ 2.2	− .17	− .23	− .20	2, 1	− .03	5.2
11554	1 48.4	+57 24	9.5	B(3)e	99.2	− 3.4	+ .07	− .02	.00	2, 2	+ 19	10.4
11606	1 48.8	+58 47	7.04	B3ne	98.8	− 2.0	− .10	.....	− .10	2	+ .09	8.6
12301	1 55.6	+63 54	5.62	cB8	98.2	+ 3.1	+ .04	+ .06	+ .05	6, 1	+ .18	9.9
12302	1 55.6	+59 12	8.1	B3e	99.5	− 1.4	− .09	.00	− .05	5, 1	+ .14	9.3
12740	1 59.8	+48 41	7.8	*B2*	103.2	−11.3	− .13	.....	− .13	3	+ .07	10.3
12856	2 0.9	+56 38	8.6	B(2)ne	100.9	− 3.6	− .04	− .07	− .06	1, 1	+ .14	10.6
12882	2 1.1	+64 33	7.54	B(2)ne	98.6	+ 3.9	− .01	.....	− .01	2	+ .19	9.2
12953	2 1.7	+57 57	5.90	cA2ea	100.7	− 2.4	+ .06	.....	+ .06	2	+ .11	10.6
13051	2 2.6	+56 31	8.7	B(o)ne	101.2	− 3.7	− .07	.....	− .07	3	+ .15	11.6
13267	2 4.6	+57 11	6.36	cB8	101.3	− 3.0	− .01	.....	− .01		+ .12	11.0
13268	2 4.6	+55 41	8.1	*Bo*	101.8	− 4.4	− .15	− .11	− .12	1, 1	+ .10	11.3
13476	2 6.6	+58 6	6.50	cAo	101.3	− 2.0	+ .16	.....	+ .16	2	+ .26	10.2
13590	2 7.6	+63 34	8.0:	*B5p*	99.6	+ 3.2	+ .02	.....	+ .02	2	+ 19	8.3
13716	2 8.6	+57 18	8.4	B1	101.8	− 2.7	− .12	− .03	− .06	1, 1	+ .15	11.0
13744	2 8.9	+57 50	7.8	cAo	101.6	− 2.2	+ .20	.....	+ .20	2	+ .30	11.2
13745	2 8.9	+55 32	7.96	B1n	102.4	− 4.3	− .09	.....	− .09	3	+ .12	10.7
MWC30	2 9.0	+56 32	10.3	Be	102.1	− 3.4	.....	+ .08	+ .08	1	+ .27	.....
13831	2 9.7	+56 17	7.9	*Bo*	102.3	− 3.6	.....	− .14	− .14	1	+ .08	11.2
13841	2 9.8	+56 34	7.21	cB2	102.2	− 3.3	− .07	− .07	− .07	3, 1	+ .13	11.8
13854	2 9.9	+56 36	6.42	cB1ea	102.2	− 3.3	− .04	− .05	− .04	3, 1	+ .17	10.7
13866	2 10.0	+56 15	7.4	cB2	102.3	− 3.6	.....	− .06	− .06	1	+ .14	11.9
13909	2 10.8	+56 38	8.7	*B2*	102.3	− 3.2	.....	− .08	− .08	1	+ .12	10.9
13970	2 10.8	+56 11	8.5	B5n	102.4	− 3.6	.....	− .07	− .07	1	+ .10	9.4
14010	2 11.1	+63 58	7.05	cB8	99.8	+ 3.8	+ .10	.....	+ .10	2	+ .23	10.9
14053	2 11.4	+56 33	8.3	*B2*	102.4	− 3.3	.....	− .07	− .07	2	+ .13	10.4
14134	2 12.1	+56 40	6.66	cB3ea	102.4	− 3.1	+ .03	+ .02	+ .03	4, 1	+ .22	10.6
14143	2 12.2	+56 43	6.66	cB1	102.4	− 3.1	+ .08	+ .05	+ .06	3, 2	+ .27	10.3
MWC33	2 12.4	+56 37	9.6	Bne	102.6	− 3.2	.....	.00	.00	1	+ .19	.....
14220	2 12.9	+52 5	7.04	B5s	104.1	− 7.4	− .12	.....	− .12	2	+ .05	8.3
14302	2 13.6	+55 52	8.4	*B2*	102.9	− 3.8	.....	− .04	− .04	2	+ .16	10.3
14322	2 13.8	+55 27	6.84	cB9	103.1	− 4.2	.00	.....	.00	2	+ .12	11.5
MWC34	2 14.2	+56 51	9.7	Be	102.6	− 2.8	.....	.00	.00	1	+ .19	.....
14372	2 14.2	+46 51	6.08	B7	106.2	−12.2	− .14	.....	− .14	2	.00	7.2
14433	2 14.8	+56 47	6.54	cA2	102.7	− 2.9	+ .13	.....	+ .13	2	+ .18	10.8
14434	2 14.8	+56 27	8.4	*B2*	102.9	− 3.2	.....	− .09	− .09	1	+ .11	10.6
14442	2 14.9	+59 6	9.3	*Bo*	101.9	− 0.7	.....	+ .04	+ .04	2	+ .26	11.4
14476	2 15.2	+56 49	8.8	*Bo*	102.8	− 2.8	.....	.00	.00	1	+ .22	11.2
MWC41	2 15.3	+56 50	9.7	B(3)e	102.8	− 2.8	.....	+ .02	+ .02	1	+ .21	10.4
14489	2 15.3	+55 23	5.22	cA2	103.3	− 4.2	+ .04	.....	+ .04	3	+ .09	10.1
14535	2 15.8	+56 47	7.46	cA2	102.9	− 2.8	+ .21	.....	+ .21	2	+ .26	11.1
14542	2 15.9	+56 56	6.95	cB9	102.8	− 2.7	+ .17	+ .17	+ .17	1, 1	+ .29	10.4
MWC43	2 16.2	+57 4	10.0	Be	102.8	− 2.5	.....	+ .04	+ .04	1	+ .23	.....
14605	2 16.5	+56 8	10.2	B(2)ne	103.2	− 3.4	.....	+ .15	+ .15	1	+ .35	10.8
14633	2 16.7	+41 2	7.3	O8	108.9	−17.4	−0.31	−0.29	−0.30	4, 1	−0.07	12.3

TABLE 3—*Continued*

HD	R.A. 1900	Decl. 1900	m	Spec.	l	b	C_1			No.	E_{1}	m_0-M
							M	W	Mean			
14818	2h18m2	+56° 10′	6.24	cB1ea	103°.4	− 3°.3	+0.06	.....	+0.06	3	+0.27	9.9
14951	2 19.5	+10 9	5.53	B7n	125.8	−44.9	− .18	.....	− .18	2	− .04	6.9
14956	2 19.6	+57 14	7.32	B1s	103.2	− 2.2	+ .16	.....	+ .16	2	+ .37	8.3
MWC46	2 19.6	+56 39	9.9	B(2)ea	103.4	− 2.8	− .03	−0.06	− .05	3, 1	+ .15	11.9
15316	2 22.8	+57 22	7.30	cA2	103.5	− 1.9	.....	+ .30	+ .30	1	+ .35	10.3
15450	2 24.2	+56 27	9.0	Bone	104.1	− 2.7	− .01	.....	− .01	4	+ .21	11.4
15497	2 24.6	+57 15	7.20	B7s	103.8	− 1.9	+ .26	.....	+ .26	3	+ .40	5.5
15558	2 25.1	+61 1	7.82	*B*	102.4	+ 1.6	+ 12	.....	+ 12	3	+ .31	.....
15570	2 25.2	+60 56	8.0:	*B*	102.4	+ 1.5	+ .20	.....	+ .20	2	+ .39	.....
15571	2 25.2	+56 59	8.0:	*B*	104.0	− 2.2	+ .02	.....	+ .02	2	+ .21	.....
15642	2 25.8	+54 54	8.6	*B2*	104.9	− 4.0	− .18	.....	− .18	3	+ .02	11.5
15690	2 26.3	+57 5	7.7:	*B3*	104.0	− 2.0	+ .18	.....	+ .18	2	+ .37	7.3
15752	2 26.8	+57 58	8.8	*Bo*	103.8	− 1.2	.....	+ .09	+ .09	2	+ .31	10.5
15785	2 27.2	+60 6	8.41	B2	103.0	+ 0.8	.....	+ .08	+ .08	1	+ .28	9.4
MWC52	2 27.5	+59 0	11.3	Be	103.5	− 2.2	.....	+ .17	+ .17	2	+ .36	.....
16243	2 31.3	+57 23	8.4	*B2*	104.6	− 1.5	+ .12	+ .11	+ .11	2, 1	+ .31	9.2
MWC55	2 32.8	+57 21	10.7	Be	104.8	− 1.4	.....	+ .05	+ 05	1	+ .24	.....
16582	2 34.4	− 0 6	4 04	B2s	139.4	−50.9	− .24	.....	− .24	2	− .04	7.3
16778	2 36.3	+59 24	7.71	cB9	104.3	+ 0.6	.....	+ .39	+ .39	1	+ .51	9.6
16908	2 37.6	+27 17	4.58	B3	119.6	−27.9	− .15	.....	− .15	3	+ .04	6.5
16968	2 38.1	+34 42	7.22	*B5*	115.8	−21.4	− .10	.....	− .10	2	+ .07	8.3
17036	2 39.0	+14 53	5.80	*B8*	127.7	−38.3	− .12	.....	− .12	2	+ .01	6.5
17081	2 39.4	−14 17	4.39	B5	159.9	−59.1	− .16	.....	− .16	1	+ .01	5.9
17088	2 39.5	+57 19	7.54	*B2*	105.6	− 1.0	+ .25	.....	+ .25	4	+ .45	7.4
17145	2 40.0	+57 15	8.0:	*B*	105.7	− 1.1	+ .28	.....	+ .28	2	+ .47	.....
MWC57	2 42.3	+61 41	10.3	B(o)ne	104.0	+ 3.0	.....	+ .15	+ .15	1	+ .37	11.6
17505	2 43.4	+60 1	7.11	O7	104.9	+ 1.6	+ 01	.....	+ 01	2	+ .24	9.9
17543	2 43.7	+17 3	5.30	B8	127.3	−35.9	− .16	.....	− .16	2	− .03	6.3
17769	2 46.0	+14 40	5.46	B6n	129.6	−37.5	− .16	.....	− .16	2	.00	6.9
17857	2 47.0	+63 43	7.78	*Bp*	103.5	+ 5.1	+ .16	.....	+ .16	2	+ .35	.....
18326	2 51.6	+60 10	7.91	*B*	105.7	+ 2.2	+ .05	.....	+ .05	2	+ .24	.....
18352	2 51.9	+60 53	7.00	B2s	105.4	+ 2.9	− .08	.....	− .08	2	+ .12	9.2
18409	2 52.4	+62 19	8.0:	*B*	104.7	+ 4.1	.00	.....	.00	2	+ .19	.....
18537	2 53.7	+51 57	5.42	B8n	109.9	− 4.8	− .13	.....	− .13	3	.00	6.2
18604	2 54.4	+ 8 31	4.69	B5	136.6	−41.1	− .18	.....	− .18	2	− .01	6.4
18883	2 57.1	+ 3 58	5.63	*B5*	141.4	−44.0	− .12	.....	− .12	2	+ .05	6.9
19243	3 0.7	+62 0	6.54	B2ne	105.7	+ 4.3	+ .06	.....	+ .06	2	+ .26	7.7
19268	3 0.9	+51 50	6.17	B5	110.9	− 4.4	− .10	.....	− .10	2	+ .07	7.3
19374	3 1.8	+17 30	6.09	B2s	131.3	−33.0	− .12	.....	− .12	3	+ .08	8.5
19624	3 4.5	+51 49	6.71	*B5*	111.4	− 4.1	− .04	.....	− .04	2	+ .13	7.4
19820	3 6.2	+59 11	7.09	O8n	107.8	+ 2.3	+ .09	.....	+ .09	3	+ .32	9.3
20017	3 7.9	+48 19	7.90	Bne	113.8	− 6.8	+ .07	+ .02	+ .04	1, 1	+ .23	.....
20041	3 8.2	+56 45	5.92	cAo	109.3	+ 0.4	+ .18	.....	+ .18	2	+ .28	9.5
20134	3 9.1	+59 41	7.51	B2e	107.8	+ 2.9	− .07	.....	− .07	3	+ .13	9.6
20315	3 11.0	+43 39	5.38	B7n	116.8	−10.4	− .10	.....	− .10	2	+ .04	6.2
20336	3 11.2	+65 17	4.76	B3e	105.0	+ 7.7	− .15	− .24	− .20	3, 1	− .01	7.0
20305	3 11.5	+49 51	5.30	B3	113.4	− 5.2	− 17	− .14	− .16	5, 1	+ .03	7.3
20418	3 12.0	+49 43	5.08	B3	113.6	− 5.3	− .17	.....	− 17	3	+ .02	7.1
20756	3 15.5	+20 47	5.17	B7s	131.9	−28.4	− .14	.....	− .14	2	.00	6.3
20809	3 16.1	+48 51	5.30	B3	114.6	− 5.6	− .15	.....	− .15	3	+ .04	7.2
21071	3 18.9	+48 45	5.91	B8	115.0	− 5.4	− .12	.....	− .12	3	+ .01	6.6
21212	3 20.3	+62 9	8.3	B2e	107.6	+ 5.7	+ .12	+0.11	+ .11	1, 1	+ .31	9.1
21278	3 20.9	+48 43	4.94	B5	115.3	− 5.3	− .10	.....	− .10	2	+ .07	6.0
21291	3 21.0	+59 36	4.42	cB9	109.1	+ 3.7	+ .06	.....	+ .06	2	+ .18	8.7
21362	3 21.7	+49 31	5.64	B8nn	115.0	− 4.5	− .09	.....	− .09	3	+ .04	6.2
21389	3 21.9	+58 32	4.76	cAoea	109.8	+ 2.9	+ .13	.....	+ .13	2	+ .23	8.7
21428	3 22.2	+49 10	4.67	B5	115.3	− 4.8	− .12	.....	− .12	2	+ .05	5.9
21448*	3 22.4	+44 42	7.37	B3	117.9	− 8.4	+ .04	.....	+ .04	2	(+ .23)	.....
21455	3 22.5	+46 37	6.20	B6	116.8	− 6.8	− .01	.....	− .01	4	+ .15	6.6
21483	3 22.7	+30 2	7.06	B3	127.0	−20.2	+0.11	.....	+0.11	3	+0.30	7.2

TABLE 3—*Continued*

HD	R.A. 1900	Decl. 1900	m	Spec.	l	b	C_1			No.	E_1	m_0-M
							M	W	Mean			
21650	3h24m6	+41° 25′	7.15	B5ne	120°.2	−10°.8	−0.09	.....	−0.09	2	+0.08	8.2
21803	3 25.8	+44 32	6.33	B2s	118.5	− 8.2	− .08	.....	− .08	2	+ .12	8.5
21856	3 26.3	+35 6	5.80	B3	124.3	−15.7	− .14	.....	− .14	3	+ .05	7.6
22192	3 29.4	+47 51	4.26	B5ne	117.0	− 5.1	− .14	.....	− .14	2	+ .03	5.6
22253	3 29.9	+56 23	6.79	B1n	112.0	+ 1.7	− .04	.....	− .04	2	+ .17	9.2
22298	3 30.3	+54 50	7.8	B2ne	112.9	+ 0.5	+ .09	+0.05	+ .06	1, 2	+ .26	9.0
MWC71	3 31.9	+61 31	9.5	B2ne	109.1	+ 6.0	+ .04	.....	+ .04	2	+ .24	10.8
22780	3 34.6	+37 16	5.57	B8nn	124.3	−13.0	− .12	.....	− .12	2	+ .01	6.3
22928	3 35.8	+47 28	3.10	B8n	118.1	− 4.8	− .16	.....	− .16	2	− .03	4.1
22951	3 36.0	+33 39	5.04	B2	126.9	−15.6	− .10	.....	− .10	2	+ .10	7.3
23180	3 38.0	+31 58	3.94	B2	128.4	−16.6	− .08	.....	− .08	2	+ .12	6.1
23193	3 38.1	+36 9	5.57	cA3	125.6	−13.3	− .05	.00	− .02	1, 1	− .01	11.1
23288	3 38.9	+23 59	5.43	B7n	134.1	−22.5	− .11	.....	− .11	2	+ .03	6.3
23302	3 39.0	+23 48	3.81	B5nea	134.2	−22.6	− .13	.....	− .13	2	+ .04	5.1
23338	3 39.3	+24 10	4.37	B8	134.1	−22.3	− .14	.....	− .14	2	− .01	5.2
23408	3 39.9	+24 4	4.02	B9s	134.2	−22.3	− .13	.....	− .13	2	− .01	4.5
23466	3 40.3	+ 5 44	5.36	B3	149.3	−35.0	− .16	.....	− .16	3	+ .03	7.4
23478	3 40.4	+32 0	6.51	B5n	128.7	−16.2	− .02	.....	− .02	2	+ .15	7.1
23480	3 40.4	+23 39	4.25	B5ne	134.6	−22.5	− .12	.....	− .12	2	+ .05	5.5
23625	3 41.5	+33 18	6.36	B3	128.0	−15.1	− .02	.....	− .02	2	+ .17	7.4
23630	3 41.5	+23 48	2.96	B5ne	134.7	−22.2	− .15	.....	− .15	2	+ .02	4.4
23675	3 41.9	+52 21	6.76	B0	115.8	− 0.4	+ .08	.....	+ .08	2	+ .30	8.6
23793	3 42.8	+10 50	5.03	B3	145.2	−31.2	− .18	.....	− .18	2	+ .01	7.2
23800	3 42.9	+52 11	6.87	B2n	116.0	− 0.4	+ .01	.....	+ .01	3	+ .21	8.4
24131	3 45.5	+34 3	5.73	B2	128.2	−14.0	− .08	.....	− .08	2	+ .12	7.9
24190	3 46.0	+33 53	7.49	B5	128.4	−14.1	− .06	.....	− .06	2	+ .11	8.3
24398	3 47.8	+31 35	2.91	cB1	130.3	−15.5	− .04	.....	− .04	2	+ .17	7.2
24431	3 48.1	+52 21	6.70	O8	116.5	0.0	.00	.....	.00	2	+ .23	9.6
24432	3 48.1	+48 45	7.02	B5s	118.9	− 2.5	+ .09	.....	+ .09	3	+ .26	6.8
24504	3 48.8	+47 35	5.34	B7n	119.7	− 3.3	− .12	.....	− .12	2	+ .02	6.3
24534*	3 49.1	+30 45	var.	Bone	131.0	−15.9	+ .04	.....	+ .04	2	(+ .26)	.....
24640	3 50.0	+34 47	5.48	B3	128.4	−12.8	− .12	.....	− .12	2	+ .07	7.2
24760	3 51.1	+39 43	2.96	B2	125.2	− 9.0	− .20	.....	− .20	2	.00	6.0
24912	3 52.5	+35 30	4.05	O7n	128.3	−12.0	− .14	.....	− .14	2	+ .09	7.9
25090	3 54.1	+62 9	7.28	B1s	110.7	+ 8.2	+ .04	.....	+ .04	2	+ .25	9.1
25204*	3 55.1	+12 12	3.3	B3	146.4	−28.0	− .17	.....	− .17	3	+ .02	5.4
25340	3 56.5	− 1 50	5.25	B7	159.7	−30.3	− .16	.....	− .16	2	− .02	6.5
25348	3 56.6	+53 3	8.4	B(1)ne	117.0	+ 1.6	.00	− .06	− .04	2, 2	+ .17	10.8
25443	3 57.4	+61 48	6.75	Bo	111.2	+ 8.2	+ .02	.....	+ .02	2	+ .24	9.0
25517	3 58.1	+44 0	9.3	*B2*	123.3	− 4.9	.....	− .01	− .01	2	+ .19	11.0
25539	3 58.3	+32 18	6.70	B3	131.4	−13.5	− .06	.....	− .06	2	+ .13	8.0
25558	3 58.4	+ 5 9	5.33	B5	153.3	−31.9	− .15	.....	− .15	2	+ .02	6.8
25638*	3 59.1	+62 4	7.0	Bon	111.2	+ 8.5	+ .08	.....	+ .08	2	+ .30	8.8
25787	4 0.2	+51 11	7.49	B3	118.7	+ 0.6	− .11	.....	− .11	2	+ .08	9.1
25799	4 0.3	+32 6	6.87	B5n	131.9	−13.3	− .08	.....	− .08	2	+ .09	7.8
25833	4 0.6	+33 11	6.61	B3	131.2	−12.5	− .08	.....	− .08	2	+ .11	8.0
25914	4 1.2	+56 50	8.1	cB3	115.0	+ 4.8	+ .13	+0.13	+ .13	1, 2	+ .32	11.4
25940	4 1.4	+47 27	4.03	B3ne	121.4	− 2.0	− .14	.....	− .14	2	+ .05	5.9
20356	4 5.0	+83 34	5.39	B5n	95.5	+23.9	− .14	.....	− .14	2	+ .03	6.8
26420	4 5.7	+41 52	7.60	B3nea	125.8	− 5.5	− .07	.....	− .07	3	+ .12	9.0
26684	4 8.2	+75 52	6.63	B5n	101.7	+18.8	− .14	.....	− .14	2	+ .03	8.0
26739	4 8.6	− 1 24	6.34	B5	161.4	−33.6	− .12	.....	− .12	2	+ .05	7.6
26906	4 10.1	+45 58	7.9	B(3)ne	123.5	− 2.1	− .06	.....	− .06	2	+ .13	9.2
26912	4 10.1	+ 8 39	4.32	B3	152.1	−27.4	− .14	.....	− .14	2	+ .05	6.2
27192	4 12.6	+50 41	5.54	B3n	120.5	+ 1.6	− .12	.....	− .12	2	+ .07	7.2
27396	4 14.3	+46 16	4.89	B4	123.8	− 1.3	− .13	.....	− .13	3	+ .05	6.4
27795	4 18.2	+45 56	7.16	B3s	124.	− 1.1	+ .02	.....	+ .02	3	+ .21	7.9
28114	4 21.0	+ 8 22	5.99	B5n	154.2	−25.4	− .10	.....	− .10	4	+ .07	7.1
28149	4 21.3	+22 16	5.41	B7n	142.2	−16.3	− .14	.....	− .14	2	.00	6.5
28446*	4 24.1	+53 42	5.86	Bon	119.5	+ 4.9	−0.08	.....	−0.08	2	+0.14	8.8

TABLE 3—*Continued*

HD	R.A. 1900	Decl. 1900	m	Spec.	l	b	C_1			No.	E_1	m_0-M
							M	W	Mean			
28497	$4^h24^m.5$	−13° 17′	5.50	B3ne	176°.3	−35°.9	−0.15	.....	−0.15	2	+0.04	7.4
29248	4 31.3	− 3 33	4.12	B2s	167.0	−29.9	− .22	.....	− .22	2	− .02	7.3
29335	4 32.1	+ 0 48	5.32	B8	162.9	−27.5	− .14	.....	− .14	2	− .01	6.2
29376	4 32.5	+ 7 7	6.89	B5	157.1	−23.9	− .14	.....	− .14	2	+ .03	8.3
E237299	4 32.9	+57 43	9.5	*B2*	117.3	+ 8.5	+ .02	.....	+ .02	2	+ .22	11.0
29763	4 36.2	+22 46	4.33	B5n	144.5	−13.7	− .16	.....	− .16	2	+ .01	5.9
29866	4 37.3	+40 36	6.10	B4ne	130.7	− 2.1	− .08	.....	− .08	3	+ .10	7.3
30076	4 39.3	− 8 41	5.87	B5ne	173.3	−30.6	− .15	.....	− .15	3	+ .02	7.3
30112	4 39.6	+ 0 23	7.28	B3	164.4	−26.1	− .15	.....	− .15	2	+ .04	9.2
30211	4 40.5	− 3 26	4.18	B5	168.2	−27.9	− .14	.....	− .14	2	+ .03	5.6
MWC91	4 43.2	+41 30	9.8	Bone	130.9	− 0.7	− .07	.....	− .07	3	+ .15	12.7
30614	4 44.1	+66 10	4.38	Oose	111.4	+14.9	− .14	.....	− .14	2	+ .09	8.3
30650	4 44.4	+43 24	7.37	B5n	129.5	+ 0.7	− .12	.....	− .12	2	+ .05	8.6
30677	4 44.6	+ 8 15	6.9	*Bo*	158.0	−20.7	− .15	.....	− .15	3	+ .07	10.3
30836	4 45.9	+ 5 26	3.78	B2s	160.7	−22.0	− .20	.....	− .20	5	.00	6.8
30870	4 46.2	+ 9 49	6.08	B5n	156.8	−19.5	− .06	.....	− .06	2	+ .11	6.9
31237	4 49.0	+ 2 17	3.87	B2s	164.0	−23.1	− .21	.....	− .21	2	− .01	6.9
31293*	4 49.4	+30 24	7.46	Aoep	140.3	− 6.7	− .04	+0.03	+ .01	2, 1	+ .11	.....
31327	4 49.7	+36 1	6.18	B2s	135.9	− 3.1	+ .08	.....	+ .08	2	+ .28	7.2
31331	4 49.7	+ 0 19	5.86	B6	165.9	−24.0	− .11	.....	− .11	2	+ .05	6.9
31617	4 52.2	+43 11	7.34	B2s	130.6	+ 1.7	− .10	.....	− .10	2	+ .10	9.6
31726	4 53.1	−14 24	5.87	*B3*	181.0	−30.1	− .20	.....	− .20	2	− .01	8.1
MWC94	4 54.2	+41 7	9.3	B(3)ne	132.4	+ 0.7	− .16	.....	− .16	2	+ .03	11.3
32190	4 56.2	+23 53	8.3	*B5*	146.4	− 9.4	.....	− .09	− .09	2	+ .08	9.3
32343	4 57.4	+58 50	5.31	B3e	118.5	+11.8	− .14	.....	− .14	2	+ .05	7.2
32446	4 58.2	+44 55	7.97	*B3*	129.8	+ 3.6	− .04	.....	− .04	2	+ .15	9.1
32481	4 58.4	+21 32	8.1	*B5*	148.7	−10.4	.....	+ .04	+ .04	2	+ .21	8.2
32612	4 59.3	−14 31	6.35	*B3*	181.8	−28.8	− .16	.....	− .16	2	+ .03	8.3
32630	4 59.5	+41 6	3.28	B4	133.0	+ 1.5	− .20	.....	− .20	5	− .02	5.3
32641	4 59.6	+22 56	6.66	B5n	147.7	− 9.3	− .06	.....	− .06	2	+ .11	7.5
32656	4 59.7	+26 17	6.56	B5n	145.0	− 7.3	− .09	.....	− .09	3	+ .08	7.6
32672	4 59.8	+38 23	7.7:	*B3*	135.3	− 0.3	− .08	.....	− .08	2	+ .11	9.1
32686	4 59.9	− 3 11	5.98	B5	170.3	−23.5	− .16	.....	− .16	2	+ .01	7.5
32990	5 2.0	+24 8	5.50	B3	147.0	− 8.2	− .08	.....	− .08	2	+ .11	6.9
32991	5 2.0	+21 34	5.95	B3ne	149.1	− 9.7	− .04	.....	− .04	3	+ .15	7.1
33090	5 2.8	+21 22	8.5	*B5*	149.4	− 9.6	.....	− .02	− .02	2	+ .15	9.0
33152	5 3.2	+36 53	8.1	B2e	136.9	− 0.4	− .01	− .04	− .03	3, 2	+ .17	9.9
33203*	5 3.5	+37 11	6.17	B2	136.6	− 0.2	+ .21	.....	+ .21	3	(+ .41)	.....
33232	5 3.7	+40 53	8.2	B(3)e	133.7	+ 2.0	.....	− .14	− .14	2	+ .05	10.0
33328	5 4.4	− 8 53	4.34	B3n	176.7	−25.2	− .16	.....	− .16	2	+ .03	6.3
33461	5 5.3	+41 6	7.9	B(1)e	133.7	+ 2.4	− .08	− .04	− .05	1, 3	+ .16	10.4
33604	5 6.3	+40 5	7.32	B3se	134.6	+ 1.9	− .12	.....	− .12	2	+ .07	9.0
33988	5 9.0	+46 19	6.94	B5ne	129.8	+ 5.9	− .02	.....	− .02	2	+ .15	7.5
34078	5 9.7	+34 12	5.81	Oqss	139.8	− 0.9	− .07	.....	− .07	3	+ .16	9.2
34085	5 9.7	− 8 19	0.34	cB8	177.0	−23.7	− .13	.....	− .13	4	.00	5.8
34233	5 10.8	+58 1	6.23	B5	120.2	+12.8	− .12	.....	− .12	3	+ .05	7.5
34251	5 10.9	+18 20	7.5:	B3n	153.1	− 9.8	− .04	.....	− .04	2	+ .15	8.7
34333	5 11.6	+36 31	7.56	*B5*	138.1	+ 0.7	− .04	.....	− .04	3	+ .13	8.2
34503	5 12.8	− 6 57	3.68	B8	175.8	−22.5	− .16	.....	− .16	2	− .03	4.7
34576	5 13.4	+36 34	7.38	B5n	138.3	+ 1.0	− .10	.....	− .10	3	+ .07	8.5
34578	5 13.4	+33 52	5.16	cA5	140.5	− 0.5	+ .03	+ .11	+ .07	2, 1	+ .04	10.4
34626	5 13.8	+36 32	8.2	*B2*	138.4	+ 1.1	− .16	−0.09	− .11	1, 2	+ .09	10.6
34656	5 14.0	+37 20	6.71	O6sf	137.7	+ 1.6	− .06	.....	− .06	1	+ .17	10.0
34748	5 14.6	− 1 31	6.42	B3	171.0	−19.5	− .16	.....	− .16	2	+ .03	8.4
34759	5 14.7	+41 43	5.12	B7	134.2	+ 4.2	− .16	.....	− .16	2	− .02	6.4
34816	5 15.0	−13 17	4.29	B1	182.3	−24.8	− .22	.....	− .22	2	− .01	8.0
34863	5 15.4	−12 25	5.29	B8n	181.5	−24.3	− .12	.....	− .12	2	+ .01	6.0
34921	5 15.8	+37 35	7.39	Bone	137.8	+ 2.0	− .01	.....	− .01	3	+ .21	9.8
34959	5 16.1	+ 3 54	6.41	B3	166.2	−16.5	− .18	.....	− .18	2	+ .01	8.5
34989	5 16.4	+ 8 20	5.71	B2	162.4	−14.1	−0.18	.....	−0.18	2	+0.02	8.6

TABLE 3—*Continued*

HD	R.A. 1900	Decl. 1900	m	Spec.	l	b	C_1			No.	E_x	m_0-M
							M	W	Mean			
35007	5h16m5	− 0° 31′	5.65	B3	170°.3	−18°.6	−0.18	.....	−0.18	3	+0.01	7.8
35039	5 16.7	− 0 29	4.65	B3	170.3	−18.5	− .19	.....	− .19	3	.00	6.8
35149	5 17.6	+ 3 27	4.99	B3n	166.9	−16.4	− .20	.....	− .20	3	− .01	7.3
35299	5 18.6	− 0 15	5.64	B3s	170.3	−18.1	− .22	.....	− .22	2	− .03	8.0
35337	5 18.9	−14 1	5.17	B3s	183.5	−24.2	− .18	.....	− .18	3	+ .01	7.3
35345	5 19.0	+35 33	8.4	B2e	139.8	+ 1.4	− .03	.....	− .03	2	+ .17	10.2
35395	5 19.3	+20 30	6.83	B2s	152.3	− 6.9	+ .02	.....	+ .02	3	+ .22	8.3
35407	5 19.4	+ 2 15	6.32	B3n	168.2	−16.6	− .14	.....	− .14	2	+ .05	8.2
35411	5 19.4	− 2 29	3.44	Bo	172.5	−18.9	− .22	.....	− .22	4	.00	7.3
35439	5 19.6	+ 1 45	4.73	B3ne	168.6	−16.8	− .16	.....	− .16	2	+ .03	6.7
35468	5 19.8	+ 6 16	1.70	B2s	164.6	−14.5	− .24	.....	− .24	2	− .04	5.0
35532	5 20.3	+16 36	6.18	B3n	155.8	− 8.9	− .16	.....	− .16	2	+ .03	8.2
35575	5 20.6	− 1 35	7.3:	B3	171.8	−18.2	− .17	.....	− .17	2	+ .02	9.4
35588	5 20.7	+ 0 25	6.02	B3n	170.0	−17.2	− .20	.....	− .20	3	− .01	8.3
35600	5 20.8	+30 7	5.72	cB9	144.5	− 1.3	− .06	+0.01	− .02	2, 1	+ .10	10.5
35619	5 21.0	+34 41	8.5	*Bo*	140.7	+ 1.3	.....	− .02	− .02	3	+ .20	11.0
35633	5 21.1	+34 27	7.9	*Bo*	140.9	+ 1.1	− .03	− .01	− .01	1, 3	+ .21	10.3
35653	5 21.2	+33 52	7.50	B1s	141.4	+ 0.8	− .04	.....	− .04	3	+ .17	9.9
35671	5 21.3	+17 53	5.31	B3	154.8	− 8.0	− .14	.....	− .14	2	+ .05	7.2
35708	5 21.6	+21 51	4.83	B3s	151.5	− 5.8	− .19	.....	− .19	3	.00	7.0
35715	5 21.6	+ 3 0	4.66	B2	167.8	−15.7	− .22	.....	− .22	2	− .02	7.8
35762	5 21.9	+ 3 45	6.61	B3	167.2	−15.3	− .16	.....	− .16	2	+ .03	8.6
35777	5 22.0	− 2 27	6.56	B5n	172.8	−18.3	− .17	.....	− .17	2	.00	8.2
35899	5 22.8	− 2 14	7.36	B5	172.7	−18.1	− .12	.....	− .12	2	+ .05	8.6
35912	5 22.9	+ 1 13	6.37	B3s	169.6	−16.3	− .18	.....	− .18	2	+ .01	8.5
35921	5 23.0	+35 18	6.71	O9	140.4	+ 1.9	− .02	.....	− .02	3	+ .21	9.7
36104	5 24.2	+12 12	7.00	*B8*	160.0	−10.4	− .18	.....	− .18	1	− .05	8.2
36113	5 24.3	+20 29	6.85	B8	153.0	− 6.0	− .12	.....	− .12	2	+ .01	7.6
36133	5 24.4	+ 3 3	7.5:	B5	168.1	−15.1	− .12	.....	− .12	2	+ .05	8.7
36151	5 24.6	− 7 21	6.55	B5	177.7	−20.1	− .16	.....	− .16	2	+ .01	8.1
36166	5 24.7	+ 1 42	5.67	B3	169.4	−15.7	− .20	.....	− .20	2	− .01	7.9
36262	5 25.4	+12 1	7.3:	B3	160.4	−10.3	− .17	.....	− .17	2	+ .02	9.4
36267	5 25.4	+ 5 52	4.32	B4n	165.7	−13.5	− .17	.....	− .17	3	+ .01	6.1
36280	5 25.5	+34 52	9.0	*B*	141.1	+ 2.1	− .12	.....	− .12	3	+ .07	.....
36285	5 25.5	− 7 31	6.24	B3	178.0	−19.9	− .20	.....	− .20	2	− .01	8.5
36337	5 25.9	+14 51	6.62	B8s	158.0	− 8.7	− .12	.....	− .12	2	+ .01	7.4
36340*	5 25.9	+ 3 16	7.9	*B3*	168.1	−14.7	.....	− .23	− .23	1	− .04	10.4
36351	5 26.0	+ 3 13	5.52	B3	168.2	−14.7	− .19	− .24	− .22	2, 1	− .03	7.9
36371	5 26.2	+32 7	4.88	cB3	143.5	+ 0.7	.00	.....	.00	4	+ .19	9.1
36374	5 26.2	+26 54	7.11	B5nn	147.8	− 2.1	− .01	.....	− .01	2	+ .16	7.6
36430	5 26.5	− 6 47	6.03	B3s	177.4	−19.4	− .19	.....	− .19	3	.00	8.2
36441	5 26.6	+26 40	8.3	*B2*	148.1	− 2.2	− .06	− .12	− .10	2, 2	+ .10	10.6
36483	5 26.9	+36 24	8.4	*B1*	140.0	+ 3.2	+ .04	.....	+ .04	4	+ .25	10.2
36486	5 26.9	− 0 22	2.48	Bo	171.5	−16.3	− .23	.....	− .23	6	− .01	6.5
36510	5 27.1	− 7 23	4.64	B2	178.0	−19.5	− .18	.....	− .18	2	+ .02	7.5
36547	5 27.4	+23 16	9.0	*B2*	151.0	− 4.0	− .01	+ .01	.00	2, 3	+ .20	10.6
36576	5 27.6	+18 29	5.50	B3ne	155.1	− 6.4	− .11	.....	− .11	2	+ .08	7.1
36591	5 27.7	− 1 40	5.30	B2s	172.8	−16.7	− .20	.....	− .20	2	.00	8.3
36646	5 28.1	− 1 48	6.46	B3	173.0	−16.7	− .19	.....	− .19	2	.00	8.7
36653	5 28.2	+14 15	5.58	B3	158.8	− 8.5	− .16	.....	− .16	2	+ .03	7.6
36695	5 28.5	− 1 14	5.37	B2n	172.5	−16.3	− .21	.....	− .21	2	− .01	8.4
36741	5 28.8	+ 1 20	6.42	B5	170.2	−15.0	− .20	.....	− .20	2	− .03	8.2
36779	5 29.0	− 1 6	6.18	B3	172.5	−16.1	− .18	.....	− .18	2	+ .01	8.3
36819	5 29.3	+23 58	5.28	B3	150.7	− 3.1	− .15	.....	− .15	3	+ .04	7.2
36822	5 29.3	+ 9 25	4.53	Boss	163.1	−10.8	− .18	.....	− .18	2	+ .04	8.1
36824	5 29.3	+ 5 35	6.71	B5	166.5	−12.8	− .14	.....	− .14	2	+ .03	8.1
36861	5 29.6	+ 9 52	3.66	O8	162.8	−10.5	− .22	.....	− .22	2	+ .01	8.1
36879	5 29.7	+21 20	7.5	*B2*	153.0	− 4.5	− .06	.....	− .06	4	+ .14	9.5
36954*	5 30.1	− 0 48	6.8	*B3*	172.3	−15.8	.....	−0.18	− .18	1	+ .01	8.9
36960	5 30.1	− 6 5	4.67	B1s	177.2	−18.3	−0.24	.....	−0.24	2	−0.03	8.5

TABLE 3—*Continued*

HD	R.A. 1900	Decl. 1900	m	Spec.	l	b	C_1			No.	E_1	m_0-M
							M	W	Mean			
37016	5^h30^m4	− 4° 29′	6.28	B2s	175°7	−17°4	−0.14	.....	−0.14	3	+0.06	8.9
37017	5 30.4	− 4 34	6.54	B2	175.8	−17.5	− .14	.....	− .14	2	+ .06	9.1
37018	5 30.4	− 4 54	4.65	B2	176.1	−17.6	− .19	.....	− .19	2	+ .01	7.6
37022*	5 30.4	− 5 27	5.36	O7	176.6	−17.9	− .02	.....	− .0.	2	+ .20	8.5
37040	5 30.5	− 4 26	6.29	B3	175.7	−17.4	− .14	.....	− .14	2	+ .05	8.1
37041	5 30.5	− 5 29	5.17	O9	176.7	−17.9	− .16	.....	− .16	2	+ .07	9.2
37043	5 30.5	− 5 59	2.87	O8s	177.1	−18.1	− .23	.....	− .23	2	.00	7.4
37055	5 30.6	− 3 19	6.33	B3	174.7	−16.9	− .18	.....	− .18	3	+ .01	8.5
37058	5 30.6	− 4 54	7.35	B3s	176.1	−17.6	− .13	.....	− .13	3	+ .06	9.1
37128	5 31.1	− 1 16	1.75	cBo	172.9	−15.8	− .20	.....	− .20	3	+ .02	7.1
37129	5 31.1	− 4 29	6.98	B3	175.8	−17.3	− .17	.....	− .17	3	+ .02	9.0
37150	5 31.3	− 5 43	6.45	B3	177.0	−17.8	− .18	.....	− .18	2	+ .01	8.6
37202	5 31.7	+21 5	3.00	B3e	153.4	− 4.2	− .21	.....	− .21	5	− .02	5.3
37209	5 31.7	− 6 8	5.62	B1s	177.4	−17.9	− .21	.....	− .21	3	.00	9.2
37232	5 31.9	+ 8 53	6.09	B3	163.9	−10.5	− .19	.....	− .19	2	.00	8.3
37303	5 32.5	− 6 0	5.75	B3n	177.4	−17.7	− .24	.....	− .24	3	− .05	8.3
37334	5 32.7	− 5 0	7.30	B3	176.5	−17.2	− .20	.....	− .20	2	− .01	9.6
37356	5 32.9	− 4 52	6.32	B3s	176.4	−17.1	− .18	.....	− .18	3	+ .01	8.4
37366	5 33.0	+30 50	7.52	*B5*	145.3	+ 1.2	− .10	.....	− .10	2	+ .07	8.6
37367	5 33.0	+29 10	6.00	B3s	146.8	+ 0.4	− .05	.....	− .05	2	+ .14	7.2
37397	5 33.2	− 1 13	6.74	B3n	173.1	−15.3	− .17	.....	− .17	3	+ .02	8.8
37438	5 33.5	+25 50	5.00	B3	149.6	− 1.3	− .20	.....	− .20	2	− .01	7.3
37468	5 33.7	− 2 39	3.78	Bo	174.5	−15.9	− .16	.....	− .16	2	+ .06	7.3
37481	5 33.8	− 6 38	5.92	B3	178.1	−17.7	− .22	.....	− .22	2	− .03	8.3
37490	5 33.9	+ 4 4	4.54	B3ne	168.4	−12.5	− .17	.....	− .17	3	+ .02	6.6
37635	5 34.8	− 9 46	6.36	B5	181.2	−18.9	− .15	.....	− .15	3	+ .02	7.8
37657	5 35.1	+43 0	6.99	B3ne	135.2	+ 8.0	− .16	.....	− .16	2	+ .03	9.0
37711	5 35.5	+16 29	4.87	B3	157.8	− 5.8	− .18	.....	− .18	3	+ .01	7.0
37742	5 35.7	− 2 0	2.05	Bon	174.1	−15.1	− .22	.....	− .22	3	.00	5.9
37744	5 35.7	− 2 53	6.07	B3	174.9	−15.5	− .20	.....	− .20	3	− .01	8.3
37756	5 35.8	− 1 11	5.00	B3	173.4	−14.7	− .21	.....	− .21	3	− .02	7.3
37903	5 36.7	− 2 18	7.8	B2	174.5	−15.0	.....	−0.10	− .10	1	+ .10	10.1
37967	5 37.2	+23 10	6.06	B3ne	152.3	− 2.0	− .12	.....	− .12	2	+ .07	7.8
38010	5 37.5	+25 24	6.86	B3ne	150.5	− 0.7	− .09	.....	− .09	2	+ .10	8.4
38191	5 38.9	+21 25	8.6	Bne	154.0	− 2.6	.....	− .05	− .05	1	+ .14	.....
38622	5 42.0	+13 52	5.20	B3s	160.9	− 5.9	− .21	.....	− .21	3	− .02	7.5
38672	5 42.4	+12 23	6.57	B8	162.2	− 6.5	− .10	.....	− .10	2	+ .03	7.2
38771	5 43.0	− 9 42	2.20	cBo	182.1	−17.1	− .16	.....	− .16	2	+ .06	7.3
39201	5 46.5	− 7 33	5.32	B3	180.5	−15.3	− .20	.....	− .20	2	− .01	7.6
39340	5 46.9	+26 25	8.1	B3ne	150.7	+ 1.6	.....	− .12	− .12	2	+ .07	9.8
E248753	5 47.3	+25 43	8.5	Bone	151.3	+ 1.3	− .07	− .05	− .06	3, 1	+ .16	11.3
39477	5 47.8	+30 28	7.46	B5n	147.3	+ 3.8	.00	.....	.00	4	+ .17	7.9
39478	5 47.8	+26 24	8.2	B2ne	150.8	+ 1.7	− .10	− .12	− .11	4, 3	+ .09	10.6
39698	5 49.1	+19 44	5.89	B3	156.7	− 1.4	− .18	.....	− .18	2	+ .01	8.0
39746	5 49.4	+27 42	7.1	*B2*	149.9	+ 2.7	− .06	.....	− .06	2	+ .14	9.1
39777	5 49.6	− 4 5	6.35	B2	177.7	−13.0	− .18	.....	− .18	2	+ .02	9.2
39970	5 50.9	+24 14	6.02	cB9	153.0	+ 1.2	+ .06	.....	+ .06	3	+ .18	10.3
40005	5 51.1	+16 21	6.91	B3	159.9	− 2.7	− .14	.....	− .14	2	+ .05	8.8
40111	5 51.8	+25 57	4.90	Bo	151.7	+ 2.3	− .16	.....	− .16	3	+ .06	8.4
40160	5 52.1	+46 31	7.24	B5	133.6	+12.4	− .17	.....	− .17	2	.00	8.8
40978	5 57.2	+46 33	6.98	B3ne	134.0	+13.2	− .14	.....	− .14	2	+ .05	8.8
41117	5 58.0	+20 8	4.71	cB1ea	157.4	+ 0.6	− .02	.....	− .02	4	+ .19	8.9
41161	5 58.2	+48 15	6.51	O9n	132.5	+14.1	− .16	.....	− .16	2	+ .07	10.5
41253	5 58.8	+ 2 52	7.5:	B5	172.6	− 7.7	− .08	.....	− .08	3	+ .09	8.5
41285	5 59.1	+16 40	7.5:	B5n	160.5	− 0.9	− .15	.....	− .15	2	+ .02	9.0
41335	5 59.4	− 6 42	5.12	B2(n)e	181.2	−12.1	− .18	.....	− .18	2	+ .02	8.0
41398	5 59.8	+28 56	7.45	Bo	149.9	+ 5.3	− .02	.....	− .02	2	+ .20	9.9
41541	6 0.7	+42 41	6.88	B5	137.8	+12.0	− .10	.....	− .10	2	+ .07	8.0
41689	6 1.6	+62 20	8.4	B2n	119.2	+20.3	.....	−0.18	− .18	1	+ .02	11.3
41690	6 1.6	+21 53	7.8	*B2*	156.3	+ 2.2	−0.04	.....	−0.04	2	+0.16	9.7

TABLE 3—*Continued*

HD	R.A. 1900	Decl. 1900	m	Spec.	l	b	C_1			No.	E_1	m_0-M
							M	W	Mean			
41692	6h 1m6	− 4° 11′	5.37	B5	179°.2	−10°.4	−0.20	.....	−0 20	2	−0.03	7.2
41753	6 1.9	+14 47	4.40	B3s	162.5	− 1.2	− .22	.....	− .22	3	− .03	6.8
41756	6 1.9	− 3 20	6.75	B5	178.5	−10.0	− .14	.....	− .14	2	+ .03	8.1
41814	6 2.2	−11 10	6.38	*B5*	185.6	−13.5	− .18	.....	− .18	2	− .01	8.0
41943	6 2.9	+13 59	7.4:	B2	163.3	− 1.4	− .14	.....	− .14	2	+ .06	10.0
42051	6 3.5	− 6 31	9.0	*B3*	181.5	−11.1	.....	+0.01	+ .01	1	+ .20	9.8
42087	6 3.7	+23 8	5.76	B2s	155.4	+ 3.2	− .05	.....	− .05	4	+ .15	7.7
42088	6 3.7	+20 31	7.40	O6	157.7	+ 1.9	− .13	.....	− .13	3	+ .10	11.2
42352	6 5.1	+13 40	6.67	B3	163.9	− 1.1	− .12	.....	− .12	3	+ .07	8.4
42379	6 5.3	+21 36	7.6	*B2*	157.0	+ 2.8	.00	.....	.00	3	+ .20	9.2
42400	6 5.4	+20 56	6.86	B8s	157.6	+ 2.5	− .03	.....	− .03	2	+ .10	7.0
42545	6 6.2	+16 9	4.92	B3n	161.8	+ 0.3	− .20	.....	− .20	2	− .01	7.2
42560	6 6.3	+14 14	4.35	B3nn	163.5	− 0.6	− .20	.....	− .20	2	− .01	6.6
E253214	6 6.4	+20 7	9.4	Bone	158.4	+ 2.3	− .02	+ .04	+ .02	2, 1	+ .24	11.6
42597	6 6.5	+ 7 26	6.91	B2	169.5	− 3.8	− .17	.....	− .17	1	+ .03	9.7
42655	6 6.8	+10 22	7.43	B5	167.0	− 2.3	− .14	.....	− .14	2	+ .03	8.8
42690	6 7.0	− 6 31	5.09	B3s	181.9	−10.3	− .20	.....	− .20	2	− .01	7.4
43078	6 9.2	+22 20	8.9	*Bo*	156.7	+ 4.0	.00	+ .05	+ .03	2, 1	+ .25	11.0
43112	6 9.4	+13 53	5.81	B2s	164.2	− 0.1	− .27	.....	− .27	5	− .07	9.3
43285	6 10.3	+ 6 6	5.95	B5ne	171.1	− 3.6	− .18	.....	− .18	2	− .01	7.6
43286	6 10.3	+ 3 59	7.4:	B6	173.0	− 4.6	− .20	.....	− .20	2	− .04	9.1
43301	6 10.4	+ 0 51	7.19	B5nn	175.8	− 6.1	− .16	.....	− .16	2	+ .01	8.7
43317	6 10.5	+ 4 19	6.44	B5	172.7	− 4.1	− .16	.....	− .16	2	+ .01	8.0
43384	6 10.8	+23 46	6.26	cB3	155.7	+ 5.0	+ .01	.....	+ .01	2	+ .20	10.4
43703	6 12.6	+23 3	8.9	*B2*	156.5	+ 5.0	+ .03	+ .04	+ .04	4, 2	+ .24	10.2
43753	6 12.9	+23 2	8.1	*B1*	156.7	+ 5.0	.00	− .04	− .03	2, 2	+ .18	10.4
43818	6 13.2	+23 30	7.03	Bos	156.2	+ 5.3	.00	.....	.00	4	+ .22	9.4
43836	6 13.3	+23 19	7.03	B0	156.3	+ 5.3	+ .11	.....	+ .11	2	+ .23	5.8
44112	6 14.9	− 7 47	5.13	B3	184.0	− 9.2	− .19	.....	− .19	3	.00	7.3
44172	6 15.3	+14 45	7.29	B5	164.1	+ 1.6	− .18	.....	− .18	2	− .01	9.0
44173	6 15.3	+11 47	6.43	B5n	166.7	− 0.2	− .16	.....	− .16	2	+ .01	8.0
44458	6 16.8	−11 44	5.49	B2ne	187.8	−10.6	− .09	.....	− .09	3	+ .11	7.7
44637	6 17.7	+15 9	8.1	B3e	164.0	+ 2.3	.....	.00	.00	1	+ .19	9.0
44700	6 18.0	+ 3 49	6.25	B3s	174.0	− 3.0	− .17	.....	− .17	2	+ .02	8.3
44701	6 18.0	− 3 14	6.58	B5n	180.3	− 6.4	− .16	.....	− .16	2	+ .01	8.1
44743	6 18.3	−17 54	1.99	cB1	193.6	−12.9	.....	− .18	− .18	1	+ .03	7.3
45166	6 20.8	+ 8 3	9.7	O	170.7	− 0.4	.....	− .15	− .15	2	+ .08	13.6
45314	6 21.6	+14 57	7.09	B2ne	164.6	+ 3.1	− .06	.....	− .06	3	+ .14	9.1
45321	6 21.6	− 4 32	6.07	B3	181.9	− 6.2	− .16	.....	− .16	2	+ .03	8.1
45418	6 22.1	− 4 17	6.88	B5n	181.7	− 6.0	− .16	.....	− .16	2	+ .01	8.4
45542	6 23.0	+20 17	4.06	B5ne	160.1	+ 5.8	− .17	.....	− .17	2	.00	5.7
45546	6 23.0	− 4 42	4.98	B3	182.2	− 5.9	− .19	.....	− .19	2	.00	7.2
45677	6 23.7	−13 0	7.46	Bep	189.7	− 9.6	− .10	.....	− .10	2	+ .09	.....
45725	6 24.0	− 6 58	4.73	B3ne	184.3	− 6.8	− .18	.....	− .18	2	+ .01	6.9
45827	6 24.6	+ 9 6	6.48	B8±	170.2	+ 0.9	− .07	.....	− .07	2	+ .06	6.9
45910	6 25.2	+ 5 57	6.70	Beq	173.1	− 0.5	.00	.....	.00	2	+ .19	.....
45995	6 25.6	+11 19	5.83	B2ne	168.3	+ 2.2	− .16	.....	− .16	2	+ .04	8.6
46056	6 26.0	+ 4 54	7.96	O8	174.0	− 0.8	− .04	− .07	− .06	3, 1	+ .17	11.3
46064	6 26.0	−13 5	6.09	*B3*	190.0	− 9.1	− .16	.....	− .16	2	+ .03	8.1
46106	6 26.3	+ 5 5	8.06	Bo	173.9	− 0.6	.00	.....	.00	1	+ .22	10.4
46149	6 26.6	+ 5 6	7.66	O8	173.9	− 0.6	− .09	.....	− .09	3	+ .14	11.2
46150	6 26.6	+ 5 0	6.80	O6	174.0	− 0.6	− .04	.....	− .04	2	+ .19	10.0
46185	6 26.8	−12 30	6.76	*B5*	189.6	− 8.7	− .18	.....	− .18	2	− .01	8.4
46202	6 26.9	+ 5 3	8.16	*B2*	174.0	− 0.5	.....	− .10	− .10	2	+ .10	10.5
46223	6 27.0	+ 4 53	7.14	O8	174.2	− 0.6	− .04	.....	− .04	2	+ .19	10.3
46300	6 27.5	+ 7 24	4.50	cAo	172.0	+ 0.7	− .13	.....	− .13	3	− .03	10.2
46328	6 27.6	−23 21	4.35	B1s	199.6	−13.3	.....	− .21	− .21	1	.00	8.0
E259431	6 27.6	+10 24	8.9	B2e	169.4	+ 2.2	− .11	.....	− .11	3	+ .09	11.3
46380	6 27.9	− 7 26	8.3	*B2*	185.2	− 6.1	− .03	+0.01	.00	1, 1	+ .20	9.9
E259597*	6 28.1	+ 8 24	8.6	B(o)ne	171.2	+ 1.3	−0.16	.....	−0.16	1	+0.06	12.1

TABLE 3—*Continued*

HD	R.A. 1900	Decl. 1900	m	Spec.	l	b	C_1			No.	E_1	m_0-M
							M	W	Mean			
46485	6h28m6	+ 4°36′	8.4	*B2*	174°6	− 0°6	+0.02	−0.01	0.00	2, 1	+0.20	10.0
46487	6 28.6	− 1 9	5.02	B3n	179.7	− 3.1	− .19	.....	− .19	2	.00	7.2
46573	6 29.1	+ 2 36	8.5	*B2*	176.4	− 1.2	− .02	.....	− .02	2	+ .18	10.2
46769	6 30.1	+ 0 58	5.69	B3s	178.0	− 1.7	− .12	.....	− .12	2	+ .07	7.4
46883	6 30.7	+10 22	8.1	*B2*	169.8	+ 2.8	+ .05	.....	+ .05	3	+ .25	9.3
46966	6 31.1	+ 6 10	7.3:	O8	173.5	+ 0.9	− .16	.....	− .16	2	+ .07	11.3
47032	6 31.5	+ 4 46	8.70	*B2*	174.8	+ 0.4	+ .04	+ .06	+ .05	4, 1	+ .25	10.0
47129	6 32.0	+ 6 13	6.06	O8e	173.6	+ 1.2	− .12	.....	− .12	2	+ .11	9.8
47240	6 32.5	+ 5 3	6.16	B1	174.7	+ 0.7	− .06	.....	− .06	3	+ .15	8.7
47299	6 32.8	− 8 34	8.4	*B3*	186.7	− 5.6	.....	− .14	− .14	1	+ .05	10.2
47395	6 33.3	+28 21	5.84	*B8*	153.9	+11.5	− .16	.....	− .16	2	− .03	6.8
47398*	6 33.3	+ 4 44	8.35	*B2*	175.0	+ 0.7	− .13	.....	− .13	1	+ .07	10.9
47417	6 33.4	+ 7 0	7.4:	B2	173.0	+ 1.8	− .10	.....	− .10	2	+ .10	9.7
47431	6 33.5	+ 4 47	6.55	*B9*	175.0	+ 0.8	.....	− .16	− .16	1	− .04	7.2
47432	6 33.5	+ 1 42	6.13	B0	177.7	− 0.6	− .05	.....	− .05	2	+ .17	8.8
47761	6 35.1	− 4 36	8.4	*Bo*	183.5	− 3.2	.....	− .06	− .06	2	+ .16	11.2
47839	6 35.5	+ 9 59	4.68	O7s	170.7	+ 3.7	− .25	.....	− .25	3	− .02	9.3
47887	6 35.7	+ 9 34	7.02	B2	171.0	+ 3.5	− .21	.....	− .21	3	− .01	10.1
47961	6 36.0	+ 9 57	7.27	B5s	170.7	+ 3.8	− .15	.....	− .15	3	+ .02	8.7
48038	6 36.3	−12 5	6.78	*B3*	190.3	− 6.4	− .08	.....	− .08	2	+ .11	8.2
48099	6 36.6	+ 6 27	6.20	O7	173.9	+ 2.3	− .18	.....	− .18	2	+ .05	10.3
48215	6 37.2	− 6 1	6.88	B5	185.0	− 3.4	− .24	.....	− .24	2	− .07	9.0
48279	6 37.5	+ 1 49	7.4	O8	178.1	+ 0.3	− .02	.....	− .02	3	+ .21	10.4
48434	6 38.3	+ 4 2	5.78	Bo	176.2	+ 1.5	− .15	.....	− .15	2	+ .07	9.2
48532	6 38.8	+20 6	8.60	*B3*	162.0	+ 9.0	.....	− .15	− .15	1	+ .04	10.5
48879	6 40.5	+67 41	5.04	B3	114.9	+25.8	− .18	.....	− .18	2	+ .01	7.2
48914	6 40.7	+ 2 37	7.5:	B5	177.8	+ 1.4	− .16	.....	− .16	2	+ .01	9.0
48977	6 41.1	+ 8 42	5.84	B3	172.4	+ 4.3	− .21	.....	− .21	3	− .02	8.2
49340	6 42.9	+69 0	5.13	B7	113.6	+26.2	− .16	.....	− .16	2	− .02	6.4
49567	6 43.9	+ 1 6	6.06	B3	179.4	+ 1.4	− .19	.....	− .19	2	.00	8.3
49787	6 45.0	− 5 24	7.30	B3e	185.4	− 1.4	− .14	.....	− .14	2	+ .05	9.2
49888	6 45.5	−12 29	7.4:	*B5*	191.7	− 4.0	− .22	.....	− .22	3	− .05	9.4
49977	6 45.9	−14 0	8.1	B2ne	193.1	− 5.2	− .05	.....	− .05	3	+ .15	10.1
50083	6 46.5	+ 5 13	6.76	B2e	176.1	+ 3.9	− .11	.....	− .11	2	+ .09	9.1
50091	6 46.5	−13 7	8.6	*B2*	192.4	− 4.7	− .13	.....	− .13	3	+ .07	11.1
50463	6 48.3	−16 6	6.99	*B5*	195.2	− 5.7	.....	− .14	− .14	2	+ .03	8.4
50707	6 49.2	−20 6	4.66	B0s	198.9	− 7.4	.....	− .20	− .20	1	+ .02	8.4
50820*	6 49.7	− 1 38	6.25	B3+Fn	182.6	+ 1.4	+ .15	.....	+ .15	2	(+ .34)	.....
51354	6 51.9	+18 2	7.13	B3ne	165.2	+10.9	− .22	.....	− .22	2	− .03	9.5
51480	6 52.4	−10 41	6.97	B8eq	190.9	− 2.3	+ .02	.....	+ .02	2	+ .15	6.7
51560	6 52.7	+37 14	7.30	B9n	147.1	+18.8	− .10	.....	− .10	2	+ .02	7.6
52266	6 55.4	− 5 40	6.97	B2n	186.8	+ 0.7	− .16	.....	− .16	2	+ .04	9.7
52382	6 55.9	− 9 4	6.36	B2	189.9	− 0.8	− .05	.....	− .05	2	+ .15	8.3
52559	6 56.6	+ 5 42	6.46	B2s	176.9	+ 6.3	− .12	.....	− .12	2	+ .08	8.9
52721	6 57.2	−11 9	6.57	B3e	191.9	− 1.5	− .06	.....	− .06	2	+ .13	7.9
52812	6 57.5	−27 5	6.66	*Bo*	206.0	− 8.8	.....	− .20	− .20	1	+ .02	10.4
52918	6 57.9	− 4 6	4.89	B3n	185.7	+ 2.0	− .20	.....	− .20	6	− .01	7.2
53179*	6 59.0	−11 24	9.1	Beq	192.3	− 1.1	.....	+ .24	+ .24	2	.....	.....
53367	6 59.7	−10 18	7.01	B1ne	191.4	− 0.6	+ .06	.....	+ .06	2	+ .27	8.7
53428	6 59.9	− 8 42	8.6	*B2*	190.0	+ 0.3	+ .04	.....	+ .04	2	+ .24	9.9
53456	7 0.0	−11 23	7.4	B5	192.4	− 1.0	− .11	.....	− .11	1	+ .06	8.6
53667	7 0.8	− 8 34	7.7	O8	190.0	+ 0.5	.....	− .06	− .06	2	+ .17	11.0
53974	7 2.0	−11 8	5.28	B2n	192.4	− 0.4	− .12	.....	− .12	2	+ .08	7.7
53975	7 2.0	−12 14	6.40	*B5p*	193.4	− 1.0	− .19	.....	− .19	2	− .02	8.1
54662	7 4.6	−10 11	6.20	O7	191.9	+ 0.6	− .15	.....	− .15	3	+ .08	10.1
55135	7 6.6	−10 16	7.16	B4ne	192.2	+ 1.0	− .11	.....	− .11	1	+ .07	8.6
55538	7 8.2	−15 19	7.8	Bo	196.8	− 1.1	− .10	− .18	− .15	3, 2	+ .07	11.2
55879	7 9.7	−10 8	5.99	O9s	192.4	+ 1.6	−0.23	.....	− .23	2	.00	10.5
55885	7 9.7	−15 13	9.4	Bo:	196.9	− 0.8	.....	− .06	− .06	2	+ .16	12.2
56806	7 13.4	−18 39	9.4	Be	200.3	− 1.6	.....	−0.08	−0.08	2	+0.11	.....

TABLE 3—*Continued*

HD	R.A. 1900	Decl. 1900	m	Spec.	l	b	C_1			No.	E_2	m_0-M
							M	W	Mean			
56847	7^h13^m6	−15° 27′	8.9	Bo	197°.5	0°.0	+0.02	−0.06	−0.03	2, 2	+0.19	11.5
57060	7 14.5	−24 23	4.90	O7f	205.4	− 4.2	.....	− .23	− .23	1	.00	9.4
57061	7 14.5	−24 47	4.40	O9	205.8	− 4.3	.....	− .25	− .25	1	− .02	9.0
57291	7 15.5	+ 3 46	6.84	B5	180.8	+ 9.6	− .18	.....	− .18	2	− .01	8.5
57539	7 16.6	− 5 43	6.59	b8n	189.4	+ 5.3	− .12	.....	− .12	2	+ .01	7.3
57682	7 17.2	− 8 48	6.17	O9s	193.0	+ 4.0	− .20	.....	− .20	2	+ .03	10.5
58050	7 18.8	+15 43	6.37	B3e	170.3	+15.7	− .19	.....	− .19	3	.00	8.6
58343	7 20.1	−16 0	5.20	B3e	198.8	+ 1.0	− .14	.....	− .14	1	+ .05	7.0
58416	7 20.4	−20 31	9.3	*B2*	202.7	− 1.1	.....	− .13	− .13	2	+ .07	11.8
58510	7 20.8	−20 59	6.73	*B2*	203.2	− 1.3	.....	− .10	− .10	2	+ .10	9.0
58784	7 22.0	+ 2 40	8.5	*B2*	182.6	+10.5	− .18	− .13	− .15	2, 2	+ .05	11.1
58978	7 22.8	−22 53	5.48	B2ne	205.1	− 1.8	.....	− .22	− .22	2	− .02	8.6
59114	7 23.4	−15 11	9.40	Bo	198.5	+ 2.1	.....	+ .06	+ .06	2	+ .28	11.3
59211	7 23.8	− 9 50	6.62	B5	193.9	+ 4.9	− .16	.....	− .16	2	+ .01	8.2
MWC180	7 24.5	−13 34	8.8	B2ne	197.2	+ 3.2	− .18	.....	− .18	3	+ .02	11.7
59543	7 25.3	−13 46	6.94	*B5*	197.5	+ 3.2	− .09	.....	− .09	2	+ .08	8.0
59864	7 26.8	−33 53	7.44	*Bo*	215.1	− 6.5	.....	− .14	− .14	1	+ .08	10.8
59882	7 26.9	− 5 21	8.5	*B3*	190.3	+ 7.7	.....	− .17	− .17	2	+ .02	10.6
60308	7 28.7	−15 14	8.30	*B*	199.1	+ 3.2	.....	+ .05	+ .05	2	+ .24	.....
60325	7 28.8	−14 7	6.24	*B5*	198.2	+ 3.8	− .14	.....	− .14	2	+ .03	7.6
60848	7 31.4	+17 7	7.2	O7ne	170.3	+19.0	− .22	.....	− .22	4	+ .01	11.6
60855	7 31.4	−14 16	5.57	*B5*	198.6	+ 4.3	− .16	.....	− .16	2	+ .01	7.1
61006	7 32.0	−33 10	7.12	*B2*	215.0	− 5.2	.....	− .18	− .18	1	+ .02	10.0
61347	7 33.7	−13 38	8.6	*B2*	198.4	+ 5.1	− .08	.....	− .08	2	+ .12	10.8
61709	7 35.5	−31 4	8.3	*B1*	213.6	− 3.5	.....	− .04	− .04	2	+ .17	10.7
61827	7 36.0	−32 20	7.52	*Oe5*	214.7	− 4.0	.....	+ .15	+ .15	1	+ .38	9.4
62150	7 37.4	−32 24	7.7	O6	214.9	− 3.9	.....	+ .07	+ .07	1	+ .30	10.1
62844	7 40.8	−32 0	8.2	*Bo*	215.0	− 3.0	.....	+ .18	+ .18	2	+ .40	9.3
63005	7 41.6	−26 15	9.0	*Bo*	210.1	+ 0.2	.....	− .16	− .16	2	+ .06	12.5
63462	7 43.9	−25 42	4.59	B3e	210.0	+ 0.9	.....	− .18	− .18	1	+ .01	6.7
64399	7 48.6	−24 51	8.3	*B2*	209.8	+ 2.2	.....	− .18	− .18	2	+ .02	11.2
64993	7 51.4	−23 48	7.5	*Bo*	209.3	+ 3.3	.....	− .14	− .14	2	+ .08	10.8
65041	7 51.7	+43 47	7.04	B3	143.6	+31.4	− .21	.....	− .21	1	− .02	9.4
65307	7 53.0	− 8 34	9.4	*B3*	196.4	+11.7	.....	− .21	− .21	1	− .02	11.7
65719	7 54.9	−25 0	9.35	*B2*	210.7	+ 3.3	.....	− .08	− .08	1	+ .12	11.5
65875	7 55.8	− 2 36	6.43	B2e	191.5	+15.4	− .20	.....	− .20	4	.00	9.4
65886	7 55.8	−25 48	9.5	*B*	211.5	+ 3.1	.....	− .07	− .07	1	+ .12	.....
66594	7 59.2	− 4 32	7.38	*B5*	193.7	+15.1	− .19	.....	− .19	2	− .02	9.1
66665	7 59.5	+ 6 29	7.6	B3	183.6	+20.6	.....	− .21	− .21	1	− .02	9.9
67880	8 4.9	−15 57	5.54	B3	204.4	+10.3	− .15	.....	− .15	2	+ .04	7.5
68761	8 8.7	−36 41	6.66	*Bo*	222.0	− 0.7	.....	− .13	− .13	1	+ .09	9.9
69106	8 10.3	−36 38	6.92	O9	222.2	− 0.5	.....	− .16	− .16	1	+ .07	10.9
71518	8 22.8	−14 36	6.55	*B5*	205.7	+14.6	− .16	.....	− .16	2	+ .01	8.1
73882	8 35.5	−40 4	7.15	O9	228.0	+ 1.4	.....	+ .08	+ .08	1	+ .31	9.5
74280	8 38.0	+ 3 46	4.32	B3n	191.2	+27.7	− .23	.....	− .23	4	− .06	6.3
74575	8 39.6	−32 50	3.70	B1	222.8	+ 6.6	.....	− .20	− .20	1	+ .01	7.2
76510	8 51.5	−13 31	8.0	*Bo*	209.1	+20.9	− .23	.....	− .23	2, 1	− .01	12.0
77581	8 58.3	−40 10	6.75	*Bo*	230.9	+ 4.6	.....	+ .10	+ .10	1	+ .32	8.4
77770	8 59.5	+50 1	7.52	*B5*	136.3	+43.2	− .24	.....	− .24	1	− .07	9.6
78584	9 4.0	+79 42	8.05	*B3*	100.0	+33.7	.....	− .17	− .17	1	+ .02	10.1
80081	9 12.6	+37 14	3.82	B0n	154.2	+45.9	− .08	.....	− .08	2	+ .04	3.9
80852	9 17.0	−31 51	8.7	*Bo*	227.5	+13.1	.....	− .13	− .13	3	+ .09	12.0
83754	9 35.5	−13 53	4.96	B3	217.0	+28.8	− .18	.....	− .18	3	+ .01	7.1
83953	9 36.7	−23 8	4.74	B3ne	224.5	+22.4	.....	− .18	− .18	2	+ .01	6.9
84567	9 41.0	−29 45	6.50	*B2*	230.0	+18.2	.....	−0.18	− .18	2	+ .02	9.4
87015	9 57.2	+22 26	5.59	B3n	179.3	+52.9	− .19	.....	− .19	3	.00	7.8
87737	10 1.9	+17 15	3.58	B8s	187.9	+52.2	− .15	.....	− .15	3	− .02	4.5
89688	10 15.9	+ 2 47	6.53	B3nn	209.8	+47.4	− .15	.....	− .15	3	+ .04	8.4
90994	10 25.2	− 0 8	4.95	B8	215.3	+47.2	− .17	.....	− .17	4	− .04	6.0
91316	10 27.5	+ 9 49	3.85	cB1	203.7	+54.0	−0.20	.....	−0.20	4	+0.01	9.3

TABLE 3—*Continued*

HD	R.A. 1900	Decl. 1900	m	Spec.	l	b	C_1 M	C_1 W	C_1 Mean	No.	E_1	m_0-M
93152	10h40m3	+31° 13′	5.37	B9n	165°6	+63°9	−0.15	.....	−0.15	2	−0.03	6.0
93521	10 42.7	+38 6	6.89	B3nn	150.1	+63.6	− .26	.....	− .26	2	− .07	9.6
97991	11 11.1	− 2 55	7.28	B2	231.8	+52.4	− .17	.....	− .17	2	+ .03	10.1
100600*	11 29.5	+17 21	6.0	B4n	209.6	+70.6	− .20	.....	− .20	2	− .02	8.0
109387	12 29.2	+70 20	3.88	B5e	91.3	+47.6	− .18	.....	− .18	3	− .01	5.6
113797	13 1.1	+36 20	5.11	B9n	63.1	+80.5	− .12	.....	− .12	2	.00	5.5
116658	13 19.9	−10 38	1.21	B2	285.4	+50.2	− .23	.....	− .23	2	− .03	4.4
120315	13 43 6	+49 49	1.91	B5nn	65.2	+65.0	− .23	.....	− .23	3	− .06	3.9
123884	14 5.1	−17 31	9.2	*B2*	296.9	+40.0	.....	−0.10	− .10	3	+ .10	11.5
129956	14 40.4	+ 1 9	5.54	B9	322.2	+50.6	− .12	.....	− .12	2	.00	5.9
138764	15 29.0	− 8 51	5.15	B8s	324.2	+35.0	− .14	.....	− .14	6	− .01	6.0
139892	15 35.6	+36 58	5.07	B8n	25.2	+52.2	− .18	.....	− .18	2	− .05	6.2
142983*	15 52.6	−13 59	4.68	Apea	324.4	+27.3	− .14	.....	− .14	4	.....	.....
143018	15 52.8	−25 50	3.00	B3n	315.2	+19.0	.....	− .24	− .24	2	− .05	5.6
143275	15 54.4	−22 20	2.54	B1n	318.1	+21.2	.....	− .21	− .21	2	.00	6.1
144206	15 59.6	+46 19	4.64	B9	39.1	+47.1	− .18	.....	− .18	2	− .06	5.5
144217	15 59.6	−19 32	2.90	B1	321.2	+22.3	.....	− .20	− .20	2	+ .01	6.4
144218	15 59.6	−19 32	5.06	B2	321.2	+22.3	.....	− .14	− .14	2	+ .06	7.6
144470	16 1.0	−20 24	4.13	B2n	320.7	+21.4	.....	− .17	− .17	4	+ .03	6.9
145502	16 6.2	−19 12	4.29	B3n	322.6	+21.3	.....	− .12	− .12	3	+ .07	6.0
147165	16 15.1	−25 21	3.08	B1	319.2	+15.7	.....	− .10	− .10	3	+ .11	5.9
147394	16 16.7	+46 33	3.91	B5	39.0	+44.1	− .20	.....	− .20	3	− .03	5.7
147888	16 19.4	−23 14	6.56	B3±	321.5	+16.4	.....	+ .01	+ .01	1	+ .20	7.4
147889	16 19.4	−24 14	8.0	B3	320.8	+15.7	.....	+ .31	+ .31	1	+ .50	6.7
147933*	16 19.6	−23 13	5.22	B3n	321.6	+16.3	.....	− .04	− .04	1	+ .15	6.4
148184	16 21.2	−18 14	4.85	B3e	325.8	+19.3	.....	− .02	− .02	3	+ .17	5.9
148546	16 23.7	−37 46	7.58	*Bo*	311.2	+ 5.9	.....	− .02	− .02	2	+ .20	10.1
148605	16 24.1	−24 54	4.87	*B3*	321.0	+14.5	.....	− .21	− .21	1	− .02	7.2
149363	16 29.1	− 5 56	7.9	O9	337.7	+25.2	− .12	− .15	− .14	2, 1	+ .09	11.8
149438	16 29.7	−28 1	2.91	Bo	319.4	+11.4	.....	− .26	− .26	2	− .04	7.1
149757	16 31.7	−10 22	2.70	Bonn	334.1	+22.1	− .13	.....	− .13	6	+ .09	6.0
149881	16 32.4	+14 40	6.59	B1	358.9	+34.8	− .19	.....	− .19	4	+ .02	10.0
150475	16 36.1	−37 39	8.6	*B2*	312.9	+ 4.2	.....	+ .01	+ .01	1	+ .21	10.1
151397	16 42.0	−39 36	9.5	*B2*	312.1	+ 2.0	.....	+ .01	+ .01	1	+ .21	11.0
151985	16 45.6	−37 51	3.64	B2	313.9	+ 2.6	.....	− .20	− .20	1	.00	6.6
152516	16 48.7	−21 43	8.08	*B5*	327.2	+12.1	.....	− .07	− .07	1	+ .10	9.0
153426	16 54.4	−38 3	7.58	*B2*	314.9	+ 1.1	.....	− .05	− .05	1	+ .15	9.5
153855	16 56.8	−31 28	6.88	*B2*	320.4	+ 4.7	.....	− .13	− .13	1	+ .07	9.4
153977	16 57.6	−24 41	9.8	*B3*	326.0	+ 8.7	.....	− .10	− .10	1	+ .09	11.4
154040	16 57.9	−39 11	9.5	*B2*	314.4	− 0.1	.....	+ .27	+ .27	1	+ .47	9.2
154090	16 58.2	−33 59	4.87	cB1ea	318.6	+ 3.0	.....	− .01	− .01	1	+ .20	9.0
154204	16 58.9	−20 21	6.17	*B3*	329.7	+11.0	.....	− .12	− .12	2	+ .07	7.9
154445	17 0.4	− 6 45	5.62	B3	347.0	+21.4	− .11	.....	− .11	4	+ .08	7.3
154450	17 0.4	−35 37	8.7	Boe	317.5	+ 1.8	.....	+ .04	+ .04	2	+ .26	10.8
154911	17 3.2	−38 30	9.2	*Bo*	315.5	− 0.5	.....	+ .02	+ .02	2	+ .24	11.4
155336	17 5.8	−32 58	9.4	*B2*	320.3	+ 2.3	.....	+ .09	+ .09	1	+ .29	10.4
155851	17 9.0	−32 34	8.1	Bone	321.0	+ 2.0	.....	− .10	− .10	2	+ .12	11.2
156110	17 10.6	+45 30	7.44	B3	37.8	+34.8	− .18	.....	− .18	2	+ .01	9.6
156134	17 10.7	−35 27	8.3	*B2*	318.9	+ 0.1	.....	+ .12	+ .12	1	+ .32	9.1
156154	17 10.8	−35 25	8.3	*Bo*	318.9	− 0.1	.....	+ .11	+ .11	2	+ .33	9.9
156201	17 11.1	−35 7	7.77	*Bo*	319.2	− 0.2	.....	+ .16	+ .16	2	+ .38	9.0
156247*	17 11.4	+ 1 19	6.0	B5	350.4	+20.1	− .09	.....	− .09	3	+ .08	7.0
156633*	17 13.6	+33 12	4.8	B3	23.5	+31.9	−0.20	.....	− .20	5	− .01	7.1
156779	17 14.4	−18 43	9.3	*B5*	333.2	+ 8.9	.....	− .08	− .08	1	+ .09	10.3
157056	17 15.9	−24 54	3.37	B2	328.2	+ 5.1	.....	− .28	− .28	2	− .08	6.9
157857	17 20.7	−10 55	7.43	O7	340.7	+11.7	.....	− .12	− .12	1	+ .11	11.2
158319	17 23.5	−16 31	8.7	B5ne	336.3	+ 8.3	.....	− .12	− .12	1	+ .05	9.9
158661	17 25.4	−17 3	8.2	*Bo*	336.1	+ 7.6	.....	− .06	− .06	3	+ .16	11.0
158705	17 25.6	−31 28	7.81	Bo	323.9	− 0.3	.....	+ .22	+ .22	2	+ .44	8.6
159176	17 28.1	−32 31	5.71	O8	323.3	− 1.3	.....	−0.10	−0.10	1	+0.13	9.3

TABLE 3—*Continued*

HD	R.A. 1900	Decl. 1900	m	Spec.	l	b	C_1 M	C_1 W	C_1 Mean	No.	E_1	m_0-M
159864	17h31m8	−17° 46′	8.6	*Bo*	336°.3	+ 5°.9	.....	−0.02	−0.02	3	+0.20	11.1
160186	17 33.4	−18 21	9.0	*B5*	336.0	+ 5.3	.....	− .09	− .09	1	+ .08	10.0
160529	17 35.3	−33 27	6.68	cA4ea	323.4	− 3.1	.....	+ .47	+ .47	1	+ .46	9.0
160641	17 36.0	−17 51	9.8	*B*	336.7	+ 5.0	.....	− .11	− .11	2	+ .08	.....
160704	17 36.3	−23 41	9.5	*B2*	331.8	+ 1.9	.....	+ .22	+ .22	4	+ .42	9.6
160730	17 36.4	−24 15	10.2	*B*	331.3	+ 1.6	.....	+ .21	+ .21	3	+ .40	.....
160762	17 36.6	+46 4	3.79	B3s	39.3	+30.4	−0.20	.....	− .20	4	− .01	6.1
160886	17 37.3	−18 16	9.7	*B5*	336.5	+ 4.5	.....	− .07	− .07	1	+ .10	10.6
161056	17 38.3	− 7 2	6.20	B5n	346.4	+10.1	+ .06	+ .03	+ .05	3, 1	+ .22	6.3
161103	17 38.5	−27 12	8.5	Bone	329.0	+ 0.4	.....	+ .04	+ .04	2	+ .26	10.6
161306	17 39.7	− 9 46	8.31	B(o)ne	344.1	+ 8.5	+ .13	.....	+ .13	5	+ .35	9.8
161789	17 42.4	−32 52	9.0	*B2*	324.6	− 4.0	.....	+ .08	+ .08	1	+ .28	10.0
161961	17 43.4	− 2 9	7.9	Bo	351.3	+11.4	− .06	− .02	− .04	4, 1	+ .18	10.5
162064	17 44.0	−19 52	8.98	*B*	336.0	+ 2.4	.....	+ .16	+ .16	1	+ .35	.....
162094	17 44.2	+34 19	6.57	B3	26.7	+26.1	− .19	.....	− .19	2	.00	8.8
162168	17 44.5	−32 58	8.6	*Bo*	324.8	− 4.5	.....	+ .15	+ .15	1	+ .37	9.9
162365	17 45.6	+15 32	8.0	*B5*	8.0	+19.1	− .17	.....	− .17	2	.00	9.6
162717	17 47.3	−24 15	9.3	*B3*	332.6	− 0.5	.....	+ .17	+ .17	1	+ .36	9.0
162718	17 47.3	−24 45	8.7	Bone	332.2	− 0.8	.....	+ .20	+ .20	4	+ .42	9.7
162978	17 48.7	−24 52	6.13	Bo	332.2	− 1.1	.....	− .14	− .14	5	+ .08	9.5
163472	17 51.2	+ 0 42	5.73	B2	354.9	+11.1	− .08	.....	− .08	5	+ .12	7.9
163535	17 51.5	−18 3	9.1	*B5*	338.4	+ 1.8	.....	+ .11	+ .11	1	+ .28	8.7
163667	17 52.2	−31 47	8.8	*Bo*	326.6	− 5.3	.....	+ .02	+ .02	1	+ .24	11.0
163777	17 52.8	−25 10	9.5:	*B*	332.4	− 2.1	.....	+ .07	+ .07	1	+ .26	.....
163800	17 52.9	−22 30	6.92	*Bo*	334.8	− 0.8	.....	.00	.00	4	+ .22	9.3
163811	17 53.0	−23 18	8.3:	*B5*	334.1	− 1.2	.....	− .05	− .05	1	+ .12	9.1
163892	17 53.4	−22 27	7.14	*B2*	334.9	− 0.8	.....	− .04	− .04	3	+ .16	9.0
164002	17 53.9	−22 33	7.15	*B5*	334.8	− 1.0	.....	− .13	− .13	2	+ .04	8.5
164018	17 54.0	−23 7	9.4	*B*	334.3	− 1.3	.....	+ .19	+ .19	2	+ .38	.....
164019	17 54.0	−28 36	9.4	*Bo*	329.6	− 4.0	.....	− .08	− .08	1	+ .14	12.3
164103	17 54.5	−14 47	8.04	*B5*	341.6	+ 2.8	+ .07	.....	+ .07	2	+ .24	8.0
164105	17 54.5	−24 39	9.2:	*B3*	333.1	− 2.2	.....	− .06	− .06	1	+ .13	10.5
164146	17 54.7	−24 12	8.3:	*B5*	333.5	− 2.0	.....	− .11	− .11	1	+ .06	9.5
164188	17 54.9	−15 48	8.7	*B3*	340.8	+ 2.2	+ .05	.....	+ .05	2	+ .24	9.2
164284	17 55.3	+ 4 23	4.81	B5ne	358.6	+11.9	− .14	.....	− .14	4	+ .03	6.2
164353	17 55.6	+ 2 56	3.92	cB3	357.4	+11.2	− .12	.....	− .12	6	+ .07	8.9
164359	17 55.6	−22 7	7.4	cB7	335.4	− 1.1	.....	− .10	− .10	3	+ .04	12.6
164384	17 55.7	−23 10	8.4	*B5*	334.5	− 1.7	.....	− .14	− .14	1	+ .03	9.8
164402	17 55.8	−22 46	5.73	Bo	334.9	− 1.5	.....	− .14	− .14	5	+ .08	9.1
164432	17 56.0	+ 6 16	6.18	B3s	0.4	+12.6	− .14	.....	− .14	5	+ .05	8.0
164438	17 56.0	−19 6	7.28	*B3*	338.1	+ 0.3	.....	+ .02	+ .02	1	+ .21	8.0
164492	17 56.3	−23 1	6.91	O7	334.7	− 1.7	.....	+ .03	+ .03	1	+ .26	9.6
164536	17 56.5	−24 15	6.87	*B3*	333.7	− 2.3	.....	− .16	− .16	2	+ .03	8.9
164637	17 57.0	−22 43	6.57	Bo	335.0	− 1.7	.....	− .16	− .16	4	+ .06	10.1
164700	17 57.3	−17 24	7.5	*B5*	339.7	+ 0.9	.....	− .07	− .07	1	+ .10	8.4
164703	17 57.3	−22 18	9.3	*B5*	335.4	− 1.5	.....	− .06	− .06	2	+ .11	10.1
164704	17 57.3	−22 53	7.65	*B5*	334.9	− 1.8	.....	− .13	− .13	2	+ .04	9.0
164717	17 57.4	−22 36	8.3	*B3*	335.2	− 1.7	.....	− .14	− .14	2	+ .05	10.1
164738	17 57.5	−17 36	7.10	*B5*	339.5	+ 0.8	.....	− .04	− .04	1	+ .13	7.8
164741	17 57.5	−25 19	9.1	*B1*	332.8	− 3.1	.....	+ .02	+ .02	3	+ .23	11.1
164794	17 57.7	−24 22	5.86	O5	333.7	− 2.6	.....	− .15	− .15	3	+ .08	9.8
164816	17 57.8	−24 19	7.1	*Bo*	333.7	− 2.6	.....	− .14	− .14	5	+ .08	10.4
164833	17 57.9	−22 50	6.86	*Bo*	335.0	− 1.9	.....	− .14	− .14	5	+ .08	10.2
164844	17 58.0	−22 34	8.0	*B5*	335.3	− 1.8	.....	− .16	− .16	2	+ .01	9.5
164852	17 58.1	+20 50	5.09	B5	14.3	+18.5	−0.15	.....	− .15	3	+ .02	6.6
164863	17 58.1	−22 30	8.4	*B*	335.4	− 1.8	.....	− .15	− .15	1	+ .04	.....
164865	17 58.1	−24 11	7.9	*B*	333.9	− 2.6	.....	+ .31	+ .31	1	+ .50	.....
164883	17 58.2	−22 30	7.1	*Bo*	335.4	− 1.8	.....	− .14	− .14	3	+ .08	10.4
164906*	17 58.3	−24 24	7.5	B(o)ne	333.7	− 2.8	.....	− .06	− .06	1	+ .16	10.3
164947*	17 58.5	−24 21	8.5	*B5*	333.8	− 2.8	.....	−0.11	−0.11	1	+0.06	9.7

TABLE 3—*Continued*

HD	R.A. 1900	Decl. 1900	m	Spec.	l	b	C_1			No.	E_1	m_0-M
							M	W	Mean			
164971	17h58m6	−23°28′	9.8	*B*	334°6	− 2°4	.....	+0.04	+0.04	1	+0.23	.....
164992*	17 58.7	−22 27	9.7	*B5*	335.5	− 1.9	.....	− .08	− .08	2	+ .09	10.7
165016	17 58.8	−24 41	7.60	*Bo*	333.5	− 3.0	.....	− .17	− .17	3	+ .05	11.1
165049	17 59.0	−15 22	8.07	*B*	341.7	+ 1.5	+0.10	+ .08	+ .09	3, 1	+ .28	.....
165052	17 59.0	−24 24	6.79	O6	333.8	− 2.9	.....	− .09	− .09	3	+ .14	10.3
165132	17 59.4	−23 43	8.0	*B3*	334.5	− 2.7	.....	− .11	− .11	1	+ .08	9.6
165174	17 59.6	+ 1 55	6.09	B2n	356.9	+ 9.8	− .12	.....	− .12	3	+ .08	8.5
165285	18 0.1	−19 58	8.73	B2ne	337.8	− 0.9	.....	+ .02	+ .02	2	+ .22	10.2
165287	18 0.1	−22 7	8.7	*B5*	335.9	− 2.0	.....	− .05	− .05	2	+ .12	9.5
165288	18 0.1	−22 28	9.1	*B5*	335.6	− 2.2	.....	− .08	− .08	2	+ .09	10.1
165319	18 0.3	−14 12	8.2	*Bo*	342.8	+ 1.9	+ .10	+ .12	+ .11	4, 2	+ .33	9.8
165320	18 0.3	−22 44	9.7	*B*	335.4	− 2.4	.....	− .10	− .10	2	+ .09	.....
165516	18 1.2	−21 27	6.22	Bo	336.6	− 1.9	.....	− .09	− .09	4	+ .13	9.2
165517	18 1.2	−25 7	8.55	*B*	333.4	− 3.7	.....	+ .12	+ .12	1	+ .31	.....
165595*	18 1.6	−22 7	8.4	*B*	336.1	− 2.3	.....	− .08	− .08	2	+ .11	.....
165612*	18 1.7	−22 54	7.7	*B3*	335.4	− 2.7	.....	− .10	− .10	2	+ .09	9.3
165655	18 1.9	−25 22	8.3	*B2*	333.3	− 4.0	.....	+ .01	+ .01	3	+ .21	9.8
165689	18 2.1	−22 17	7.9	*B5*	336.0	− 2.6	.....	− .12	− .12	2	+ .05	9.1
165765	18 2.5	−22 44	9.4	*B5*	335.7	− 2.8	.....	− .13	− .13	2	+ .04	10.7
165793	18 2.6	−36 41	6.58	*Bo*	323.4	− 9.5	.....	− .18	− .18	1	+ .04	10.2
165808	18 2.7	−16 26	7.4	B5	341.1	+ 0.2	.....	− .03	− .03	2	+ .14	8.0
165812	18 2.7	−22 10	7.89	*B5*	336.2	− 2.6	.....	− .12	− .12	2	+ .05	9.1
165857	18 2.9	−22 11	8.7	*B5*	336.2	− 2.6	.....	− .10	− .10	2	+ .07	9.8
165892	18 3.1	−21 25	9.2	*B*	336.9	− 2.3	.....	+ .10	+ .10	3	+ .29	.....
165921	18 3.2	−24 1	7.4	Bo	334.6	− 3.6	.....	− .08	− .08	4	+ .14	10.3
165998	18 3.5	−21 35	8.5	*B*	336.8	− 2.4	.....	+ .24	+ .24	2	+ .43	.....
166033	18 3.7	−23 40	8.2	*B*	335.0	− 3.5	.....	− .09	− .09	1	+ .10	.....
166056	18 3.8	−24 8	9.7	*B*	334.6	− 3.7	.....	+ .01	+ .01	1	+ .20	.....
166107	18 4.0	−23 48	7.64	*B5*	334.9	− 3.6	.....	− .11	− .11	1	+ .06	8.8
166125	18 4.1	−14 12	9.1	B4	343.3	+ 1.1	.....	+ .09	+ .09	1	+ .27	9.1
166182	18 4.4	+20 48	4.32	B2s	14.9	+17.1	− .20	.....	− .20	7	.00	7.3
166188	18 4.4	−18 13	9.0	B2e	339.8	− 1.0	.....	+ .09	+ .09	4	+ .29	10.0
166192	18 4.4	−23 56	8.3	*B5*	334.8	− 3.8	.....	− .03	− .03	1	+ .14	8.9
166286	18 4.8	−16 46	7.58	Bo:	341.1	− 0.4	.....	− .01	− .01	1	+ .21	10.0
166287	18 4.8	−16 50	7.6	Bo	341.1	− 0.4	.....	− .03	− .03	2	+ .19	10.2
166291	18 4.8	−19 12	9.0	*B3*	339.0	− 1.5	.....	− .01	− .01	2	+ .18	9.9
166304	18 4.9	−16 44	9.1	Bo	341.2	− 0.4	.....	− .04	− .04	2	+ .18	11.7
166331	18 5.1	+10 45	9.3	*B*	5.6	+12.7	− .12	.....	− .12	3	+ .07	.....
166418	18 5.4	−16 44	8.2	Bo	341.2	− 0.5	.....	+ .07	+ .07	2	+ .29	10.1
166443	18 5.5	−20 44	8.8	*Bo*	337.7	− 2.4	.....	− .08	− .08	4	+ .14	11.7
166481	18 5.7	−22 8	9.6	*B*	336.5	− 3.1	.....	+ .04	+ .04	2	+ .23	.....
166539	18 6.0	−15 37	8.7	Bo	342.3	0.0	− .04	− .03	− .04	4, 1	+ .18	11.3
166540	18 6.0	−16 55	8.0	Bo	341.1	− 0.7	.....	− .04	− .04	3	+ .18	10.6
166546	18 6.0	−20 27	7.17	*B1*	338.0	− 2.4	.....	− .13	− .13	3	+ .08	10.2
166566	18 6.1	−15 42	7.9	B1se	342.2	− 0.1	− .02	− .01	− .02	5, 1	+ .19	10.2
166568*	18 6.1	−18 45	9.0	*B2*	339.5	− 1.6	.....	− .05	− .05	2	+ .15	11.0
166628	18 6.4	−19 28	7.14	*B2*	338.9	− 2.0	.....	+ .16	+ .16	3	+ .36	7.6
166666	18 6.6	−15 36	9.2	B2e	342.4	− 0.3	+ .04	.....	+ .04	3	+ .24	10.5
166689	18 6.7	−16 24	7.34	Bo	341.7	− 0.6	.....	− .09	− .09	3	+ .13	10.3
166734	18 6.9	−10 46	8.8	Boea	346.6	+ 2.2	+ .36	+ .40	+ .39	5, 2	+ .61	8.4
166764*	18 7.0	−16 27	10.4	*B5*	341.7	− 0.7	.....	− .14	− .14	2	.....	.....
166787	18 7.1	−19 47	8.4	*B3*	338.8	− 2.3	.....	+ .10	+ .10	2	+ .29	8.6
166803	18 7.2	−15 13	7.9	Bo	342.8	0.0	−0.03	.....	− .03	2	+ .19	10.5
166852	18 7.4	−22 45	8.50	*B2*	336.2	− 3.8	.....	− .03	− .03	2	+ .17	10.3
166920	18 7.7	−17 19	10.5	*B5*	341.0	− 1.2	.....	− .03	− .03	2	+ .14	11.1
166934	18 7.8	−18 51	8.4	*B3*	339.6	− 2.0	.....	+ .01	+ .01	2	+ .20	9.2
166963	18 7.9	−16 36	9.7	B5	341.6	− 0.9	.....	− .04	− .04	2	+ .13	10.4
166964	18 7.9	−17 10	8.8	*B5*	341.1	− 1.2	.....	− .05	− .05	2	+ .12	9.6
166965	18 7.9	−19 2	8.8	*B2*	339.5	− 2.1	.....	+ .03	+ .03	2	+ .23	10.2
166967	18 7.9	−25 20	8.3	*B5*	334.0	− 5.1	.....	−0.12	−0.12	1	+0.05	9.5

TABLE 3—*Continued*

HD	R.A. 1900	Decl. 1900	m	Spec.	l	b	C_1			No.	E_1	m_0-M
							M	W	Mean			
166999	18h 8m1	−19° 9′	9.5	*B5*	339°.4	− 2°.2	.....	−0.08	−0.08	2	+0.09	10.5
167000	18 8.1	−20 41	9.2	*B5*	338.1	− 2.9	.....	− .03	− .03	2	+ .14	9.8
167088	18 8.6	−19 6	8.5	*B3*	339.5	− 2.3	.....	− .12	− .12	2	+ .07	10.2
167090	18 8.6	−20 30	9.4	*B5*	338.3	− 2.9	.....	− .07	− .07	2	+ .10	10.3
167224*	18 9.1	−18 59	7.9	*B5*	339.7	− 2.3	.....	− .10	− .10	2	+ .07	9.0
167263	18 9.3	−20 25	6.02	*B1*	338.4	− 3.1	.....	− .14	− .14	3	+ .07	9.1
167264	18 9.3	−20 46	5.42	Bo	338.1	− 3.2	.....	− .13	− .13	2	+ .09	8.7
167287*	18 9.4	−19 1	7.0	*Bo*	339.7	− 2.5	.....	− .09	− .09	5	+ .13	10.0
167288	18 9.4	−23 9	8.4	*B5*	336.1	− 4.4	.....	− .03	− .03	1	+ .14	9.0
167330	18 9.6	−12 34	8.4	*Bo*	345.3	+ 0.7	+0.12	+ .13	+ .13	4, 2	+ .35	9.9
167332	18 9.6	−16 0	9.7	B9	342.4	− 1.0	.....	− .03	− .03	2	+ .09	9.5
167336	18 9.6	−18 24	8.9	*B5*	340.3	− 2.1	.....	+ .10	+ .10	2	+ .27	8.6
MWC287	18 9.7	−20 23	8.7	Bone	338.5	− 3.1	.....	− .02	− .02	1	+ .20	11.2
167397*	18 9.9	−17 0	8.2	*Bo*	341.5	− 1.5	.....	− .06	− .06	4	+ .16	11.0
167411	18 10.0	−18 17	7.9	*B3*	340.4	− 2.2	.....	− .03	− .03	2	+ .16	9.0
167412	18 10.0	−18 29	8.6	*B5*	340.2	− 2.3	.....	− .12	− .12	2	+ .05	9.8
167432*	18 10.1	−17 9	9.5	*B5*	341.4	− 1.6	.....	− .06	− .06	2	+ .11	10.3
167436	18 10.1	−20 3	9.3	*B5*	338.9	− 3.0	.....	− .11	− .11	2	+ .06	10.5
167451	18 10.2	−13 36	8.7	Bo	344.5	0.0	+ .17	.....	+ .17	2	+ .39	9.9
167478*	18 10.3	−18 28	9.2	*B5*	340.3	− 2.3	.....	− .05	− .05	2	+ .12	10.0
167479	18 10.3	−18 49	8.2	*B3*	340.0	− 2.5	.....	− .10	− .10	2	+ .09	9.8
167543	18 10.6	−14 40	8.8	Bo	343.6	− 0.5	+ .05	+ .03	+ .04	3, 2	+ .26	10.9
167611*	18 10.9	−18 35	9.6	*B5*	340.2	− 2.5	.....	− .07	− .07	2	+ .10	10.5
167633	18 11.0	−16 33	8.2	Bo	342.0	− 1.5	.....	− .04	− .04	5	+ .18	10.8
167657	18 11.1	−16 26	8.7	B6	342.2	− 1.5	.....	− .06	− .06	2	+ .10	9.4
167659	18 11.1	−19 0	7.3	*B2*	339.9	− 2.8	.....	− .05	− .05	2	+ .15	9.3
167722	18 11.4	−19 46	9.3	*B5*	339.3	− 3.2	.....	− .08	− .08	2	+ .09	10.3
167747	18 11.5	−17 58	9.7	*B5*	340.9	− 2.3	.....	+ .04	+ .04	2	+ .21	9.8
167771	18 11.6	−18 30	6.37	O8	340.4	− 2.6	.....	− .11	− .11	4	+ .12	10.0
167815	18 11.8	−19 42	7.59	B2	339.4	− 3.3	.....	− .06	− .06	3	+ .14	9.6
167838	18 11.9	−15 28	6.64	Bo	343.1	− 1.2	+ .06	+ .08	+ .08	3, 3	+ .30	8.4
167863	18 12.0	−18 51	6.57	*B5*	340.1	− 2.9	.....	− .09	− .09	2	+ .08	7.6
167902	18 12.2	−18 0	9.4	*B5*	340.9	− 2.5	.....	− .10	− .10	2	+ .07	10.5
167971	18 12.5	−12 17	7.34	O8	346.0	+ 0.2	+ .20	+ .24	+ .23	2, 2	+ .46	8.6
167999	18 12.6	−16 41	9.4	*B5*	342.1	− 1.9	.....	− .04	− .04	3	+ .13	10.1
168021AB*	18 12.7	−18 39	6.9	*Bo*	340.4	− 2.9	.....	− .03	− .03	6	+ .19	9.5
168021C	18 12.7	−18 39	7.4	*Bo*	340.4	− 2.9	.....	− .03	− .03	1	+ .19	10.0
168078	18 12.9	−17 6	9.8	*B5*	341.8	− 2.2	.....	− .04	− .04	2	+ .13	10.5
168080	18 12.9	−18 12	9.2	*B2*	340.8	− 2.7	.....	− .12	− .12	2	+ .08	11.6
168112	18 13.1	−12 8	8.5	*Bo*	346.2	+ 0.1	.....	+ .19	+ .19	2	+ .41	9.5
168138	18 13.2	−19 29	9.1	*B3*	339.7	− 3.4	.....	− .07	− .07	2	+ .12	10.5
168162	18 13.3	−15 31	9.4	B5	343.2	− 1.5	.....	+ .18	+ .18	2	+ .35	8.6
168163	18 13.3	−16 20	8.9	*B3*	342.5	− 1.9	.....	+ .12	+ .12	2	+ .31	8.9
168183	18 13.4	−14 2	8.2	*Bo*	344.5	− 0.8	.....	.00	.00	2	+ .22	10.6
168186	18 13.4	−17 52	10.5	*B5*	341.2	− 2.7	.....	− .07	− .07	2	+ .10	11.4
168199	18 13.5	+13 44	6.18	B5n	9.2	+12.1	−0.13	.....	− .13	3	+ .04	7.5
168207	18 13.5	−14 12	9.4	B5	344.4	− 0.9	.....	+ .05	+ .05	2	+ .22	9.5
168230*	18 13.6	−18 54	9.5	*B3*	340.3	− 3.2	.....	+ .18	+ .18	2	+ .37	9.1
168279*	18 13.8	−18 11	9.1	*B5*	340.9	− 2.9	.....	− .10	− .10	2	+ .07	10.2
168302	18 13.9	−16 3	9.4	B8	342.8	− 1.9	.....	+ .28	+ .28	2	+ .41	7.3
168352	18 14.1	−17 7	8.9	*B2*	341.9	− 2.5	.....	+ .02	+ .02	2	+ .22	10.4
168308	18 14.2	−17 6	9.6	*B3*	341.9	− 2.5	.....	+ .04	+ .04	2	+ .23	10.2
168418	18 14.4	−17 2	9.6	*B3*	342.0	− 2.5	.....	+ .03	+ .03	2	+ .22	10.3
168444	18 14.6	−14 53	8.86	B4	343.9	− 1.5	.....	+ .12	+ .12	2	+ .30	8.7
168552	18 15.2	−17 11	8.3	*B3*	342.0	− 2.7	.....	+ .04	+ .04	2	+ .23	8.9
168571	18 15.3	−17 26	8.0	*B2*	341.8	− 2.9	.....	+ .13	+ 13	2	+ .33	8.7
168675	18 15.9	−17 57	9.1	*B5*	341.4	− 3.2	.....	+ .02	+ .02	2	+ .19	9.4
168726	18 16.1	−16 39	9.5	B8	342.5	− 2.7	.....	− .01	− .01	2	+ .12	9.5
168748	18 16.2	−17 9	10.5	*B5*	342.1	− 2.9	.....	+ .05	+ .05	2	+ .22	10.6
168765	18 16.3	−17 28	9.5	*B5*	341.8	− 3.1	.....	+0.05	+0.05	2	+0.22	9.6

TABLE 3—*Continued*

HD	R.A. 1900	Decl. 1900	m	Spec.	l	b	C_1			No.	E_1	m_0-M
							M	W	Mean			
168797	18h16m5	+ 5° 24′	6.04	B5n	2°0	+ 7°7	−0.12	.....	−0.12	6	+0.05	7.3
168941	18 17.2	−27 0	9.3	*Bo*	333.5	− 7.8	.....	−0.16	− .16	1	+ .06	12.8
168957	18 17.3	+25 1	6.86	B5e	20.2	+16.1	− .17	.....	− .17	3	.00	8.5
169014	18 17.5	−16 46	9.1	Bo	342.6	− 3.0	.....	.00	.00	2	+ .12	8.7
169033	18 17.6	−12 3	5.73	B8	346.8	− 0.8	− .09	.....	− .09	7	+ .04	6.2
169034	18 17.6	−13 39	8.6	Bo	345.3	− 1.6	.....	+ .45	+ .45	2	+ .67	7.8
169271	18 18.8	−18 20	9.0	*B3*	341.4	− 4.0	.....	+ .03	+ .03	3	+ .22	9.7
169419	18 19.4	−17 35	9.5	*Bo*	342.1	− 3.8	.....	+ .11	+ .11	4	+ .33	11.1
169454	18 19.6	−14 2	6.84	cBoe	345.2	− 2.2	+ .30	+ .28	+ .29	2, 2	+ .51	8.8
169601	18 20.3	−17 51	9.8	*B*	342.0	− 4.1	.....	+ .05	+ .05	2	+ .24	.....
169704	18 20.9	−21 35	9.4	*B5*	338.7	− 6.0	.....	− .04	− .04	1	+ .13	10.1
169727	18 21.0	−13 43	9.5	*Bo*	345.6	− 2.3	.....	+ .21	+ .21	2	+ .43	10.4
169753*	18 21.1	− 9 15	7.8	*B2*	349.6	− 0.2	+ .18	+ .22	+ .20	3, 2	+ .40	8.0
169754	18 21.1	−11 25	9.0	*B2*	347.7	− 1.2	.....	+ .36	+ .36	2	+ .56	8.1
169755	18 21.1	−14 34	9.4	Bo	344.9	− 2.7	.....	+ .12	+ .12	2	+ .34	10.9
169798	18 21.3	+22 39	6.72	B5s	18.4	+14.3	− .19	.....	− .19	2	− .02	8.5
169827	18 21.4	−17 21	8.2	*B5*	342.5	− 4.1	.....	+ .03	+ .03	2	+ .20	8.4
170028	18 22.3	+26 10	6.83	B3n	21.8	+15.6	− .18	.....	− .18	3	+ .01	9.0
170051	18 22.4	+26 23	6.87	B5	22.0	+15.6	− .18	.....	− .18	3	− .01	8.5
170061	18 22.4	−14 47	9.4	Bone	344.9	− 3.1	.....	+ .05	+ .05	2	+ .27	11.4
170097	18 22.6	−16 46	8.4	*Bo*	343.2	− 4.1	.....	− .07	− .07	3	+ .15	11.3
170111	18 22.7	+26 23	6.36	B5n	22.0	+15.6	− .17	.....	− .17	3	.00	8.0
170159	18 22.9	−13 4	8.6	*Bo*	346.5	− 2.4	+ .08	+ .12	+ .11	2, 2	+ .33	10.2
170177	18 23.0	−13 34	9.6	*B2*	346.0	− 2.7	.....	+ .25	+ .25	1	+ .45	9.4
170235	18 23.2	−25 19	6.23	B2e	335.6	− 8.2	.....	− .08	− .08	1	+ .12	8.4
170453	18 24.4	−14 17	9.2	*B2*	345.6	− 3.2	.....	+ .03	+ .03	2	+ .23	10.6
170580	18 25.1	+ 4 0	6.50	B5	1.8	+ 5.2	− .07	.....	− .07	3	+ .10	7.4
170604	18 25.2	−16 39	8.4	*B3*	343.6	− 4.6	.....	− .07	− .07	1	+ .12	9.8
170650	18 25.5	+23 48	5.72	B5	19.8	+13.9	− .16	.....	− .16	3	+ .01	7.2
170700	18 25.7	−14 11	8.8	*Bo*	345.8	− 3.5	.....	− .04	− .04	2	+ .18	11.4
170714	18 25.8	− 5 51	7.31	B5n	353.2	+ 0.4	+ .04	.....	+ .04	3	+ .21	7.4
170716	18 25.8	−12 24	9.6	*Bo*	347.4	− 2.7	.....	+ .03	+ .03	2	+ .25	11.7
170740	18 25.9	−10 52	5.80	B3	348.8	− 2.0	+ .03	.....	+ .03	10	+ .22	6.5
170783	18 26.1	+ 4 34	7.70	*B5*	2.4	+ 5.2	− .03	.....	− .03	3	+ .14	8.3
170938	18 26.9	−15 46	8.1	*Bo*	344.5	− 4.5	.....	+ .28	+ .28	2	+ .50	8.5
170978	18 27.1	−24 11	6.75	*B3*	337.0	− 8.5	.....	− .11	− .11	1	+ .08	8.4
171012	18 27.3	−18 26	6.98	Bosea	342.2	− 5.9	.....	+ .06	+ .06	2	+ .28	8.9
171198	18 28.3	−12 20	9.7	*Bo*	347.8	− 3.2	.....	+ .12	+ .12	2	+ .34	11.2
171201	18 28.3	−21 37	9.4	*B*	339.5	− 7.5	.....	− .04	− .04	1	+ .15	.....
171348	18 29.3	−22 10	8.0	B3e	339.1	− 8.0	.....	− .13	− .13	1	+ .06	9.8
171392	18 29.5	−14 23	9.4	*B2*	346.1	− 4.7	.....	− .01	− .01	2	+ .19	11.1
171406	18 29.6	+30 49	6.43	B5n	26.8	+15.9	− .14	.....	− .14	3	+ .03	7.8
171432*	18 29.7	−18 38	7.1	*B3*	342.3	− 6.5	.....	− .03	− .03	1	+ .16	8.2
171469	18 29.9	−15 48	9.5	*B2*	344.9	− 5.2	.....	+ .04	+ .04	2	+ .24	10.8
171589	18 30.6	−14 12	8.3	Bo	346.4	− 4.6	.....	− .03	− .03	2	+ .19	10.9
171611	18 30.7	−20 24	7.37	*B5*	340.8	− 7.5	.....	− .03	− .03	1	+ .14	8.0
171780	18 31.6	+34 22	5.93	B5n	30.4	+17.0	− .18	.....	− .18	3	− .01	7.6
171871	18 32.0	+51 2	7.39	B2s	47.1	+22.6	− .14	.....	− .14	3	+ .06	10.0
171876	18 32.0	−15 31	8.7	*B8p*	345.3	− 5.5	.....	− .01	− .01	1	+ .12	8.7
172175	18 33.6	− 7 57	9.7	*Bo*	352.2	− 2.3	.....	+ .13	+ .13	2	+ .35	11.2
172252	18 34.1	−11 58	9.6	*Bo*	348.7	− 4.3	.....	+ .21	+ .21	2	+ .43	10.5
172256	18 34.1	−22 45	8.6	*B5*	339.1	− 9.2	.....	− .14	− .14	1	+ .03	10.0
172367	18 34.7	− 7 20	9.6	Bo	352.9	− 2.2	.....	+ .06	+ .06	2	+ .28	11.5
172427	18 35.0	−10 48	9.7	*B2*	349.9	− 4.0	.....	+ .03	+ .03	2	+ .23	11.1
172510	18 35.5	−14 51	8.81	*B2*	346.3	− 5.9	.....	− .02	− .02	2	+ .18	10.6
173087	18 38.5	+34 38	6.12	B5	31.3	+15.8	− .15	.....	− .15	2	+ .02	7.6
17321	18 39.1	− 7 13	7.9	B1e	353.5	− 3.2	− .06	− .08	− .07	2, 2	+ .14	10.5
173370	18 39.8	+ 1 57	5.04	Bon	1.7	+ 1.0	− .14	.....	− .14	6	− .02	5.6
173375	18 39.8	−17 39	7.06	*B3*	344.3	− 8.1	.....	− .05	− .05	1	+ .14	8.3
173438	18 40.2	− 4 42	8.6	*Bo*	355.9	− 2.3	+0.15	+0.23	+0.20	2, 2	+0.42	9.6

TABLE 3—*Continued*

HD	R.A. 1900	Decl. 1900	m	Spec.	l	b	C_1			No.	E_1	m_0-M
							M	W	Mean			
173637	18h41m2	− 8° 2′	9.0	*Bo*	353.°0	− 4.°0	.....	+0.01	+0.01	2	+0.23	11.3
173987	18 43.2	− 6 34	9.0	*Bo*	354.6	− 3.8	.....	− .01	− .01	2	+ .21	11.4
173991	18 43.2	−12 40	9.2	*B2*	349.1	− 6.6	0.00	− .01	− .01	3, 2	+ .19	10.9
174179	18 44.2	+31 39	5.78	B3s	28.9	+13.4	− .21	.....	− .21	4	− .02	8.1
174237	18 44.5	+52 53	5.76	B5n	49.6	+21.3	− .18	.....	− .18	3	− .01	7.4
174261	18 44.6	+21 3	6.93	B5n	19.3	+ 8.7	− .14	.....	− .14	2	+ .03	8.3
174298	18 44.8	+23 57	6.51	B2s	21.9	+10.0	− .12	.....	− .12	2	+ .08	9.0
174391	18 45.2	+15 49	6.54	B3s	14.6	+ 6.2	− .17	.....	− .17	2	+ .02	8.6
174511	18 45.7	− 7 54	8.6	*B2*	353.7	− 4.9	− .12	− .13	− .13	2, 2	+ .07	11.1
174571	18 46.0	+ 8 35	9.1	*B2*	8.3	+ 2.7	− .02	+ .12	+ .08	4, 3	+ .28	10.1
174585	18 46.1	+32 42	5.77	B3	30.1	+13.5	− .19	.....	− .19	4	.00	8.0
174638*	18 46.4	+33 15	var.	B8+B2	30.6	+13.7	− .13	.....	− .13	3	.....	.....
174959	18 48.1	+36 25	6.01	B5s	33.8	+14.7	− .16	.....	− .16	2	+ .01	7.5
175081	18 48.6	+37 24	7.08	B5n	34.7	+15.0	− .16	.....	− .16	3	+ .01	8.6
175141	18 48.9	−19 59	8.88	*B5*	343.1	−11.1	.....	− .06	− .06	1	+ .11	9.7
175426	18 50.2	+36 51	5.51	B3	34.3	+14.5	− .20	.....	− .20	2	− .01	7.8
175514	18 50.6	+ 9 13	9.0	Bo1	9.4	+ 2.0	+ .04	+ .10	+ .08	5, 3	+ .30	10.8
175544	18 50.7	+ 0 8	7.73	*B3*	1.4	− 2.3	− .05	.....	− .05	3	+ .14	9.0
175754	18 51.7	−19 17	7.03	*Bop*	344.1	−11.4	.....	− .20	− .20	4	+ .02	10.8
175803	18 52.0	+19 43	7.97	*B3*	18.9	+ 6.6	− .06	.....	− .06	2	+ .13	9.3
175863	18 52.3	+59 53	6.94	B4e	57.2	+22.5	− .11	.....	− .11	2	+ .07	8.3
175876	18 52.3	−20 33	6.73	*Oe5*	342.7	−12.2	.....	− .20	− .20	2	+ .03	11.0
176162	18 53.8	−12 58	5.36	B7	350.0	− 9.0	− .12	.....	− .12	4	+ .02	6.3
176254	18 54.3	+20 29	6.72	B3s	19.8	+ 6.5	− .11	.....	− .11	3	+ .08	8.4
176304	18 54.5	+10 0	6.52	B2s	10.5	+ 1.5	− .02	.....	− .02	3	+ .18	8.3
176502	18 55.5	+40 33	6.12	B5s	38.3	+15.1	− .18	.....	− .18	2	− .01	7.8
176542	18 55.7	+15 13	8.94	*B5*	15.3	+ 3.7	− .07	.....	− .07	3	+ .10	9.8
176582	18 55.9	+39 5	6.25	B5	36.9	+14.4	− .14	.....	− .14	2	+ .03	7.6
176630	18 56.1	− 6 20	7.69	*B5*	356.3	− 6.5	− .07	.....	− .07	2	+ .10	8.6
176818	18 57.0	+21 22	6.86	B3	20.9	+ 6.3	− .06	.....	− .06	3	+ .13	8.2
176819	18 57.0	+20 42	6.55	B2	20.3	+ 6.0	− .06	.....	− .06	3	+ .14	8.6
176871	18 57.2	+26 9	5.50	B3n	25.2	+ 8.5	− .13	.....	− .13	4	+ .06	7.3
176914	18 57.4	+28 16	6.78	B5n	27.1	+ 9.4	− .14	.....	− .14	2	+ .03	8.2
177003	18 57.7	+50 24	5.24	B3	47.9	+18.6	− .20	.....	− .20	2	− .01	7.5
177006	18 57.7	+32 15	7.1	*B5*	30.8	+11.1	− .15	.....	− .15	2	+ .02	8.6
177014	18 57.7	−19 34	9.1	*B5*	344.4	−12.8	.....	+ .02	+ .02	2	+ .19	9.4
177015	18 57.7	−20 16	7.57	B3e	343.7	−13.1	.....	− .08	− .08	2	+ .11	9.0
177109	18 58.2	+33 29	6.22	B3n	31.9	+11.6	− .14	.....	− .14	2	+ .05	8.1
177284	18 58.9	− 2 10	9.2	*B3*	0.3	− 5.2	− .10	.....	− .10	2	+ .09	10.8
177559	19 0.1	−19 38	8.2	*B5*	344.6	−13.3	.....	− .09	− .09	2	+ .08	9.2
177593	19 0.3	+34 0	7.12	B5n	32.6	+11.4	− .14	.....	− .14	2	+ .03	8.5
177624	19 0.4	+ 9 29	6.93	B5n	10.8	0.0	− .01	.....	− .01	3	+ .16	7.4
177648	19 0.5	+23 11	6.94	B3e	22.9	+ 6.5	− .05	.....	− .05	3	+ .14	..2
177752	19 0.9	− 0 59	8.7	*B3*	1.6	− 5.1	− .05	.....	− .05	2	+ .14	9.9
177812	19 1.1	+ 3 6	8.9	*B2*	5.2	− 3.2	+ .12	+ .15	+ .14	3, 1	+ .34	9.5
177989	19 1.8	−18 53	9.1	*B5*	345.5	−13.4	.....	− .17	− .17	2	.00	10.7
178129	19 2.3	+ 3 17	7.8	B3	5.5	− 3.4	+ .07	.....	+ .07	3	+ .26	8.2
178175	19 2.4	−19 27	5.41	B3ne	345.0	−13.7	.....	− .13	− .13	2	+ .06	7.2
178329	19 3.1	+41 16	6.15	B3s	39.6	+14.1	− .20	.....	− .20	2	− .01	8.4
178475	19 3.7	+35 57	5.13	B5n	34.7	+11.6	− .17	.....	− .17	3	.00	6.7
178487	19 3.7	−10 22	8.7	*Bo*	353.5	−10.0	− .03	− .06	− .05	1, 1	+ .17	11.4
178540	19 3.9	+24 34	6.66	B5	24.5	+ 6.4	− .14	.....	− .14	2	+ .03	8.0
178591	19 4.1	+40 54	6.94	*B5*	39.3	+13.7	− .12	.....	− .12	2	+ .05	8.2
178849*	19 5.1	+34 35	6.63	B3s	33.6	+10.8	+ .34	.....	+ .34	2	(+ .53)	.....
178912	19 5.4	+33 5	8.3	*B5*	32.2	+10.0	− .17	.....	− .17	2	.00	9.9
179202	19 6.5	−23 12	8.1	*B*	341.9	−16.2	.....	−0.11	− .11	1	+ .06	9.3
179406	19 7.3	− 8 7	5.37	B3n	356.0	− 9.8	− .04	.....	− .04	3	+ .15	6.5
180126	19 10.2	+ 9 37	8.2	*B3*	12.0	− 2.1	− .04	.....	− .04	2	+ .15	9.4
180163	19 10.4	+38 58	4.46	B5s	38.1	+11.8	− .20	.....	− .20	5	− .03	6.3
180398	19 11.3	+12 56	8.0	B(3)ne	15.1	− 0.7	−0.07	.....	−0.07	2	+0.12	9.4

TABLE 3—*Continued*

HD	R.A. 1900	Decl. 1900	m	Spec.	l	b	C_1			No.	E_1	$m_v - M$
							M	W	Mean			
180554	19h11m9	+21°13′	4.60	B5n	22°.4	+ 3°.2	−0.14	.....	−0.14	3	+0.03	6.0
180587	19 12.0	+10 49	8.6	*B5*	13.3	− 1.9	− .15	.....	− .15	3	+ .02	10.1
180629	19 12.1	−17 7	7.8	*B5*	348.2	−14.8	.....	−0.13	− .13	3	+ .04	9.1
180844	19 13.0	+32 57	7.01	B5	32.9	+ 8.6	− .19	.....	− .19	2	− .02	8.8
180968	19 13.5	+22 51	5.40	Bonn	24.0	+ 5.7	− .12	.....	− .12	3	+ .10	8.6
181164	19 14.3	+25 53	7.32	B3s	26.7	+ 5.0	− .16	.....	− .16	2	+ .03	9.3
181360	19 15.1	+23 7	7.50	B3	24.4	+ 3.5	− .08	.....	− .08	2	+ .11	8.9
181409	19 15.3	+33 13	6.32	B3	33.3	+ 8.3	− .20	.....	− .20	3	− .01	8.6
181492	19 15.6	+31 47	6.64	B4	32.1	+ 7.5	− .16	.....	− .16	3	+ .02	8.4
181858	19 17.0	− 8 23	6.49	B5s	356.8	−12.1	− .13	.....	− .13	2	+ .04	7.8
181963	19 17.4	+25 25	7.26	B3s	26.6	+ 4.1	− .10	.....	− .10	2	+ .09	8.8
181987*	19 17.5	+25 23	7.3	B3n	26.8	+ 4.2	− .07	.....	− .07	2	+ .12	8.7
182032	19 17.7	+22 19	7.7	B3	24.0	+ 2.6	− .11	.....	− .11	2	+ .08	9.3
182078	19 17.9	+22 21	7.9	*B3*	24.3	+ 2.5	− .15	.....	− .15	2	+ .04	9.8
182255	19 18.7	+26 4	4.92	B8s	27.4	+ 4.2	− .16	.....	− .16	2	− .03	5.9
182568	19 20.2	+29 26	4.86	B5	30.5	+ 5.5	− .17	.....	− .17	2	.00	6.5
183013	19 22.4	+21 27	7.23	B3	23.8	+ 1.2	− .12	.....	− .12	2	+ .07	8.9
183143	19 23.0	+18 5	6.93	cB9eα	20.9	− 0.5	+ .38	.....	+ .38	3	+ .50	8.9
183144	19 23.0	+14 5	6.26	B5n	17.5	− 2.6	− .17	.....	− .17	2	.00	7.9
183261	19 23.6	+20 2	7.15	B3n	22.7	+ 0.2	− .14	.....	− .14	2	+ .05	9.0
183362	19 24.1	+37 44	6.36	B3ne	38.2	+ 8.8	− .18	.....	− .18	2	+ .01	8.5
183537	19 25.0	+20 4	6.39	B5nn	22.9	0.0	− .16	.....	− .16	2	+ .01	7.9
183570	19 25.1	−16 23	7.25	*B5*	350.3	−17.3	.....	− .10	− .10	3	+ .07	8.4
E231616	19 25.9	+18 3	10.3	*Bo*	21.3	− 1.2	.....	+ .13	+ .13	1	+ .35	11.8
184171	19 28.1	+34 14	4.85	B5s	35.5	+ 6.4	− .18	.....	− .18	3	− .01	6.5
184279	19 28.6	+ 3 34	6.78	B2se	8.9	− 9.0	− .19	.....	− .19	2	+ .01	9.7
184502	19 29.7	+16 3	6.81	B3	20.0	− 3.1	− .17	.....	− .17	2	+ .02	8.9
184915	19 31.5	− 7 15	5.04	Bon	359.6	−14.7	− .14	.....	− .14	2	+ .08	9.4
184927	19 31.6	+31 4	7.4	*B2*	33.2	+ 4.2	− .20	.....	− .20	2	.00	10.4
184930	19 31.6	− 1 31	4.28	B8n	4.8	−12.1	− .17	.....	− .17	3	− .04	5.4
184942	19 31.7	+25 36	7.46	B3	28.4	+ 1.4	− .10	.....	− .10	3	+ .09	9.0
185268	19 33.2	+29 7	6.26	B5n	31.6	+ 2.9	− .17	.....	− .17	2	.00	7.9
185418	19 33.9	+17 2	7.42	B3	21.3	− 3.4	− .10	.....	− .10	3	+ .09	9.0
185507	19 34.3	+ 5 10	5.17	B3	11.1	− 9.5	− .10	.....	− .10	3	+ .09	6.7
185534	19 34.4	−21 32	7.7	*B5*	346.2	−21.4	.....	− .13	− .13	1	+ .04	9.0
185780	19 35.7	+40 24	7.47	B2	41.7	+ 8.2	− .17	.....	− .17	3	+ .03	10.3
185842	19 36.0	− 2 33	7.12	B5s	4.4	−13.5	− .14	.....	− .14	2	+ .03	8.5
185859	19 36.1	+20 15	6.44	Bo	24.4	− 2.2	+ .04	.....	+ .04	3	+ .26	8.5
185915	19 36.4	+23 29	6.41	B8	27.2	− 0.6	− .11	.....	− .11	3	+ .02	7.1
185936	19 36.5	+13 35	5.84	B5	18.7	− 5.7	− .15	.....	− .15	4	+ .02	7.3
186412	19 39.1	+22 15	6.53	B5	26.4	− 1.8	− .16	.....	− .16	2	+ .01	8.1
186587	19 40.2	+10 32	7.36	B5	16.5	− 8.0	− .06	.....	− .06	2	+ .11	8.2
186618	19 40.4	+47 1	7.6	B1n	47.9	+10.8	− .25	.....	− .25	1	− .04	11.5
186660	19 40.6	− 3 7	6.50	B3s	4.4	−14.8	− .12	.....	− .12	3	+ .07	8.2
186777	19 41.4	+31 10	7.35	B7s	34.3	+ 2.5	− .14	.....	− .14	2	.00	8.5
186980	19 42.4	+31 52	7.28	O8	35.0	+ 2.7	− .11	.....	− .11	2	+ .12	10.9
186994	19 42.5	+44 43	7.3	*Bo*	46.1	+ 9.3	− .22	.....	− .22	2	.00	11.2
187320	19 44.3	+19 24	7.5	B2n	24.7	− 4.3	− .10	.....	− .10	4	+ .10	9.8
187350	19 44.4	− 1 21	8.3	*B2*	6.5	−14.8	− .07	− .11	− .10	3, 2	+ .10	10.6
187459	19 45.0	+33 12	6.35	Bon	36.5	+ 2.9	− .06	.....	− .06	2	+ .16	9.1
187567	19 45.5	+ 7 39	6.39	B3ne	14.7	−10.6	− .13	−0.16	− .14	2, 1	+ .05	8.2
187811	19 46.8	+22 21	4.91	B5ne	27.5	− 3.2	− .18	.....	− .18	2	− .01	6.6
187879	19 47.2	+40 20	5.62	B2	42.8	+ 6.3	− .14	.....	− .14	2	+ .06	8.2
187961	19 47.6	+10 6	6.48	B5n	17.1	− 9.8	− .13	.....	− .13	2	+ .04	7.8
188001	19 47.9	+18 25	6.29	O7f	24.3	− 5.5	− .10	.....	− .10	2	+ .13	9.9
188209	19 49.0	+46 47	5.51	O8s	48.5	+ 9.4	− .17	.....	− .17	4	+ .06	9.6
188252	19 49.2	+47 41	5.70	B2s	49.3	+ 9.8	− .18	.....	− .18	2	+ .02	8.6
188293	19 49.3	− 8 29	5.78	B5n	0.5	−19.2	− .16	.....	− .16	2	+ .01	7.3
188439	19 50.1	+47 34	6.15	B2nn	49.3	+ 9.6	− .19	.....	− .19	3	+ .01	9.1
188461	19 50.2	+41 6	6.82	B3s	43.7	+ 6.2	−0.18	.....	−0.18	2	+0.01	9.0

TABLE 3—*Continued*

HD	R.A. 1900	Decl. 1900	m	Spec.	l	b	C_1			No.	E_1	m_0-M
							M	W	Mean			
188618	19h50m9	−18° 11′	9.2	*B5*	351°.2	−23°.7	.....	−0.10	−0.10	2	+0.07	10.3
188665	19 51.2	+57 16	5.04	B5	57.9	+14.4	−0.18	.....	− .18	2	− .01	6.7
188891	19 52.3	+40 8	7.22	B3	43.1	+ 5.3	− .17	.....	− .17	2	+ .02	9.3
188892	19 52.3	+38 13	4.87	B7s	41.5	+ 4.3	− .18	.....	− .18	3	− .04	6.3
189066	19 53.1	+35 59	6.04	B3	39.7	+ 3.0	− .18	.....	− .18	2	+ .01	8.2
189178	19 53.7	+40 6	5.43	B3n	43.2	+ 5.1	− .16	.....	− .16	3	+ .03	7.4
189432	19 54.9	+37 50	6.28	B7s	41.4	+ 3.7	− .14	.....	− .14	2	.00	7.4
189550*	19 55.5	+19 37	7.5	*B2*	26.3	− 6.4	− .10	− .18	− .16	2,3	+ .04	10.2
189687	19 56.2	+36 46	5.15	B3	40.7	+ 2.9	− .16	.....	− .16	2	+ .03	7.1
189775	19 56.6	+51 47	6.02	B8n	53.5	+10.9	− .17	.....	− .17	2	− .04	7.1
189818	19 56.9	+57 32	7.08	B3	58.5	+13.9	− .18	.....	− .18	2	+ .01	9.2
189921	19 57.4	+10 26	6.80	B7s	18.6	−11.7	− .16	− .17	− .16	2, 1	− .02	8.0
190025	19 57.9	+42 46	7.29	B3	45.9	+ 5.9	− .16	.....	− .16	2	+ .16	10.9
190066	19 58.1	+21 52	6.55	cBo	28.4	− 5.7	− .06	.....	− .06	2	+ .16	10.1
190467	20 0.0	+36 8	8.2	*B2*	40.6	+ 1.9	− .04	.....	− .04	4	+ .16	
E227415	20 0.1	+35 16	9.9	B3	39.9	+ 1.4	.....	+ .08	+ .08	1	+ .27	10.2
E227460	20 0.6	+35 59	9.9	B3	40.5	+ 1.7	.....	+ .28	+ .28	1	+ .47	8.8
190603	20 0.7	+31 56	5.69	cBoeβ	37.2	− 0.6	+ .13	.....	+ .13	4	+ .35	8.7
E227586	20 1.8	+35 20	8.9	B1	40.1	+ 1.1	.....	− .02	− .02	1	+ .19	11.2
190864	20 1.9	+35 19	7.8	O6	40.1	+ 1.1	− .04	− .10	− .07	4, 1	+ .16	11.2
E227611	20 2.0	+35 37	8.7	Bne	40.4	+ 1.3	.....	+ .01	+ .01	1	+ .20	.....
+35°3955	20 2.2	+35 32	7.3	Bo	40.3	+ 1.2	− .08	− .03	− .04	2, 3	+ .18	9.9
190919	20 2.2	+35 24	7.30	cB1	40.2	+ 1.1	+ .08	− .04	.00	3, 2	+ .21	11.3
190944	20 2.3	+40 24	8.5	B(2)e	49.4	+ 7.2	− .03	.....	− .03	3	+ .17	10.3
+35°3956	20 2.3	+35 29	7.9	B5	40.3	+ 1.1	.....	− .05	− .05	2	+ .12	8.7
E227634	20 2.3	+35 29	8.0	B1	40.3	+ 1.1	.....	− .03	− .03	2	+ .18	10.3
190967	20 2.4	+35 6	7.92	*B3*	40.0	+ 0.9	− .01	.....	− .01	2	+ .18	8.9
190993	20 2.5	+23 19	5.08	B3	30.3	− 5.7	− .18	.....	− .18	3	+ .01	7.2
E227696	20 2.8	+35 27	8.3	B2	40.3	+ 1.0	.....	− .04	− .04	1	+ .16	10.2
191139	20 3.3	+36 7	8.3	*B5*	41.0	+ 1.3	− .11	.....	− .11	2	+ .06	9.5
191201	20 3.6	+35 26	7.12	Bo	40.4	+ 0.9	− .03	− .10	− .07	3, 2	+ .15	10.0
E227767	20 3.6	+35 18	8.8	B2	40.3	+ 0.8	.....	− .14	− .14	1	+ .06	11.4
191263	20 3.9	+10 26	6.23	B5s	19.5	−13.1	− .17	− .18	− .18	2, 1	− .01	7.9
E227836	20 4.3	+35 50	9.6	B2e	40.8	+ 1.0	.....	+ .02	+ .02	1	+ .22	11.1
191395	20 4.6	+39 28	8.4	*B2*	43.9	+ 3.0	− .10	− .11	− .11	3, 2	+ .09	10.8
E227877	20 4.6	+35 10	9.2	B3n	40.4	+ 0.6	.....	− .08	− .08	1	+ .11	10.6
191495	20 5.1	+35 14	8.12	B1	40.4	+ 0.5	− .08	− .12	− .11	2, 2	+ .10	11.0
E227960	20 5.4	+35 45	9.6	Bo	40.9	+ 0.8	.....	− .10	− .10	1	+ .12	12.7
191566*	20 5.5	+35 11	7.7	B2	40.4	+ 0.4	− .05	.....	− .05	3	+ .15	9.7
191610	20 5.7	+36 33	4.82	B3ne	41.6	+ 1.2	− .20	.....	− .20	5	− .01	7.1
191612	20 5.7	+35 26	7.8	O7	40.7	+ 0.5	+ .01	− .04	− .02	2, 2	+ .21	10.8
191639	20 5.8	− 9 9	6.45	B2	1.8	−23.2	− .14	.....	− .14	3	+ .06	9.0
E228007	20 5.9	+35 28	9.0	B3n	40.7	+ 0.5	.....	− .03	− .03	1	+ .16	10.1
E228041	20 6.2	+35 12	9.2	B3ne	40.5	+ 0.4	.....	+ .03	+ .03	1	+ .22	9.9
E228053	20 6.3	+36 24	8.9	*Bo*	41.5	+ 1.0	.....	+ .07	+ .07	2	+ .29	10.8
191746	20 6.4	+28 8	6.94	B3	34.7	− 3.7	− .12	.....	− .12	2	+ .07	8.6
E228104	20 6.9	+35 35	9.1	B(3)ne	40.9	+ 0.4	.....	.00	.00	1	+ .19	10.0
191877	20 7.0	+21 35	6.11	Bo	29.4	− 7.6	− .12	.....	− .12	2	+ .10	9.3
191917	20 7.2	+35 39	7.8	B1	41.0	+ 0.4	.....	− .11	− .11	1	+ .10	10.7
191978	20 7.5	+41 4	8.2	*B2*	45.5	+ 3.5	− .06	.....	− .06	2	+ .14	10.2
192281	20 9.0	+39 58	7.47	O5	44.8	+ 2.6	+ .07	.....	+ .07	2	+ .30	9.9
192422	20 9.7	+38 28	7.10	Bos	43.6	+ 1.6	+ .05	.....	+ .05	2	+ .27	9.1
192445	20 9.8	+36 2	7.12	B2ne	41.6	+ 0.2	− .12	.....	− .12	2	+ .08	9.6
E228438	20 10.1	+36 20	8.9	Bone	41.9	+ 0.3	− .08	.....	− .08	2	+ .14	11.8
192517	20 10.2	+29 54	6.94	B3s	36.7	− 3.4	− .14	.....	− .14	3	+ .05	8.8
192539	20 10.3	+31 41	7.38	B2s	38.1	− 2.4	− .04	.....	− .04	2	+ .16	9.3
192575	20 10.5	+67 58	6.79	B2s	68.7	+17.9	− .06	.....	− .06	2	+ .14	8.8
192639	20 10.8	+37 3	7.02	O7f	42.6	+ 0.6	+ .03	.....	+ .03	3	+ .26	9.7
192685	20 11.0	+25 17	4.82	B3n	33.0	− 6.2	−0.18	.....	− .18	5	+ .01	7.0
E228548	20 11.4	+39 40	10.3	B(2)ne	44.8	+ 2.0	.....	+0.19	+0.19	2	+0.39	10.6

TABLE 3—*Continued*

HD	R.A. 1900	Decl. 1900	m	Spec.	l	b	C_1			No.	E_1	m_0-M
							M	W	Mean			
192968	20h12m7	+40°39′	7.9	*B2*	45°.7	+ 2°.4	−0.17	.....	−0.17	2	+0.03	10.7
192987	20 12.8	+36 45	6.32	B5n	42.6	+ 0.1	− .17	.....	− .17	3	.00	7.9
193009	20 12.9	+32 4	7.02	Bone	38.7	− 2.6	− .06	.....	− .06	2	+ .16	9.8
193183	20 13.8	+37 55	7.12	B2s	43.6	+ 0.5	+ .08	.....	+ .08	3	+ .28	8.2
193220	20 14.0	+25 20	6.78	B3	33.4	− 6.7	− .16	.....	− .16	2	+ .03	8.8
193237*	20 14.1	+37 43	4.88	B1eq	43.5	+ 0.4	+ .06	.....	+ .06	6	(+ .27)	.....
193322	20 14.6	+40 25	5.82	O8	45.8	+ 2.0	− .07	.....	− .07	14	+ .16	9.2
E228841	20 14.8	+38 34	9.1	*Bo*	44.3	+ 0.9	.....	+0.10	+ .10	3	+ .32	10.8
193443	20 15.2	+37 57	7.4	*B1*	43.8	+ 0.3	+ .03	.....	+ .03	2	+ .24	9.3
193514	20 15.5	+38 57	7.29	O8	44.7	+ 1.0	+ .10	.....	+ .10	4	+ .33	9.5
193516	20 15.5	+37 28	9.1	B1(e)	43.5	0.0	+ .08	.....	+ .08	2	+ .29	10.7
193536	20 15.6	+46 0	6.28	B2	50.4	+ 5.1	− .17	.....	− .17	2	+ .03	9.1
193683	20 16.5	+31 42	7.40	B3s	38.9	− 3.5	− .19	.....	− .19	2	.00	9.6
193911	20 17.7	+24 7	5.41	B8ne	32.8	− 8.1	− .12	.....	− .12	2	+ .01	6.1
194279	20 19.7	+40 26	7.05	cB1	46.3	+ 1.2	+ .33	.....	+ .33	3	+ .54	8.8
194335	20 20.0	+37 10	5.68	B3ne	43.8	− 0.8	− .18	.....	− .18	12	+ .01	7.8
E229221	20 20.1	+38 11	9.6	B(o)e	44.6	− 0.2	.....	+ .28	+ .28	2	+ .50	10.0
194779	20 22.4	+41 1	7.66	*B*	47.1	+ 1.2	.00	.....	.00	2	+ .19	.....
194839	20 22.8	+41 3	7.45	B2se	47.2	+ 0.9	+ .34	.....	+ .34	3	+ .54	6.7
194883	20 23.0	+54 22	7.24	B3e	57.9	+ 9.1	− .10	.....	− .10	2	+ .09	8.8
195089	20 24.1	+41 42	7.24	B3	47.8	+ 1.3	− .12	.....	− .12	2	+ .07	9.0
195407	20 26.0	+36 39	7.72	B3e	44.1	− 2.1	.00	.....	.00	1	+ .19	8.6
195556	20 27.0	+48 37	4.89	B3	53.6	+ 5.1	− .17	.....	− .17	3	+ .02	7.0
195592	20 27.2	+43 59	7.15	Bose	50.0	+ 2.3	+ .30	.....	+ .30	3	+ .52	7.4
195810	20 28.4	+10 58	3.98	B7	23.4	−17.8	− .16	.....	− .16	2	− .02	5.2
195965	20 29.3	+47 53	6.82	B2	53.3	+ 4.4	− .15	.....	− .15	2	+ .05	9.5
195985	20 29.4	+44 39	7.50	B5	50.8	+ 2.4	− .13	.....	− .13	2	+ .04	8.8
195986	20 29.4	+42 51	6.41	B6s	49.4	+ 1.3	− .16	.....	− .16	2	.00	7.8
196006	20 29.5	+32 34	7.08	B3s	41.3	− 5.1	− .18	.....	− .18	2	+ .01	9.2
196025	20 29.6	+ 6 32	6.86	B5	19.7	−20.5	− .18	.....	− .18	2	− .01	8.5
196035	20 29.7	+20 38	6.28	B3s	31.7	−12.4	− .17	.....	− .17	2	+ .02	8.3
196243	20 31.0	+29 55	7.41	B5	39.4	− 7.0	− .14	.....	− .14	2	+ .03	8.8
196421	20 32.2	+57 35	8.2	*B5*	61.3	+10.0	− .03	.....	− .03	3	+ .14	8.8
196740	20 34.2	+23 46	5.04	B7n	34.9	−11.4	− .17	.....	− .17	2	− .03	6.3
196775	20 34.4	+15 29	5.92	B3	28.1	−16.4	− .18	.....	− .18	2	+ .01	8.0
197036	20 36.0	+45 19	6.46	B3n	52.0	+ 1.9	− .14	.....	− .14	2	+ .05	8.3
197345	20 38.0	+44 55	1.33	cA2ea	51.9	+ 1.4	− .10	.....	− .10	2	− .05	7.2
197419	20 38.5	+35 5	6.50	B3s	44.4	− 5.0	− .19	.....	− .19	2	.00	8.7
197460	20 38.8	+36 2	8.2	*B2*	45.2	− 4.5	.....	+ .01	+ .01	2	+ .21	9.7
197511	20 39.1	+49 59	5.41	B3s	56.0	+ 4.4	− .14	.....	− .14	2	+ .05	7.3
197637	20 39.9	+79 4	6.78	B3s	79.8	+22.2	− .14	.....	− .14	2	+ .05	8.6
197702	20 40.3	+31 20	8.2	*B3*	41.8	− 7.7	− .05	.....	− .05	3	+ .14	9.4
197770	20 40.7	+56 46	6.36	B2s	61.4	+ 8.6	+ .03	.....	+ .03	3	+ .23	7.8
197911	20 41.6	+62 51	7.7	*B5*	66.2	+12.7	− .13	.....	− .13	2	+ .04	9.0
198183	20 43.5	+36 7	4.47	B5ne	45.9	− 5.2	− .15	.....	− .15	3	+ .02	5.9
198478	20 45.5	+45 45	4.89	cB2ea	53.4	+ 0.9	+ .05	.....	+ .05	4	+ .25	8.6
198512	20 45.7	+53 32	7.95	B2ne	59.3	+ 6.0	− .04	.....	− .04	4	+ .16	9.8
198625	20 46.5	+46 17	6.48	B4n	53.9	+ 1.1	− .10	.....	− .10	2	+ .08	7.8
198781	20 47.6	+63 40	6.38	B1n	67.3	+12.3	− .07	− .18	− .14	3, 1	+ .07	9.5
198784	20 47.6	+37 36	6.97	B3	47.6	− 4.8	− .04	.....	− .04	3	+ .15	8.1
198820	20 47.9	+32 28	6.35	B5s	43.7	− 8.2	− .15	.....	− .15	5	+ .02	7.8
198846*	20 48.1	+34 17	7.1	Ognn	45.1	− 7.0	− .13	.....	− .13	3	+ .10	10.9
198895	20 48.4	+55 7	8.26	B2e	60.8	+ 6.7	+ .14	.....	+ .14	2	+ .34	8.9
199081	20 49.7	+44 0	4.68	B3	52.6	− 0.8	− .16	.....	− .16	2	+ .03	6.7
199140	20 50.1	+28 8	6.44	B1s	40.7	−11.4	− .18	.....	− .18	3	+ .03	9.8
199216	20 50.7	+49 9	7.13	B1s	56.6	+ 2.3	+ .11	.....	+ .11	4	+ .32	8.5
199218	20 50.7	+40 20	6.48	B5ne	50.0	− 3.4	− .17	.....	− .17	2	.00	8.1
199308	20 51.3	+55 58	7.61	*B3*	61.7	+ 7.0	− .07	.....	− .07	2	+ .12	9.0
199356	20 51.6	+39 55	7.02	B3ne	49.8	− 3.8	− .03	.....	− .03	3	+ .16	8.1
199478	20 52.4	+47 2	5.76	cB8ea	55.2	+ 0.9	+0.09	+0.09	+0.09	2, 1	+0.22	9.7

TABLE 3—*Continued*

HD	R.A. 1900	Decl. 1900	m	Spec.	l	b	C_1 M	C_1 W	C_1 Mean	No.	E_1	m_0-M
199579	20h53m1	+44°33′	6.01	O6	53°.4	− 0°.9	−0.12	.....	−0.12	2	+0.11	9.7
199661	20 53.6	+56 29	6.14	B3	62.3	+ 7.1	− .20	−0.20	− .20	3, 1	− .01	8.4
200120	20 56.4	+47 8	4.86	B3ne	55.7	+ 0.4	− .22	.....	− .22	3	− .03	7.3
200310	20 57.6	+45 46	5.24	B3ne	54.9	− 0.7	− .20	.....	− .20	2	− .01	7.5
200775	21 0.4	+67 47	7.20	B5e	71.4	+14.0	+ .07	.....	+ .07	3	+ .24	7.1
200857	21 1.0	+54 51	7.16	B2	61.8	+ 5.2	+ .16	.....	+ .16	8	+ .36	7.6
201254	21 3.2	+14 16	6.86	B5	31.6	−22.6	− .15	.....	− .15	2	+ .02	8.3
201345	21 3.9	+33 0	7.76	*Bo*	46.4	−10.3	− .22	.....	− .22	3	.00	11.7
201522	21 5.1	+46 51	7.8	B3ne	56.5	− 0.9	− .14	.....	− .14	3	+ .05	9.6
201666	21 6.0	+45 20	7.52	*B5*	55.6	− 2.0	− .10	.....	− .10	2	+ .07	8.6
201733	21 6.4	+45 6	6.52	B5e	55.5	− 2.2	− .19	.....	− .19	2	− .02	8.3
201795	21 6.8	+38 33	7.7	*B3*	50.8	− 6.9	− .13	.....	− .13	2	+ .06	9.5
201819	21 7.0	+35 53	6.40	B1n	48.9	− 8.8	− .18	.....	− .18	2	+ .03	9.8
201836	21 7.1	+47 17	6.36	B5	57.1	− 0.8	− .11	.....	− .11	2	+ .06	7.5
201910	21 7.5	+40 47	7.30	B5n	52.5	− 5.4	− .16	.....	− .16	2	+ .01	8.8
201912	21 7.5	+29 18	6.77	B6	44.2	−13.4	− .16	.....	− .16	4	.00	8.2
202124	21 8.8	+44 7	7.83	*B*	55.1	− 3.2	− .05	.....	− .05	2	+ .14	.....
202214	21 9.3	+59 35	5.65	O9s	66.0	+ 7.7	− .08	.....	− .08	3	+ .15	9.1
202253	21 9.5	+43 28	7.70	*B3*	54.7	− 3.8	− .06	.....	− .06	2	+ .13	9.0
202347	21 10.1	+45 12	7.47	B5	56.0	− 2.8	− .16	.....	− .16	2	+ .01	9.0
202349	21 10.1	+37 21	7.34	*B3*	50.4	− 8.2	− .17	.....	− .17	2	+ .02	9.4
202654	21 12.2	+47 33	6.32	B5n	57.9	− 1.2	− .16	.....	− .16	2	+ .01	7.8
202850	21 13.5	+38 59	4.28	cA0	52.1	− 7.5	− .03	− .06	− .05	3, 2	+ .05	9.4
202883	21 13.7	+29 55	8.11	*B5*	45.6	−14.0	− .15	.....	− .15	2	+ .02	0.6
202900	21 13.8	+78 34	6.95	B3	80.5	+20.6	− .06	.....	− .06	2	+ .13	8.2
202904	21 13.8	+34 29	4.42	B3ne	48.9	−10.8	− .17	.....	− .17	4	+ .02	6.5
203025	21 14.6	+58 10	6.41	B3e	65.5	+ 6.1	− .02	.....	− .02	3	+ .17	7.4
203064	21 14.8	+43 31	5.06	O8nn	55.4	− 4.4	− .16	.....	− .16	2	+ .07	9.1
203245	21 16.0	+49 6	5.65	B5	59.4	− 0.7	− .14	.....	− .14	2	+ .03	7.0
203374	21 16.7	+61 25	6.64	Bone	68.0	+ 8.4	+ .01	.....	+ .01	2	+ .23	8.9
203467	21 17.3	+64 27	5.18	B3ne	70.2	+10.5	− .13	.....	− .13	2	+ .06	7.0
203664	21 18.6	+ 9 30	8.3	B2n	30.2	−28.5	− .20	.....	− .20	2	.00	11.3
203699	21 18.8	+13 37	6.71	B5e	33.7	−26.0	− .20	.....	− .20	2	− .03	8.5
203731	21 19.0	+40 16	7.42	B3ne	53.7	− 7.3	− .07	.....	− .07	3	+ .12	8.8
203938	21 20.2	+46 44	7.10	*B2*	58.3	− 2.7	+ .13	.....	+ .13	3	+ .33	7.8
204116	21 21.4	+54 57	7.96	Bon	64.0	+ 3.2	+ .09	.....	+ .09	3	+ .31	9.7
204150	21 21.6	+60 23	7.61	Bon	67.7	+ 7.2	− .15	.....	− .15	3	+ .07	11.0
204172	21 21.7	+36 14	5.84	Bo	51.3	−10.6	− .19	.....	− .19	3	+ .03	9.5
204403	21 23.2	+36 41	5.20	B3	51.9	−10.5	− .18	.....	− .18	2	+ .01	7.3
204536	21 24.2	+46 8	6.88	B5	58.4	− 3.6	− .12	.....	− .12	3	+ .05	8.1
204722	21 25.5	+43 54	7.52	B3ne	57.1	− 5.5	− .10	.....	− .10	3	+ .09	9.1
204770	21 25.8	+66 22	5.42	B5n	72.2	+11.3	− .16	− .13	− .14	2, 1	+ .03	6.8
204827	21 26.1	+58 18	8.3	*B*	66.7	+ 5.3	+ .15	.....	+ .15	2	+ .34	.....
204860	21 26.3	+45 4	6.96	B5n	58.0	− 4.7	− .14	.....	− .14	2	+ .03	8.4
205021	21 27.4	+70 7	3.32	B1	74.9	+14.0	− .25	.....	− .25	2	− .04	7.2
205060	21 27.7	+42 16	7.07	B5(n)e	56.2	− 6.9	− .11	.....	− .11	2	+ .06	8.2
205139	21 28.3	+60 1	5.52	B1s	68.1	+ 6.4	− .08	.....	− .08	2	+ .13	8.2
205196	21 28.6	+57 4	7.36	Bos	66.2	+ 4.1	+ .15	.....	+ .15	3	+ .37	8.7
205618	21 31.4	+29 18	8.2	B3ne	47.9	−17.1	− .17	.....	− .17	2	+ .02	10.3
205794	21 32.6	+57 1	8.7	B3	66.5	+ 3.7	.....	− .02	− .02	1	+ .17	9.7
E235565	21 34.3	+51 3	8.8	B2ne	62.9	− 1.0	− .20	.....	− .20	2	.00	11.8
206165	21 35.2	+61 38	4.87	cB2	69.8	+ 7.0	+ .02	.....	+ .02	3	+ .22	8.8
206183	21 35.3	+56 32	7.6	Bo	66.5	+ 3.1	.....	− .11	− .11	1	+ .11	10.7
206267	21 35.9	+57 2	5.64	O6n	66.9	+ 3.4	− .06	.....	− .06	2	+ .17	8.9
206327	21 36.3	+61 6	8.7	B2	69.5	+ 6.6	− .09	.....	− .09	3	+ .11	10.9
206672	21 38.6	+50 44	4.78	B3	63.3	− 1.7	− .16	.....	− .16	2	+ .03	6.8
206773	21 39.3	+57 17	6.98	Bone	67.4	+ 3.4	− .05	.....	− .05	3	+ .17	9.7
207198	21 42.2	+61 59	5.97	O9s	70.7	+ 6.9	+ .03	.....	+ .03	3	+ .26	8.7
207260	21 42.6	+60 40	4.46	cA2	69.9	+ 5.7	+ .15	+0.18	+ .16	3, 1	+ .20	8.6
207308	21 42.9	+61 50	7.6	B2	70.6	+ 6.6	−0.01	.....	−0.01	3	+0.19	9.3

TABLE 3—*Continued*

HD	R.A. 1900	Decl. 1900	m	Spec.	l	b	C_1			No.	E_1	m_0-M
							M	W	Mean			
207329	21h43m1	+51° 39′	7.45	B2e	64°.4	− 1°.4	+0.03	.....	+0.03	3	+0.23	8.8
207330	21 43.1	+48 51	4.26	B3	62.6	− 4.9	− .16	.....	− .16	3	+ .03	6.2
207538	21 44.6	+59 14	7.03	O9ss	69.2	+ 4.5	+ .03	.....	+ .03	3	+ .26	9.7
207563	21 44.8	+20 0	6.16	B3	43.6	−26.0	− .16	.....	− .16	2	+ .03	8.2
207673	21 45.6	+40 40	6.49	cA0	57.7	−10.3	+ .16	+0.11	+ .13	1, 1	+ .23	10.4
207757*	21 46.2	+12 9	7.5	Bep	37.7	−31.9	+ .06	.....	+ .06	3	.....	.....
207793	21 46.5	+52 14	6.56	B2n	65.1	− 1.3	+ .06	.....	+ .06	3	+ .26	7.7
207872	21 47.1	+59 43	8.2	B3n	69.7	+ 4.6	+ .04	.....	+ .04	2	+ .23	8.8
207951	21 47.8	+61 20	8.3	B2	70.8	+ 5.9	.....	− .05	− .05	1	+ .15	10.3
208057	21 48.5	+25 27	5.05	B3	48.3	−22.5	− .18	.....	− .18	2	+ .01	7.2
208095	21 48.8	+55 20	5.54	B8	67.3	+ 1.0	− .16	.....	− .16	2	− .03	6.6
208218	21 49.7	+62 13	6.76	B1s	71.5	+ 6.4	+ .01	.....	+ .01	3	+ .22	8.8
208220	21 49.7	+43 1	9.8	Bo	60.0	− 8.9	− .24	.....	− .24	2	− .02	13.8
208392	21 50.9	+62 8	7.10	B3ne	71.6	+ 6.3	.00	.....	.00	3	+ .19	8.0
208501	21 51.5	+56 8	6.01	B8s	68.0	+ 1.4	+ .26	.....	+ .26	3	+ .39	4.1
208682	21 52.9	+64 52	5.85	B3ne	73.4	+ 8.4	− .14	.....	− .14	2	+ .05	7.7
208905	21 54.3	+60 49	6.90	B2	71.2	+ 5.0	− .07	.....	− .07	2	+ .13	9.0
208947	21 54.7	+65 41	6.28	B3	74.0	+ 8.9	− .12	− .14	− .13	2, 1	+ .06	8.1
208973	21 54.9	+33 9	8.1	*B3*	54.6	−17.4	− .12	.....	− .12	2	+ .07	9.8
209008	21 55.1	+ 6 14	5.99	B5s	34.4	−37.5	− .16	.....	− .16	2	+ .01	7.5
209162	21 56.2	+62 47	8.7	B8	72.4	+ 6.5	.....	− .01	− .01	1	+ .12	8.7
209296	21 57.2	+56 14	8.3	B(5)e	68.7	+ 1.0	.00	.....	.00	3	+ .17	8.7
209339	21 57.6	+62 0	6.48	Bo	72.1	+ 5.7	− .12	.....	− .12	3	+ .10	9.7
209409	21 58.1	− 2 38	4.66	B6ne	26.0	−43.8	− .14	.....	− .14	2	+ .02	5.9
209419	21 58.2	+52 24	5.66	B5	66.7	− 2.2	− .16	.....	− .16	3	+ .01	7.2
209454	21 58.4	+61 4	7.9	B3n	71.7	+ 4.9	.....	− .06	− .06	1	+ .13	9.2
209481	21 58.7	+57 31	5.50	O9n	69.6	+ 2.0	− .12	.....	− .12	3	+ .11	9.2
209744	22 0.6	+59 19	6.74	B2n	70.9	+ 3.3	+ .01	.....	+ .01	3	+ .21	8.3
209961	22 2.0	+47 45	6.16	B3	64.5	− 7.6	− .16	.....	− .16	3	+ .03	8.2
209975	22 2.1	+61 48	5.17	O9	72.4	+ 5.3	− .12	.....	− .12	3	+ .11	8.9
210352A	22 4.8	+60 38	9.0	B2	72.0	+ 4.1	.....	− .08	− .08	1	+ .12	11.2
210352B	22 4.8	+60 38	9.8	B5	72.0	+ 4.1	.....	+ .10	+ .10	1	+ .27	9.5
210424	22 5.2	−12 4	5.40	B5	16.3	−50.5	− .16	.....	− .16	2	+ .01	6.9
210628	22 6.6	+55 36	6.87	B5s	69.5	− 0.2	− .04	.....	− .04	2	+ .13	7.6
210809	22 7.9	+51 56	7.6	O8	67.7	− 3.4	− .06	.....	− .06	2	+ .17	10.9
210839	22 8.1	+58 56	5.19	O6nf	71.5	+ 2.5	− .04	.....	− .04	2	+ .19	8.4
211924	22 15.5	+ 5 17	5.35	B7	38.0	−41.8	− .04	.....	− .04	3	+ .10	5.7
212044	22 16.4	+51 21	7.08	B2e	68.4	− 4.6	− .16	.....	− .16	2	+ .04	9.8
212076	22 16.6	+11 42	4.93	B3e	43.9	−37.3	− .16	.....	− .16	3	+ .03	6.9
212120	22 16.9	+46 2	4.66	B5	65.7	− 9.2	− .15	.....	− .15	2	+ .02	6.1
212222	22 17.6	+41 36	6.27	B7	63.5	−13.0	− .14	.....	− .14	2	.00	7.4
212455	22 19.3	+54 44	8.0	cB3	70.6	− 2.1	+ .09	.....	+ .09	2	+ .28	11.5
212571	22 20.2	+ 0 52	4.64	B1ne	34.8	−45.8	− .18	.....	− .18	2	+ .03	8.0
212883	22 22.4	+36 57	6.39	B2s	61.8	−17.5	− .16	.....	− .16	2	+ .04	9.1
212978	22 23.1	+39 19	6.07	B3	63.2	−15.5	− .18	.....	− .18	2	+ .01	8.2
213087	22 23.9	+64 37	5.66	B1	76.1	+ 6.3	.00	+0.02	+ .01	2, 1	+ .22	7.7
213322	22 25.5	+53 44	6.59	B5	70.9	− 3.2	− .10	.....	− .10	2	+ .07	7.7
213405	22 26.0	+64 36	8.0	*Bo*	76.2	+ 6.2	+ .04	.....	+ .04	8	+ .18	10.0
213420	22 26.1	+42 36	4.54	B3	65.4	−13.0	− .15	.....	− .15	4	+ .04	6.5
213571	22 27.3	+69 40	7.16	B5s	78.9	+10.6	− .14	.....	− .14	2	+ .03	8.6
213976	22 30.1	+40 16	7.00	B5	64.9	−15.4	− .14	.....	− .14	2	+ .03	8.4
214167	22 31.4	+39 7	6.55	B2	64.5	−16.5	− .24	.....	− .24	1	− .04	9.8
214168	22 31.4	+39 7	5.83	B3ne	64.5	−16.5	− .14	.....	− .14	3	+ .05	7.7
214240	22 31.8	+49 33	6.20	B3	69.7	− 7.4	− .11	.....	− .11	2	+ .08	7.8
214263	22 31.9	+37 19	6.75	B3	63.7	−18.1	− .20	.....	− .20	2	− .01	9.0
214432	22 33.0	+38 55	7.4	B3n	64.7	−16.8	− .15	.....	− .15	2	+ .04	9.3
214652	22 34.6	+36 51	6.67	B3	63.9	−18.8	− .15	.....	− .15	2	+ .04	8.6
214680	22 34.8	+38 32	4.91	O9s	64.8	−17.3	− .23	.....	− .23	4	.00	9.4
214923	22 36.5	+10 19	3.61	B8	47.7	−41.4	− .14	.....	− .14	1	− .01	4.5
214930	22 36.6	+23 19	7.30	B3s	56.8	−30.7	−0.12	.....	−0.12	3	+0.07	9.0

TABLE 3—*Continued*

HD	R.A. 1900	Decl. 1900	m	Spec.		b	C_1			No.	E_1	m_0-M
							M	W	Mean			
214993	22h37m0	+39°43′	5.18	B1s	65°8	−16°5	−0.20	.....	−0.20	5	+0.01	8.7
215191	22 38.4	+37 17	6.22	B3	64.8	−18.8	− .14	.....	− .14	2	+ .05	8.1
215227	22 38.6	+44 12	8.9	Bne	68.2	−12.6	− .09	.....	− .09	3	+ .10	.....
215371	22 39.6	+64 48	6.76	B3	77.6	+ 5.7	− .11	.....	− .11	3	+ .08	8.4
215733	22 42.2	+16 43	7.2	*B2*	53.9	−37.0	− .18	.....	− .18	3	+ .02	10.1
216014	22 44.2	+64 32	6.83	Bo	77.9	+ 5.3	+ .05	.....	+ .05	3	+ .27	8.8
216044	22 44.5	+54 36	8.6	*B2*	73.7	− 3.7	− .08	.....	− .08	3	+ .12	10.8
216200	22 45.8	+41 26	5.84	B3	68.2	−15.7	− .07	.....	− .07	2	+ .12	7.2
216248	22 46.3	+58 8	10.0	*B*	75.4	− 0.6	− .06	+0.02	.00	3, 2	+ .19	.....
216411	22 47.6	+58 28	7.16	Bos	75.7	− 0.4	+ .15	.....	+ .15	2	+ .37	8.5
216438	22 47.8	+53 11	8.6	*B2*	73.6	− 5.2	− .13	.....	− .13	3	+ .07	11.1
216532	22 48.6	+61 54	8.4	*B3*	77.3	+ 2.6	+ .03	+ .08	+ .06	2, 1	+ .13	9.7
216629	22 49.4	+61 36	9.4	*B*	77.2	+ 2.3	+ .25	+ .25	+ .25	7, 2	+ .44	.....
216658	22 49.6	+61 36	9.1	*B*	77.3	+ 2.3	+ .19	+ .19	+ .19	5, 2	+ .38	.....
216711	22 50.0	+62 4	9.2	*B*	77.5	+ 2.7	+ .21	+ .14	+ .16	4, 4	+ .35	.....
216898	22 51.8	+61 46	8.3	*B2*	77.6	+ 2.4	+ .10	+ .08	+ .09	4, 1	+ .29	9.3
216916	22 51.9	+41 4	5.54	B3s	69.1	−16.5	− .17	.....	− .17	4	+ .02	7.6
216927	22 52.0	+58 22	8.7	*B*	76.2	− 0.7	+ .24	+ .27	+ .26	3, 1	+ .45	.....
217035	22 52.6	+62 19	7.76	*B5*	77.9	+ 2.9	+ .07	+ .04	+ .05	2, 1	+ .22	7.8
217050	22 52.7	+48 9	5.20	B3ne	72.2	−10.1	− .17	.....	− .17	4	+ .02	7.3
217061	22 52.8	+62 5	9.0	*B*	77.8	+ 2.6	+ .18	+ .20	+ .19	4, 2	+ .38	.....
217101	22 53.1	+38 48	6.07	B2	68.3	−18.7	− .17	.....	− .17	2	+ .03	8.9
217227	22 54.2	+43 18	7.02	B3s	70.4	−14.7	− .16	.....	− .16	2	+ .03	9.0
217297	22 54.7	+63 10	7.36	Bo	78.4	+ 3.5	+ .01	.....	+ .01	2	+ .23	9.7
217463	22 55.8	+62 14	9.2	*B2*	78.2	+ 2.6	+ .09	+ .12	+ .11	2, 2	+ .31	10.0
217543	22 56.3	+38 10	6.39	B3ne	68.6	−19.5	− .16	.....	− .16	2	+ .03	8.4
217675	22 57.3	+41 47	3.63	B5n	70.3	−16.3	− .14	.....	− .14	3	+ .03	5.0
217811	22 58.2	+43 31	6.32	B3s	71.2	−14.8	− .12	.....	− .12	2	+ .07	8.0
217817	22 58.3	+59 18	6.87	B3	77.3	− 0.2	− .10	.....	− .10	3	+ .09	8.4
217891	22 58.8	+ 3 17	4.58	B5e	48.0	−50.4	− .16	.....	− .16	2	+ .01	6.1
217943	22 59.2	+59 54	6.57	B3	77.7	+ 0.2	− .10	.....	− .10	2	+ .09	8.1
218342	23 2.1	+62 41	7.46	B2	79.0	+ 2.8	+ .10	.....	+ .10	3	+ .30	8.4
218344	23 2.1	+50 33	7.17	B3	74.6	− 8.5	− .18	.....	− .18	2	+ .01	9.3
218376	23 2.4	+58 53	4.93	cB1	77.7	− 0.8	− .18	.....	− .18	3	+ .03	10.2
218407	23 2.7	+45 33	6.56	B3	72.8	−13.2	− .15	.....	− .15	3	+ .04	8.5
218440	23 3.0	+59 13	6.28	B3s	77.9	− 0.5	− .12	.....	− .12	2	+ .07	8.0
218537	23 3.7	+63 6	6.19	B3	79.3	+ 3.1	− .12	− .12	− .12	3, 1	+ .07	7.9
218674	23 4.8	+49 7	6.53	B3n	74.4	−10.0	− .10	.....	− .10	2	+ .09	8.1
218723	23 5.2	+64 41	6.62	B3	80.1	+ 4.5	− .10	.....	− .10	3	+ .09	8.2
218915	23 6.7	+52 31	7.06	O9s	76.0	− 6.9	− .10	.....	− .10	2	+ .13	10.7
219063	23 7.9	+64 11	7.22	B5	80.2	+ 3.9	− .12	.....	− .12	2	+ .05	8.5
219188	23 8.9	+ 4 27	6.93	B2n	52.3	−50.8	− .14	.....	− .14	3	+ .06	9.5
219523	23 11.3	+63 44	7.07	B5	80.4	+ 3.4	− .10	.....	− .10	2	+ .07	8.2
219688	23 12.7	− 9 44	4.56	B5n	37.4	−62.5	− .11	.....	− .11	2	+ .06	5.7
220057	23 15.7	+60 36	6.82	B5	79.8	+ 0.3	− .08	.....	− .08	4	+ .09	7.8
220058	23 15.7	+55 15	8.51	B(1)ne	78.1	− 4.8	− .13	.....	− .13	3	+ .08	11.6
220562	23 19.6	+56 59	6.76	B5	79.0	− 3.4	− .01	.....	− .01	3	+ .16	7.2
220598	23 19.9	+35 49	6.82	B5n	72.4	−23.5	− .16	.....	− .16	3	+ .01	8.4
221253	23 25.4	+58 0	4.89	B3	80.2	− 2.6	− .18	.....	− .18	3	+ .01	7.0
221711	23 29.4	+54 56	7.41	B3	79.9	− 5.7	− .08	.....	− .08	2	+ .11	8.8
222263	23 34.0	+56 26	8.7	*B5*	81.0	− 4.4	− .01	.....	− .01	2	+ .16	9.2
222568	23 36.6	+67 48	8.1	*B3*	84.0	+ 6.5	+ .03	.....	+ .03	2	+ .22	8.8
223128	23 41.8	+66 13	5.94	B2s	84.2	+ 4.9	− .14	.....	− .14	5	+ .06	8.5
223152	23 42.0	+50 41	7.47	B5	80.7	−10.3	− .12	.....	− .12	3	+ .05	8.7
223229	23 42.6	+46 16	5.84	B3	79.8	−14.6	− .16	.....	− .16	2	+ .03	7.8
223329	23 43.6	+55 5	7.56	*B5*	81.9	− 6.0	− .10	.....	− .10	2	+ .07	8.7
223385	23 44.0	+61 40	5.61	cA2ea	83.4	+ 0.4	+ .25	+ .23	+ .24	4, 2	+ .29	9.1
223387	23 44.0	+56 40	9.1	B(o)ne	82.3	− 4.5	− .06	−0.10	− .09	2, 2	+ .13	12.1
223924	23 48.6	+56 16	8.3	*B2*	82.9	− 5.0	− .15	.....	− .15	2	+ .05	10.9
223960	23 48.9	+60 18	6.98	cA0ea	83.7	− 1.1	+0.21	.....	+0.21	3	+0.31	10.3

TABLE 3—*Continued*

HD	R.A. 1900	Decl. 1900	m	Spec.	l	b	C_1			No.	E_1	m_0-M
							M	W	Mean			
223987	$23^h49^m.2$	+61° 3′	7.56	Bo	83°.9	− 0°.4	.....	+0.08	+0.08	1	+0.30	9.4
224055	23 49.7	+61 17	7.16	cB3ea	84.0	− 0.1	+0.20	.....	+ .20	3	+ .39	9.9
224151	23 50.5	+56 53	6.05	B1	83.3	− 4.5	− .06	.....	− .06	4	+ .15	8.6
224404	23 52.5	+59 28	6.4?	B8n	83.9	− 2.0	− .02	− .08	− .05	3, 1	+ .08	6.7
224424	23 52.7	+59 9	8.4	Boea	84.0	− 2.3	+ .21	.....	+ .21	4	+ .43	9.3
224544	23 53.7	+31 48	6.36	B5ne	78.7	−29.2	− .15	.....	− .15	2	+ .02	7.8
224559	23 53.8	+45 52	6.46	B3ne	81.7	−15.4	− .18	.....	− .18	2	+ .01	8.6
224572	23 53.9	+55 12	4.93	B2n	83.4	− 6.2	− .17	.....	− .17	3	+ .03	7.7
224590	23 54.1	+59 29	9.7	B3n	84.2	− 2.0	.....	− .04	− .04	1	+ .15	10.9
224868	23 56.3	+60 17	7.36	B5	84.6	− 1.3	− .06	.....	− .06	2	+ .11	8.2
224905	23 56.6	+59 54	8.5	B3n	84.6	− 1.7	.....	− .08	− .08	1	+ .11	9.9
225094	23 58.3	+63 5	6.26	cB2ea	85.3	+ 1.4	+ .03	+ .02	+ .02	3, 1	+ .22	10.2
225095	23 58.3	+55 0	7.56	B1e	84.0	− 6.5	− .10	.....	− .10	2	+ .11	10.4
225146	23 58.8	+60 33	8.6	Bo	85.0	− 1.1	.....	− .02	− .02	1	+ .20	11.1
225160	23 58.9	+61 40	8.2	O8ea	85.1	+ 0.1	− .04	−0.04	− .04	2, 2	+ .19	11.4
225190	23 59.2	+53 43	7.55	*B3*	83.9	− 7.8	− .13	.....	− .13	2	+ .06	9.3
225257	23 59.7	+57 58	6.51	B3	84.8	− 3.6	−0.10	.....	−0.10	2	+0.09	8.1

NOTES TO TABLE 3

8768 HD magnitude 8.0.
21448 Double.
24534 X Persei, spectrum variable, magnitude 6.2–6.9.
25204 λ Tauri.
25638 Magnitude of A; combined color.
28446 Magnitude of A; combined color.
31293 Has interstellar D lines.
33203 Double.
36340 HD magnitude 9.0.
36954 HD magnitude 8.1.
37022 Four stars, 5.36 O7, 6.84 B2, 6.85 Bo, 7.93 B2; combined color equivalent to Bo.
E259597 Poor.
47398 Poor.
50820 Composite.
53179 Z Canis Majoris, spectrum peculiar
100600 Magnitude of A; combined color.
142983 HD spectrum B3p.
147933 Magnitude of A; combined color.
156247 U Ophiuchi.
156633 ω Herculis.
1649 6 HD magnitude 9.0.
164947 HD magnitude 10.0.
164992 HD magnitude 10.7.
165595 HD magnitude 9.4.
165612 HD magnitude 8.9.
166508 HD magnitude 10.3.
166764 Spectrum doubtful.
167224 HD magnitude 8.9.
167287 HD magnitude 8.3.
167397 HD magnitude 9.2.
167432 HD magnitude 10.6; combined magnitude and color.
167478 HD magnitude 10.3.
167611 HD magnitude 10.6.
168021A Magnitude of A; color of AB.
168230 HD magnitude 10.6.
168279 HD magnitude 10.6.
169753 RZ Scuti.
171432 HD magnitude 8.1.
174638 β Lyrae.
178849 Double.
181987 Z Vulpeculae.
189550 HD magnitude 8.5.
191566 Magnitude of A; combined color.
193237 P Cygni, spectrum peculiar.
198846 Y Cygni.
207757 Spectrum peculiar.

proper motions of the *Boss General Catalogue* and corrected them for the estimated absorption. With these we included new solutions obtained from radial velocities and from close pairs of B stars with the same color excess. The new scale of absolute magnitudes and the previous one for 733 stars are given in Table 4.

In the present work we have not attempted to distinguish between stars with sharp lines and those with nebulous lines except for the c stars. There are thirty or forty stars with outstanding color excesses which are probably unrecognized c stars. Likewise, among

the fainter B stars of the *Henry Draper Catalogue*, the presence or absence of the bright *Hα* line is not known. We have therefore used the mean absolute magnitudes of Table 4 without trying to allow for individual differences which, for a large portion of the stars observed, cannot be recognized.

Results.—The photoelectric colors of B stars furnish an excellent means for the study of selective space absorption in the galaxy, and the observational results in Table 3 have been communicated in advance to several astronomers who were interested in this question.

TABLE 4

MEAN ABSOLUTE VISUAL MAGNITUDES

Spectrum	1332 Stars	733 Stars	Difference
cB, cA	−5.5	.....	.....
O	−4.5	−4.0	−0.5
Bo	−3.9	−3.2	−0.7
B1	−3.6	−2.5	−1.1
B2	−3.0	−1.8	−1.2
B3	−2.2	−1.3	−0.9
B4	−1.9	−0.9	−1.0
B5	−1.6	−0.7	−0.9
B6	−1.4	−0.5	−0.9
B7	−1.1	−0.3	−0.8
B8	−0.8	−0.2	−0.6
B9	−0.4	+0.1	−0.5

At the McDonald Observatory symposium some of the general conclusions we presented were:

1. The color excesses of B stars are as closely correlated with the intensities of interstellar lines as the intensities of those interstellar lines in the same stars are correlated with each other.

2. The reddest B stars are strongly concentrated toward the galactic equator. They are especially numerous toward the center of the galaxy, but do not occur near the anticenter.

3. In several bright regions of the Milky Way—namely, the small cloud in Sagittarius, the cloud in Cygnus, and the double cluster in Perseus—there are no B stars of normal color. The average color excess ranges from 0.10 to 0.20 mag., and hence all these star groups would look at least twice as bright if we could see them in the clear.

4. The apparent distribution of the reddened B stars shows that the absorption in the galaxy is obviously so irregular and spotted that a constant coefficient of absorption cannot be used for any large region of space. The assumption of a uniform absorbing layer near the plane of the galaxy will have to be revised.

This investigation has been supported by grants from the Alumni Research Fund of the University of Wisconsin, from the Rumford Fund of the American Academy of Arts and Sciences, and from the Observatory Council of the California Institute of Technology.

CARNEGIE INSTITUTION OF WASHINGTON
MOUNT WILSON OBSERVATORY,
UNIVERSITY OF WISCONSIN
WASHBURN OBSERVATORY
August 1939

THE GENERAL ILLUMINATION DURING A TOTAL SOLAR ECLIPSE

JOHN Q. STEWART AND C. D. MACCRACKEN

ABSTRACT

Although Halley noted at the total eclipse of May 3, 1715, that diffused daylight from outside the moon's shadow was an important factor in determining the general brightness, its study since has been neglected. Observations of it during the long eclipse of June 8, 1937, at sea, from the Isthmian freighter "Steelmaker," are given. Other relevant observations are reviewed. Remarks about the "globular corona" are included. A roughly approximate mathematical theory of scattering by pure air into the umbra is presented. The results are discussed for the noon point, as compared with the sunrise or sunset points, and for lunar shadows of different sizes and with the observer at varying distances off center. From two methods it is concluded that the integrated brightness of the horizon glow at the noon point at mid-totality, June 8, 1937, was of the order 1/5000th zenith sea-level sun, or 100 full moons. This estimate may be too large by a small factor; but it is certain that diffused daylight far outshines the corona, even at the darkest eclipses. Careful observations of general brightness on October 1, 1940, will be desirable.

It is emphasized that for study of the corona's structure a large shadow with the sun near the zenith is a requisite (and it is desirable also that the observer be at a high elevation). A list of six eclipses, 1940–1973, is given which come particularly close to this standard. In four of these the noon point is far at sea.

In short reports[1] of observations made from the freighter "Steelmaker" of the total solar eclipse of June 8, 1937, attention was called to the unexpectedly bright glow which ringed the sky above the horizon. A detailed account has not been published previously.

I. OBSERVATIONS FROM THE "STEELMAKER"

During the 7^m6^s of observed totality (easily a record) the ship was proceeding along the central line of the shadow path, course 88° true, at a reduced speed of 8 or 9 knots. The G.C.T. of mid-totality was observed as $20^h30^m27^s$; ship's time, 11:30:27 A.M. Ship's position was W. 133°38′, N. 9°49′.5. The exact noon point of the eclipse, at W. 130°27′, N. 9°54′, was only 191 nautical miles to the east. The sun's computed zenith distance during totality was 14°.2.

Although the importance of precise observations of general sky illumination was not fully recognized in advance, several officers and members of the crew were instructed in rehearsals to assist in

[1] J. Q. Stewart and James Stokley, *Pub. A.S.P.*, **49**, 186, 1937; *Pop. Astr.*, **45**, 358, 1937 (but the longitude there is incorrectly given as W. 130°38′, for 133°38′); *Pub. A.A.S.*, **9**, 58, 1937. See also *U.S. Steel News*, **3**, 12, 1938, and *Yale Review*, **29**, 51, 1939.

identifying what stars became visible and to note the appearance of the moon's shadow. The party was prepared for third-magnitude stars; but the dusk was unexpectedly bright, and Venus, Mercury, Sirius, Rigel, Betelgeuse, and possibly Procyon and Capella were all that were reported. At mid-totality ordinary newspaper print could just be read.

The accounts of the "Steelmaker" observers, compiled immediately afterward, afford the following description of the passage of the shadow. The results are given in detail because no comparable account exists. Astronomers at eclipses have been so occupied with instrumental study of the sun itself that observation of the general twilight illumination is a neglected field.

Weather conditions are of importance. On June 8, sky transparency remained excellent all morning but worsened rapidly after noon. Many cumulus clouds were low on the horizon, and close at hand low clouds scudded with the fresh breeze, which was from E. by N. The zenith remained continuously unobscured, although between first and second contacts there was an occasional alto-cirrus overcast. But the transparency which had permitted a daylight sextant altitude of Venus at 9:00 A.M. was, around the zenith, unabated through totality.

Just before 10:00 A.M. first contact was timed, and a few minutes later the ship's radio operator tuned in the broadcast of totality from Canton Island. Seventy-seven minutes after the shadow left Canton it reached the "Steelmaker." This must be the first time that the moon's approach was directly clocked. The mate saw Venus shining out astern at 11:23. An arc of slate-blue shadow was rising then very swiftly up the western sky, overtaking the ship. Second contact was signaled at 11:26:56. So far as is known, no other ships were in the shadow track. There was no land within 1300 miles of the noon point.

The shadow's advance was not noticeable across the dull-slate sea. In the sky the shadow was clearly visible—a great dusky blue umbrella with tawny "twilit" sky ringing its moving rim. Only half a minute after second contact the shadow's western edge, nearly 150 miles away, was already evident. Above far clouds to the west diffused daylight completed a band of illuminated sky which ex-

tended altogether around the horizon. (A similar view of the farther margin of the oncoming shadow is depicted on Mr. Howard Russell Butler's painting of the approach of the moon's shadow on June 8, 1918, at Baker, Oregon.)

At mid-totality the saffron margin of daylit sky extended uniformly around the horizon of the "Steelmaker," except perhaps due eastward, where the sky was overcast. The yellow-tan glow reached then to a uniform altitude of about 14°. Where it met the blue shadow, it seemed almost as sharp edged as a sharp-edged cloud. The shadow, dusky blue with a slight purplish tinge, was darkest at the zenith.

Even at mid-totality the corona contributed no appreciable fraction of the general illumination. The sky did not brighten much near the corona, although the non-appearance of Aldebaran, 12° from the sun, is indicative of a slight brightening. No shadows were cast by the corona's steely light. The dusk was markedly deepest at mid-totality and decreased again as totality progressed. When deepest, the dusk was not decidedly more than during a heavy thunderstorm on a summer day.

At 6 minutes the oncoming light rode far up the west. No one noticed its gradation into blue; but when the diamond ring appeared, the sky was blue around the sun. The dull-blue shadow hurried down the east, its farther margin lost beyond the overcast.

Measures of the corona's brightness were secured[2] by two methods. Photographs of it with short-focus cameras were unsatisfactory. Gyroscopic stabilization of camera platforms would result in very marked improvement,[3] but coronal photography is not a promising field at sea. Airplanes or stratosphere balloons offer a stabler base.

Visual inspection of the corona, on the other hand, can be carried out very well at sea. Viewed so near the zenith, it was extraor-

[2] James Stokley, *Pub. A.A.S.*, **9**, 59, 1937. The radio operator, the second assistant engineer, the deck engineer, and a member of the crew made the measurement with photocells. Stokley himself used a Macbeth illuminometer, and the results agreed in indicating that this corona's total light was roughly equal to the light of the full moon. (More precise measures on land gave about half the full moon's light.)

[3] H. L. Cooke, *Report of the Canadian Air Board for 1922*, pp. 62–69; U.S. Patents 1586070–1, May 25, 1926.

dinarily sharp. The foggy, feathery appearance of the streamers common at lower solar altitudes was absent. The streamers exhibited hard geometrical outlines, but the longest was visible for only 2 diameters of the sun. Between this and a multitude of short needle-like spikes circling the moon, only a few minutes of arc in length, the gradation in size was fairly continuous. Captain Earl D. Lucas (observing from the wheelhouse roof) compared the streamers to searchlight beams shining across a fog.

The inner corona, pure white and brilliant, showed no yellow tinge where it met the moon, and appeared unusually narrow—no doubt partly because of the splendid seeing which permitted following details of spikes close to the moon and partly because of the extraordinarily large difference between the angular diameters of moon and sun. For the latter reason the chromosphere was hidden during most of totality. Through field glasses one received the impression that the inner corona as a separate entity might be nonexistent—that its apparently uniform brightness could represent closely crowded short radial spikes. Even the most unobservant members of the crew were impressed by the large prominences.

One of the crew, W. S. Milliken, sketched the corona from the boat deck, giving especial attention to colors. The moon's disk, he noted, was "grayish blue with brown center." At second contact, for a fraction of a minute after removing his blindfold, he was more struck with a "pearly gray silver" halo around the dark moon, in which the streamers seemed imbedded, than with the streamers themselves. On his sketch he marked this halo as extending continuously out from the dark moon's edge about a radius and one half, or 22′, not quite at an even distance all around but nearly so. In color its light resembled the streamers; it was a magnitude or more lower in surface brightness, according to Stewart's recollection. Around its outer edge, Milliken noted, the sky was dark blue with a purplish tinge.

This apparition strongly suggests the "globular corona" recorded for the Hayden Planetarium–Grace expedition on Major Stevens's photographs[4] $1\frac{3}{4}$ hours later. Because of the low sun near the Peruvian coast, these photographs, although from about 25,000

[4] Statement from Harvard Observatory, *The Sky*, September, 1937.

feet, were taken through an air path about twice the optical length of the air path above the "Steelmaker." Canton Island's less favorable location, at sea-level and with the sun at 22° altitude, made the air path toward the sun there longer still. The halo was not noticed by Mr. Charles Bittinger, the painter, nor, apparently, by other members of the party at Canton Island. At least one more eclipse will be required to confirm its existence.

At eclipses astronomers have been, for many years, completely engrossed by exacting, prearranged programs. Worth-while contributions can be expected from acute observers who are free to look around. Certain types of observation can be made from fair-sized ships at sea, or airplanes, almost as well as from land.

For the courtesy which made the two astronomers welcome as guests on the ship from Honolulu to Brooklyn, thanks are due to Captain Logan Cresap, marine superintendent, and Mr. John McAuliffe, president, of the Isthmian Steamship Company (which is a subsidiary of the United States Steel Corporation), and to representatives of the Company at several ports. Acknowledgments are due also to the Matson Navigation Company, to Mr. Donald Morrison, to Dr. Gustavus W. Cook, and to Princeton University.

II. OLDER OBSERVATIONS, AND DISCUSSION

The antique but still stimulating historical summary by Robert Grant[5] includes several comments on the general twilight illumination during total eclipses. At Lodi in Lombardy, for example, during the eclipse of the morning of July 8, 1842, two reddish zones were seen extending along the horizon, one to the south, the other to the north.[6] "They were of a dull copper color, totally different from the ruddy hue of the aurora or the twilight. The rest of the heavens passed without any degradation [i.e., sharply?] to a dark azure inclining to violet." Stars of the first magnitude were seen, but not of the second. The noon point was in western Siberia, almost 3000 miles east and north of Lombardy. The sun's altitude in western Europe was low, and the elongation of the moon's shadow there to east and west accounts (see sec. iii) for the failure of the copper-colored zones to continue along the eastern and western horizon at

[5] *History of Physical Astronomy*, pp. 358–412, London, 1852. [6] *Ibid.*, p. 370.

Lodi. At one or two recent eclipses, with the sun at low altitudes, photographs of the horizon glow have been taken which show it similarly rising higher in the sky to north and south than to east and west.

Grant's records make it plain that not uncommonly stars considerably fainter than the first magnitude are visible to the unaided eye. It was Edmond Halley who called attention to diffused daylight from outside the moon's shadow as an important factor in determining the general brightness, and on this principle explained the fact that at London the obscurity at the total eclipse of May 3, 1715, was less intense than in parts of England which were more deeply immersed in the moon's shadow. Remarkably little attention has been paid to the problem since.

On June 8, 1937, Dana K. Bailey, of the Hayden Planetarium–Grace expedition, stationed with Serge A. Korff at Moro, Peru, at 2400 feet elevation (the sun's altitude during eclipse being only 8°) reported[7] that stars of the third magnitude became visible.

Evidently the position of the "Steelmaker," although the best position occupied by astronomers known to history with regard to length of totality, was not the best with regard to lack of illumination (but see secs. v and vi). We tentatively attributed the unexpected brightness to a very high, thin haze, because Stewart had not noticed the saffron color from Garden City, Long Island, on January 24, 1925, or from Locke Mills, Maine, on August 31, 1932. The visible arcs of low sky had a bluish-white hue at these places, which were near the shadow edge. The discussion in subsequent sections shows that scattering of sunlight from outside the 1937 shadow by pure air would have diffused about the amount and color of light observed from the ship. The hypothesis of an unusual stratospheric haze therefore is withdrawn.[8]

It would be possible to quote statements in the recent literature which imply that most of the general illumination comes from the corona rather than from the scattered daylight, although the con-

[7] Dorothy Bennett, *Pop. Astr.*, **45**, 356, 1937.

[8] Report of Princeton University Observatory for 1937, *Pub. A.A.S.*, **9**, 197, 1938. Mr. E. W. Woolard, of the United States Weather Bureau, in correspondence during the late summer of 1937 suggested, after conversation with Dr. Humphreys, that scattering by pure air might be adequate.

trary is definitely the case, as Dr. W. J. S. Lockyer and others[9] have indicated. Lockyer's interesting paper contains an inadequate statement of theory: "At the sunrise and sunset ends of the track the illumination will be greatest, and it will be least on that portion where the sun is on the meridian during totality. Further, the nearer the sun is to the zenith during totality the more the illumination will be reduced." The discussion below indicates the exact opposite for long eclipses. If the moon's shadow is small, as it was for the eclipse he discussed, his statement holds—indeed, an eclipse total at noon may even be annular elsewhere.

The papers quoted by Grant would repay careful re-examination by a modern student of archeological bent. Grant's quotations are not uniformly trustworthy, as is indicated by his assigning a wrong date to the annular eclipse of September 18, 1838, which Joseph Henry observed in Princeton, New Jersey.

III. AN APPROXIMATE ANALYTICAL SURVEY OF THE PROBLEM

Because of the importance of secondary and tertiary scattering, a complete mathematical study of the diffusion of sunlight into the moon's shadow in the air would be very involved. The "primary" scattering of direct sunlight occurs only outside the shadow. Under the shadow "secondary" scattering from the rays coming in more or less horizontally throws light into the air overhead. And other scattering diverts some of it down again. These latter two processes do not increase the general brightness, but they are just the processes which mask faint details of the corona. Other secondary and tertiary scattering in the lower air reinforces the original horizontal incoming beam, reducing the effective extinction and tending to increase the general brightness in the shadow.

All these processes occur at all levels in the atmosphere where the density, and so the efficiency per unit volume as scattering agent, of air has values widely various. The scattering is sharply dependent upon the wave length of the light. Even if the air is altogether haze-free, the presence of shadowing masses of clouds or mountains, or of bright snow fields, would introduce an additional complication. Molecules do not scatter equally in all directions; scattered light is

[9] W. J. S. Lockyer, *M.N.*, **87**, 668, 1927; **88**, 97, 1927; G. Armellini and G. Conti, *A.N.*, **230**, 434, 1927.

polarized. The energy of solar radiation is a function of wave length, as is also the sensitivity of the eye to radiant energy.

All these considerations are concerned in calculations of sky brightness in normal twilight and when the uneclipsed sun is above the horizon.[10] At eclipses the variation in color and brightness of the partly eclipsed sun, due to limb effect just outside the umbra, requires also to be included.

The following treatment is simplified to a point which reduces accuracy to orders of magnitude only.

Taking the earth's radius as r, the height y above sea-level of a point P in the air which appears at an altitude θ to an observer at O is, approximately,

$$y = x \tan \theta + \frac{x^2}{2r}, \tag{1}$$

where x is $\overline{OP} \cos \theta$, and x^2/r^2 has been neglected.

The scattering of an element of air at P will be linearly proportional to the density of the air there. Hulburt,[11] extending well-known tables of W. J. Humphreys,[12] adopted for n, the number of molecules per cubic centimeters

$$n = n_0 e^{-py}, \tag{2}$$

where, below $y = 10^6$ cm (or 10 km), p is 1.11×10^{-6} cm^{-1}; and above, p is 1.54×10^{-6} cm^{-1}.

At a distance z outside the edge of the umbra of the moon's shadow (z being measured at right angles to the axis of the shadow cone in the plane tangent to the earth at the center of the umbra) the fraction, σ, of the sun's disk exposed can, nearly enough, be represented by

$$\sigma = Az + Bz^2, \tag{3}$$

σ not being too large. Here A and B depend upon the distances at the particular eclipse of the sun and moon from the earth's shadowed surface. For the noon point, June 8, 1937, the moon's distance was

[10] E. O. Hulburt, *J. Opt. Soc. Amer.*, **28**, 227, 1938.

[11] *Ibid.*, eq. (3).

[12] *Physics of the Air*, p. 74, Philadelphia, 1929.

354,000 km. A shift of 103 km in z corresponded, therefore, to a shift of 1′ of the moon's disk in front of the sun's. The ratio of angular semidiameters, moon to sun, was about 16′.9/15′.8. Two disks in this ratio were cut from graph paper, and a count of squares showed that, with $0 < \sigma < 0.08$ and $0 < z < 600$ km, A was 924×10^{-7} km^{-1} and B was 1.38×10^{-7} km^{-2}. Because of darkening at the limb, the fraction of full sunlight available to illumine air at distance z is less than σ. The ratio of light (compared to full sun) to area, ζ_λ, becomes less the shorter the wave length. It varies through the visible region roughly from $\frac{1}{2}$ to $\frac{3}{4}$ for the region of the limb which is effective.[13] In an exact solution ζ_λ would have to be found as a function of z as well as of λ. In the relations immediately following, ζ_λ is assumed independent of z.

Combining (1), (2), and (3), the total energy scattered in all directions from a unit volume of air at P is proportional to

$$S = k_\lambda I_\lambda (Az + Bz^2) e^{-p(x \tan \theta + x^2/2r)}, \tag{4}$$

where I_λ is the intensity of primary sunlight at P. The factor k_λ is the scattering coefficient and is a function of the wave length λ.

For an eclipse with the sun at the zenith, the umbra projects as a circle on the earth's surface, of radius b, and

$$z = x - b, \tag{5}$$

if O is at the center of the shadow. For the eclipse of June 8, 1937, b was about 124 km at the noon point. The zenith distance of the sun there, practically at the position of the "Steelmaker," can be taken, nearly enough, as zero.

The energy which reaches O directly from P along the line PO is reduced by secondary scattering below the value S of (4). The length PO is x sec θ, but the density of air along PO varies with its elevation above sea-level. The total air mass along OP is derived by substituting (1) in (2), multiplying by dx sec θ, and integrating from O to x. This, in turn, must be multiplied by the scattering coefficient (which is proportional to k_λ). The exponential function is taken of the resultant quantity with sign reversed, and this repre-

[13] G. Abetti, *The Sun*, pp. 315–317, New York, 1938.

sents the fraction of the energy S which survives as far as O in the direct beam along PO.

The final brightness of the sky as seen from O at altitude θ requires integrating this result, in turn, with regard to all elements P outside the shadow along a straight line OP of indefinite extent. In addition, in an exact treatment, the solid angles of the elemental ray cones would be considered. The full analytical treatment is intricate, and in order to feel out the problem the two integrations were performed numerically in illustrative special cases. Furthermore, in order to avoid complication in dealing with scattering in different directions, it was assumed that half the scattered energy S of (4) moved toward O (and that the other half moved out to space). This assumption can be correct only with respect to order of magnitude. It finds partial justification in the well-known principle that the brightness of an extended surface is independent of the distance.

The sunlight effective in producing the horizon glow always comes from regions fairly close to the limb. It was taken as equivalent approximately to black-body radiation at a temperature of 5700°. The corresponding computed intensity I_λ from Planck's formula as a function of wave length is listed in Table 1. The energy wavelength distribution is a bit flatter to the redward of the maximum than it is for the whole sum. Table 1 also gives the scattering coefficient k_λ in a special form. It was computed from the well-known Rayleigh formula relating scattering to refractive index; values of the latter were taken from the *International Critical Tables*.[14] Table 1 also includes, for reference, the relative sensitivity, S_λ, of an average eye to light of different wave lengths.[15]

The projection of the umbra of the moon's shadow on the earth's surface can be taken, in general, practically as an ellipse with a semimajor axis, a, extending in the azimuth of the moon and enlarged over the radius of the shadow cone, b, by the factor, cosec h, or the cosecant of the sun's altitude. The semiminor axis, b, is equal to the radius of the cone at the region of intersection with the earth's surface. Consequently, the eccentricity of the ellipse is cot h and its

[14] **7**, 2–3, New York, 1930.

[15] R. A. Houstoun, *Vision and Colour Vision*, p. 81, London, 1932.

area is πb^2 cosec h. Evidently in eclipses of moderate or long duration the area is much greater where the sun is at a low altitude than it is at the noon point, for cosec h increases faster than b^2 decreases, for such eclipses, with decreasing h.

For example, inspection of the co-ordinates of the shadow track, June 8, 1937, in the American Ephemeris shows that the diameter of the moon's shadow cone where it intersected the earth was about 125 miles at the sunset point and about 155 miles at the noon point.

From the foregoing formulae numerical results were worked out for sky brightness at various altitudes as seen from the noon point,

TABLE 1*

SCATTERING COEFFICIENT, SOLAR INTENSITY, AND EYE SENSITIVITY

λ	k_λ	I_λ	S_λ	$S_\lambda I_\lambda k_\lambda$	ξ_λ
3000.....	1.142	0.44	0.000	0.0000	0.32
4000.....	0.338	.86	.0004	0.0116	.42
5000.....	0.135	.99	.33	4.4105	.51
6000.....	0.065	.93	.63	3.8084	.59
7000.....	0.034	.80	.004	0.0109	.64
8000.....	0.020	0.65	0.000	0.0000	0.68

* λ is wave length in angstroms. k_λ refers to extinction produced by Rayleigh scattering by pure air; if I_0 is the initial intensity, then $I_0 e^{-k_\lambda}$ is the surviving intensity in the direct beam if the light has passed through 7.991 km of air at sea-level density (the height of the homogeneous atmosphere). I_λ is the intensity of sunlight from near the solar limb, computed from Planck's formula for a temperature of 5700° K, in terms of the intensity at the maximum, which is at λ 5070. S_λ is the relative sensitivity of the eye to radiant energy of different wave lengths, the maximum being 1.00 at about λ 5575. ξ_λ is the intensity of radiation close to the sun's limb (0.95 of a radius from the center), in terms of the intensity at the center of the disk.

both for an observer at the center of the shadow and for one off center. Results also were secured for a sea-level position on the central line near the coast of Peru and for an airplane there at an elevation of 25,000 feet. Two wave lengths, one in the violet and one in the yellow, were used. These computations were made by Messrs. O. H. Reeder, H. Johnson, Jr., and especially by C. D. MacCracken, undergraduates in Princeton University.

Because of the approximate character of these computations, it is not worth while to publish tables of the results. The results in detail substantiate statements made in the next section, which introduces also supplementary principles relating to sky brightness during eclipse.

One important general consideration remain[s] [t]o be emphasized. The illumination from the horizon glow during a[n] eclipse, traveling into the shadow more or less horizontally, does [not] in itself reduce the shadow's blackness in the sky overhead. It [is] the scattering downward of that glow by the air above the obse[rver] which masks faint stars and faint details of the corona.

IV. RESULTS OF COMPUTATIONS OF SCATTERI[NG] OF LIGHT INTO THE MOON'S SHADOW IN THE

The numerical integrations described in sect[ion] iii yield sky brightnesses expressed in arbitrary units. In ord[er] to get a rough absolute calibration, similar numerical integrati[ons] were carried out for the uneclipsed zenith sun. H. H. Kimb[all] observation[16] served here—that with a clear blue sky near sea-l[evel] and with the sun near the zenith, about 1/9th as much light fall[s] on a horizontal surface from the sky as directly from the sun. The [con]clusion indicated (but see sec. v) that for the position of the "[Wh]eelmaker" at mid-totality the total light of the horizon glow all [a]round the sky due to Rayleigh scattering by pure air would hav[e] been roughly 1/5000th as bright as is the zenith sun at sea-level [in] computing this result, the effective limb light was assumed to [be] about 0.7 as intense per unit area of the solar disk as is the aver[age] light of the whole disk ($\zeta = 0.7$; in Table 1, ξ is the ratio to [the] light at the center of the disk, not to the mean).

As for the color of the light in the horizon glow [the] extinction increases as scattering increases. Outside the shadow [the] yellow light will be scattered much less than blue (cf. Table 1); [but] under the shadow there is no direct sunlight to be scattered, [and] secondary scattering reduces the strength of incoming beams. [The] reduction factor there, increasing exponentially with distance, [o]vercomes, in the violet and blue, if the shadow is wide enough, th[e] initial disadvantage of the yellow. If the shadow is wider still, [it] should predominate in the horizon glow, at least in its lower [p]art. But near the edge of any lunar shadow the diffused sunlight [fro]m that side should be almost the normal blue. It should be incre[ased] a little in average wave length as a result of the lower effective t[e]mperature of

[16] *Monthly Weather Review*, **42**, 650, 1914.

the limb light; but the increase is slight and at an annular eclipse blue sky presumably remains blue.

It is worth noting, in this general connection, that the conventional statement that normal daytime sky is blue because scattering sharply increases as the wave length decreases is incomplete. And it is incomplete wholly aside from the energy frequency characteristic of sunlight. If the earth were so large as to be nearly flat with respect to the distance which red light can travel through sea-level atmosphere before being reduced, by scattering, to half its initial intensity, then the sky around the horizon on a transparent day would be, not blue, but the color of a white surface in sunlight. Actually, the clearest sky is a bit less blue, and brighter, around the horizon than at the zenith. On a day with slight haze the horizon sky is made yellowish or white by the relative increase in scattering of the longer waves. When sunlit air beyond the margin of a thunderstorm can be seen at a distance, with the line of sight passing under the shadowing storm-clouds, sometimes a saffron color appears which closely resembles that seen during the 1937 eclipse. Presumably haze in the air beneath the clouds so increases the scattering as to make the relatively small cloud-area the approximate optical equivalent of the moon's shadow.

The total light from the horizon glow at an eclipse, integrated around the circle, is computed as greater as seen from a high airplane than as seen from sea-level, because the dip of the horizon exposes low elevation, relatively dense, sunlit air. However, the upper limit of the glow, where it meets the shadow, would come at a lower true angular altitude from the airplane than at sea-level, because the scattering from high-elevation air is so small.

For the position of the "Steelmaker" the numerical computations indicate an effective upper bound lower than the observed 14° at mid-totality. Secondary scattering was neglected in these computations; if included, it would tend to reduce the discrepancy, as well as to increase the estimated total illumination.

Examination of the detailed computations shows that 90 per cent of the diffused daylight in the horizon glow at any azimuth in an eclipse shadow comes from air closer (horizontally) to the observer than roughly 250 miles.

At Moro, Peru (W. 78°10′5″, S. 9°8′5″), the sun's altitude during totality on June 8, 1937, was about 8°; the shadow's semimajor axis there was about 400 miles, nearly east and west. Its semiminor axis, as indicated above, was about 62 miles. This indicates at once that no appreciable diffused daylight would have been visible above the horizon in the direction of the setting sun or in the opposite direction, at mid-totality. The glow would have reached the highest and would have been the strongest toward the north and south. Consequently, as compared with the noon position, the general illumination would have been reduced, owing to this effect alone, by a factor of the order of $\frac{1}{2}$.

Detailed comparison of this sunset position with that of the "Steelmaker" is instructive. The sunlight's intensity in the effective circle of scattering air would have been reduced at Moro in the ratio sin 8°/sin 76°, or 1/7. But the whole mass of air around the shadow would scatter just as much light from the low altitude as from the zenith beam if it were not for the increased shielding of low-elevation by high-elevation air on account of the longer air paths. For, if a volume of air is flooded with sunlight, the direction of the sun does not affect the amount of scattering. Referring to the values of k_λ in Table 1, it is evident that with an air path half a dozen times that for the zenith sun the factor of reduction at sea-level due to such shielding would amount to about $e^{-0.2}$ at λ 7000, to $e^{-0.4}$ at λ 6000, and to $e^{-2.0}$, or 0.15, at λ 4000 (secondary scattering would make the reductions less severe). Averaging, the reduction factor in the general illumination at Moro due to the shielding would have been roughly $\frac{2}{3}$. It would have been much more important in the violet than in the red.

On the other hand, the diminution in the radius of the moon's shadow cone by about 25 km would make for a relative increase, in Peru, of the horizon glow by a factor dependent in part upon the average extinction in an air path of that length. This is because sunlight scattered toward the center by a given element of air outside the shadow would itself be reduced by further scattering before it reached the observer, as has already been emphasized. A horizontal air path of 25 km at sea-level reduces by pure Rayleigh scattering the intensity in the direct beam to about 35 per cent for

λ 4000, but for λ 6000 the corresponding reduction is much less marked—to about 80 per cent. Since much of the light in the horizon glow comes in along paths through high-level air, of much diminished density, it is at once evident that the general illumination—striking some average for color and path—would not have been increased more than a few per cent—say 10 per cent—by the diminution of 25 km in *b*.

The diminution in *b* also would tend to increase the angular width of the horizon glow, as seen from the shadow's center, approximately in the ratio 124/100. Its integrated brightness would increase by a ratio somewhat less, for the brightest part would lie at the lowest angular altitudes, where scattering would be greatest. We adopt a factor 1.15 to represent this effect.

In addition, the elevation of the Peruvian party was about 2400 feet, where the barometric pressure is reduced to 700 mm, as compared with the 760 mm at sea-level. Thus the mass of scattering air overhead was reduced to about 0.9, as compared with sea-level. The sky brightness overhead would have been reduced in no greater proportion (see below).

The combination of the five factors—nominally, $\frac{1}{2}$, $\frac{2}{3}$, 1.1, 1.15, and 0.9—amounts to a theoretical reduction of roughly a magnitude in overhead sky brightness for Moro, as compared with the post of the "Steelmaker," 3700 miles west of Balboa. The difference in the faintest stars recorded at the two locations is roughly 2 mag. In the Pacific the limit seems to have been near Betelgeuse, as contrasted with "third magnitude" at Moro. Such observations must be subject to a considerable personal equation. At certain other stations in Peru stars as faint as magnitude 3 were not noticed.

Furthermore, the sky brightness changes during totality—but, from all that has been said, it is clear that the integrated brightness of the horizon glow during totality due to scattering by pure air is not enormously sensitive to the observer's position in a shadow. Along the exact central line there should be a diminution of the order of only 1 mag. in the general brightness between second or third contact and mid-totality. If the observer is off center to north or south, the brightness at mid-totality, although not at the contacts, is correspondingly increased. Near the sunrise or sunset point

the general illumination should be several times less at mid-totality than at the noon point, if the moon's shadow is large; but if the shadow is small, it is the noon point which has the greater integrated horizon glow. The difference in general brightness at mid-totality for a large shadow and a small one also can range only over a magnitude or two.

Even in the limiting case of zero duration of totality, with equal apparent diameters of moon and sun, the average intensity of sunlight in the effective circle 250 miles around the infinitesimal shadow is reduced by an average factor of the order of 100, as compared with no eclipse. Since the sky with zenith uneclipsed sun gives about 1/9th of the sun's brightness, it is evident that the sky glow in this limiting eclipse will amount to the order of 1/1000th of the zenith sea-level sun. (If the moon were nearer and correspondingly smaller in linear size, this brightness would be greater, owing to the smaller penumbra.) Deep immersion in a large shadow cuts down decidedly the blue and green light, because of atmospheric extinction, but affects the yellow and red principally only through the reduction in the angular height of the glow.

The obliquity of the shadow as it strikes through the air near the sunrise and sunset points should give rise to a very pretty phenomenon—indicated by Professor Russell in conversation. At the sunrise point the shadow is moving vertically downward toward the observer, with a speed of more than half a mile per second. Consequently, a few seconds before second contact the sky overhead should be dark, but instantaneously after third contact the whole sky should be sunlit, for the shadow has "gone to earth." At the sunset point the order of these two aspects reverses; there the shadow, as it were, comes out of the earth at second contact.

V. ESTIMATES OF THE HORIZON GLOW AND OVERHEAD BRIGHTNESS DURING TOTALITY

In section iii the rough estimate was presented that the total brightness of the horizon glow at the noon point on June 8, 1937, was 1/5000th of the zenith sea-level sun. Supplementing this, an independent approach can be made by considering the disappearance of the coronal streamers after third contact. Equation (3), with the

values of A and B already indicated, shows that for the first minute or so of time after third contact the area of photosphere exposed increased linearly with the time. The velocity of the shadow eastward across the sea was about 35 km/min. After 1 minute, 1/300th of the disk was exposed. Taking the effective darkening at the limb for the first minute as $\frac{1}{2}$, the illumination from the photosphere immediately after third contact was increasing at the rate of 1/36,000th of the zenith sea-level sun per second.

The coronal streamers certainly disappeared within a few seconds after third contact. The horizon glow just before third contact stretched far up the western sky and, as stated above, must have been a magnitude or so brighter than at mid-totality—say, 1/2000th of the full sun. The returning photosphere would not have attained this brightness until 18 seconds after third contact.

Light from the photosphere would be much more effective, however, in masking the corona than light from the horizon glow, for four reasons. First, a factor of 2 is introduced because of the effect of polarization on the intensity of scattered light. Light from the horizon glow must have been plane polarized, and so only 50 per cent effective in producing secondary scattering overhead. Light from the sun direct, of course, was unpolarized. Second, referring once more to Table 1, the greater relative strength of the photosphere in blue light, even at the limb, as compared with the horizon glow, would have resulted in a second increase in efficiency in the scattering it produced. Just before third contact, the horizon glow itself must have been richer in blue, to the west, than at mid-totality. The factor in favor of the photosphere, nevertheless, must have been significant; assume that it was 2. Third, the glare of the photosphere beside the corona must have reduced an eye's sensitivity to contrast and so caused a premature disappearance of the streamers. The factor of correction necessitated by this effect cannot be estimated offhand; if it is also taken as 2, then the sky brightness masking the corona would effectively have been doubled only $2\frac{1}{4}$ seconds after third contact. This seems a reasonable agreement with the observed disappearance of the streamers, but obviously considerable uncertainty remains.

The three factors already mentioned come into account even if

the air is perfectly free of dust and haze. The presence of such foreign matter, through diffraction and refraction, would increase still further the sky brightness within a few degrees of the photosphere—and this, fourth, factor might well be the greatest of all.

The argument of this section roughly confirms *1/5000th of the zenith sea-level sun* as the integrated brightness of the horizon glow at mid-totality at the noon point, June 8, 1937 (but suggests that this estimate ought to be reduced somewhat).

Kimball[16] found that the intensity of zenith sunlight at sea-level on a horizontal surface was about 9000 foot-candles on a clear day. Thus the total brightness of the horizon glow at mid-totality comes out, from the foregoing estimate, as 1.8 foot-candles. Its intensity, on a vertical surface, would have been $\frac{1}{2}(2/\pi)$ times this, or 0.6 foot-candle. The intensity on a horizontal surface would have been much less because of the grazing angles.

Taking the full moon's brightness as about 1/500,000th the sun's, the total horizon glow was equivalent to roughly no more than 100 full moons—or 200 coronas. Per unit angular area, however, the horizon glow would have averaged only about 1/25th of the full moon's surface brightness; its color probably averaged a bit redder than the zenith moon.

The relative weakness in blue of the horizon glow at mid-totality, combined with its disadvantage due to polarization already mentioned, would have made it four or five times less effective in masking faint stars and coronal structure than the ratio 1/5000th of the sun would indicate. Such masking depends on secondary (and tertiary) scattering.

The average brightness in the moon's shadow overhead, caused by scattering of the horizon glow, comes out per unit angular area as less than 1/10,000th that of the normal daytime sky. If multiple scattering were included, this estimate would be increased. Remembering that there are 20626.5 square degrees in a hemisphere and that the integrated brightness of the normal daytime sky is greater than 1/9th of the sun (which is the intensity on a horizontal surface), the average brightness of the shadow in the sky works out as less than, say, 1/12,500th of the moon's surface brightness. Thus, the average illumination in the moon's blue shadow in the air over-

head, owing to secondary scattering alone, was, per unit angular area, perhaps five hundred times fainter than the illumination in the horizon glow.

The moon's shadow was blue, not orange. Blue light had a factor of roughly 5 in its favor over orange, with regard to efficiency of the secondary scattering; but the blue in the horizon glow at the center of the shadow may have been reduced by an even greater factor, as seen from sea-level. Presumably the strength of blue remaining at high elevations in the air helps to account for the shadow's color—but this illustrates another complexity in the general problem. Another factor accounting for the blueness of the shadow is multiple scattering, which would be significant only in the blue and violet. Blue is readily removed from direct beams, but it does not readily dissipate from the sky.

VI. THE COMPARISON OF ECLIPSE SITES

The quantitative conclusions presented above are uncertain within a factor of 2 or more. They are given in detail chiefly as suggesting further study—and especially observations at future eclipses. When adequate observations become available, it will be possible to make the theoretical treatment less imprecise; cf. Hulburt's interesting study[11] of normal twilight.

For taking instrumental observations of sky brightness during a total solar eclipse, moving photographic films, exposed through two or three different color filters toward various altitudes and azimuths, doubtless will be preferable to a bank of photoelectric cells. The latter would require being connected to recording galvanometers, and calibration might be more difficult. In addition, sky conditions should be noted carefully with regard to clouds and transparency.

When spectroscopic studies of the chromosphere are in question, the considerations advanced in this paper are of no importance with regard to the selection of eclipse sites. Sky brightness is very significant, however, when the structure of the outer corona is to be examined. In comparing different eclipses and different positions for observation at the same eclipse, there is little advantage in drawing detailed numerical conclusions from this preliminary study; but three principles stand out.

1. Provided the moon's shadow is moderately large at a given eclipse, there is not a very large gain to be expected in general darkness at another eclipse with the maximum shadow.

2. Small zenith distance for the eclipsed sun is very important for obtaining distinctness of the corona. At low solar altitudes the absolute brightness of the corona is reduced by atmospheric extinction, which is particularly effective in the shorter wave lengths. Furthermore, even though the brightness of the horizon glow is less with a low sun, sharply increased secondary scattering in the long air path toward the corona will more than counterbalance this diminution, leading to increased masking at large zenith distances—again particularly in short wave lengths. The combination of these two influences, with a low sun, can result in reducing the difference between corona and sky-foreground by a magnitude or more, as compared with an eclipse near the zenith.

3. If the observer can attain a high elevation above sea-level, the differential between corona and sky is further increased. With large lunar shadows the masking in the blue and violet, with pure air, does not decrease as rapidly with elevation as the barometric pressure decreases, because, as has already been indicated, short waves in the horizon glow are blocked out at sea-level and are effective only at high elevations. With a zenith sun the gain in the differential at 5 miles of elevation again could be more than a magnitude, as compared with sea-level. With a low sun the gain could be more.

The noon point, June 8, 1937, offered perhaps the best view of the corona in modern history; it is unfortunate that full advantage was not taken of it. The elevation which Major Stevens and his party attained would have earned them a still better view had it not been deteriorated by the low altitude of the sun.

Three conditions determine that an eclipse be observable at the zenith in the darkest overhead sky: (1) moon at perigee; (2) earth at aphelion; and (3) latitude of noon point equal to sun's declination. The requirement that the noon point lie on the earth's equator is significant for duration but not for darkness. Future eclipses which come somewhere near meeting the three requirements for maximum darkness are readily selected from tables of eclipses. In Table 2 are

listed the six eclipses from 1939 through 1975 which have durations[17] at the noon point[18] longer than $4^m.2$ and for which the sun's zenith distance is less than 30°. That of 1940 will be almost as near the ideal as was that of 1937; while the latter's two successors in the saros, in 1955 and 1973, will be a shade better still. The noon point itself will be on land only in 1973 (in French West Africa). In 1955 the noon point will be in the China Sea close to Manila, but in 1940 and 1947 it will be deep in the South Atlantic, while in 1958 and 1965 it will be in the far Pacific but in the neighborhood (by airplane) of the Tuamotu Archipelago.

TABLE 2

DARK ECLIPSES

DATE	DURATION	NOON POINT		SUN	
		Latitude	Longitude	Declination	Zenith Distance
1940 Oct. 1	$5^m.7$	−19°	W. 16°	− 3°	16°
1947 May 20	5.2	− 2	W. 25	+20	22
1955 June 20	7.2	+15	E. 117	+23	8
1958 Oct. 12	5.2	−26	W. 139	− 7	19
1965 May 30	5.3	− 4	W. 137	+22	26
1973 June 30	7.2	+19	E. 6	+23	4

It is evident that study of the corona's structure from sea and air offers decided possibilities during the next 25 years. Even if apparatus under development[19] designed to accentuate contrast and reveal the corona without an eclipse should succeed, astronomers still will observe the corona at eclipses in order to push our knowledge of the sun's surroundings to contrasts still more delicate.

PRINCETON UNIVERSITY OBSERVATORY
June 17, 1939

[17] S. A. Mitchell, *Eclipses of the Sun*, 3d ed., p. 55, 1932.

[18] Von Oppolzer, *Canon der Finsternisse*, 1887.

[19] A. M. Skellett, *Proc. Nat. Acad. Sci.*, **20**, 461, 1934. (Television technique is used as a supplement to the coronagraph.)

THE MATHEMATICAL CHARACTERISTICS OF SUNSPOT VARIATIONS. II

JOHN Q. STEWART AND FORREST C. EGGLESTON

ABSTRACT

The study is continued of the mathematical form $R = F\theta^a e^{-b\theta}$ as representing the course of sunspot numbers during a given outburst or cycle. The Case 2 solutions described in the first paper are found, after detailed computation, to represent the observed annual numbers with an average residual, regardless of sign, of 7.2 Wolf numbers. Probably most of this difference is due to the inherent randomness which is superposed on the underlying smooth trend of spot numbers, but it also includes small systematic errors, perhaps due to a somewhat imprecise method of determining the time of the start of an outburst. The total discrepancy, O−C, regardless of sign, averages 16 per cent of the average value of an annual sunspot number and this tends to be independent of the amplitude of a cycle.

The systematic difference between observed and computed times of maxima, which in the first paper was considered to show that the mathematical form $F\theta^a e^{-b\theta}$ was only approximately applicable, can be attributed, on the other hand, it is suggested, to variations introduced by the Zurich method of smoothing the monthly numbers—upon which the "observed" times of maxima depend. The conclusion of the present paper is that the suggested mathematical form is not likely to be improved upon. Additional auxiliary tables for this function are given which are specially applicable to the problem of fitting the monthly numbers of an incompleted cycle. The problem of predicting the remainder of the present cycle, No. 17, is touched upon.

In the first paper[1] methods were developed for fitting the form

$$R = F(r - s)^a e^{-b(r-a)} \qquad (1)$$

to the annual sunspot numbers of a given "outburst," of average duration about eleven years. Here R is the Wolf number for the varying year r. During a single cycle, F, a, b, and s are constant: s is the time of the start of the outburst; F is a scale factor; r runs from s to plus infinity. For $r < s$, R is zero.

XIV. DETAILED RESIDUALS OF CASE 2 SOLUTIONS

Table 7 of Paper I presented sample residuals, O − C, between observed and computed annual sunspot numbers. The complete set of such residuals for all the Case 2 solutions of Table 5 is presented here in Table 12,[2] which is in exactly the form of Table 1.

[1] John Q. Stewart and H. A. A. Panofsky, *Ap. J.*, **88**, 385–407, 1938. That paper contained three slight misprints. In the equation at the top of p. 389, preceding (7), the sign of $M_0(s - t)^2$ should be negative. In (7) M_2/M_1 ought to be M_2/M_0. At the foot of p. 404 write $I(a/\sqrt{a} + 1, a)$.

[2] The sections, tables, and equations of this paper are numbered consecutively with those of the first one ("Paper I").

TABLE 12

CASE 2 SOLUTIONS: O−C

CYCLE NUMBER	MINIMUM YEAR	OBSERVED *minus* COMPUTED SPOT NUMBERS FOR YEARS AFTER MINIMUM													
		0	1	2	3	4	5	6	7	8	9	10	11	12	13
1	1755	+9.4	+ 8.0	+15.7	+ 1.2	−20.8	−23.6	+ 6.5	− 0.7	+ 2.9	+10.3	+6.1	.....	.....	.....
2	1766	+3.4	+11.8	−11.1	− 8.3	− 9.1	− 3.0	+10.1	+ 0.8	+11.6	.....	.....	.....	.....	.....
3	1775	−2.9	+ 6.2	+16.9	+ 7.6	−28.9	−27.8	+ 2.5	+ 6.0	+ 8.5	.....	.....	.....	.....	.....
4	1784	+4.4	+ 8.7	+17.4	+15.6	− 8.5	−16.1	−22.7	−19.2	− 1.0	+ 5.7	+16.1	+4.7	+5.9	+0.4
5	1798	−1.6	+ 1.0	− 3.7	− 1.5	− 2.1	− 5.4	+ 5.8	+10.8	− 0.4	+ 3.5	+ 0.1	−2.0	.....	.....
6	1810	−2.4	+ 0.1	+ 3.6	+ 6.9	− 5.0	− 1.9	− 2.5	−4.9	− 4.6	+ 1.5	+ 3.2	+0.4	+1.2	.....
7	1823	+0.7	+ 6.1	+ 1.7	− 3.5	−13.2	− 9.7	+ 1.0	+19.6	+12.5	+ 5.5	.....	.....	.....	.....
8	1833	−4.2	+ 6.0	+ 6.7	+ 3.0	−10.0	−27.4	− 7.7	+ 6.7	+ 5.8	+ 8.5	.....	.....	.....	.....
9	1843	+3.2	+10.6	+22.2	+ 2.2	− 8.1	− 6.2	−27.9	−31.6	− 3.5	+11.8	+14.6	+7.5	+0.1	.....
10	1856	+0.4	+ 5.8	+ 1.9	+ 8.8	− 2.3	−13.4	−13.0	− 7.1	+13.0	+ 9.6	+ 4.0	.....	.....	.....
11	1867	+0.3	+18.6	− 1.4	+ 8.9	−28.1	− 9.5	− 6.9	+ 2.8	− 4.6	+ 1.0	+ 7.7	.....	.....	.....
12	1878	+1.4	+ 3.4	+20.2	− 2.0	−13.7	− 7.1	+ 6.8	+12.5	+ 0.1	− 1.9	− 1.6	.....	.....	.....
13	1889	+1.8	+ 0.3	+ 3.9	+ 6.1	− 2.1	− 6.8	− 4.7	− 7.1	− 5.4	+ 7.7	+ 1.3	+3.7	.....	.....
14	1901	−0.3	− 0.7	− 0.1	− 6.2	+ 1.5	− 8.7	+ 8.3	+ 7.3	+14.8	− 0.7	− 6.5	−3.8	.....	.....
15	1913	−2.9	+ 5.7	+21.5	−14.1	− 0.5	−15.9	− 4.5	− 2.1	+ 6.0	+ 5.0	.....	.....	.....	.....
16	1923	+1.9	+ 3.8	0.0	− 7.0	− 8.6	+ 9.8	+13.6	+ 0.4	− 1.2	− 2.4	.....	.....	.....	.....
17	1933	−1.6	+ 2.6	+ 5.3	− 1.1	− 1.9	.....	.....	.....	.....	.....	.....	.....	.....	.....

The residuals have a slight systematic character, but not that which was anticipated from Tables 8 and 9 (see Sec. XV below). Instead, they show that form (1) provides, in general, a better fit than was concluded in Paper I.

We have spent a good deal of labor in analyzing the residuals of Table 12. In every cycle they show that the Case 2 computed curve tends to run a little high during the first several years, then low, and finally high again. Attempts to modify form (1) by an empirical additive correction did not lead to a significant reduction in these residuals.

TABLE 13*

RELATION OF RESIDUALS TO SUMS OF SPOT NUMBERS

Cycle Number	M_0	Sum O − C	Cycle Number	M_0	Sum O − C
1	467	105.2	9	694	149.5
2	537	69.2	10	547	79.3
3	615	107.3	11	620	89.8
4	843	146.0	12	382	70.7
5	277	38.3	13	463	50.9
6	236	38.2	14	373	58.9
7	392	73.5	15	444	78.2
8	653	86.0	16	410	48.7

* M_0 is the sum of the annual numbers between successive minima (from Table 2), and the values of O−C are summed for each cycle from Table 12.

A suitable modification of equation (10) might result in a marked improvement. That problem will best be attacked through a study of the monthly, instead of the annual, observed numbers. It is not discussed in the present paper.

In Table 13 the sum, regardless of sign, of the observed *minus* the computed spot numbers of Table 12 is compared with the sum of the observed spot numbers—that is, nearly enough, with the respective values of M_0 from Table 3. The sum of all the residuals, O − C, for the 178 years 1755–1932, inclusive, represented in the sixteen completed cycles is 1289.7. Hence, the average residual, regardless of sign, for a computed annual spot number is 7.2 Wolf numbers.[3]

Arranging the sixteen cycles in the order of increasing M_0, and

[3] Our statement in a recent note (*Phys. Rev.*, **55**, 1102, 1939) that it was "7%" is open to misinterpretation.

dividing them arbitrarily into three about equal groups, we are led to Table 14. The sum of all the M_0's for each group is the sum of the observed annual spot numbers (subject to an insignificant correction due to the way M_0 was computed[4]). The column in Table 14 headed "Ratio" gives the ratios to these sums of the respective sums of the residuals.

Evidently the Case 2 solutions have an average discrepancy, regardless of sign, of about 16 per cent. This percentage discrepancy is independent of the height of maximum of the outburst.

TABLE 14

PERCENTAGE RESIDUALS

Group	Cycles	Sum of the M_0's	Sum of the O — C's	Ratio (Percentage)
I.....	6, 5, 14, 12, 7	1660	279.6	17
II.....	16, 15, 13, 1, 2, 10	2868	431.5	15
III.....	3, 11, 8, 9, 4	3425	578.6	17

XV. CRITICISM OF THE ZURICH TIMES OF MAXIMA

In the first paper,[5] on the other hand, the conclusion was indicated that form (1) fits cycles of intermediate height the most closely. That conclusion was not based upon the complete solutions presented in Table 12, which had not been computed, but upon the discrepancies between computed and observed times of maxima, as presented in Table 8 for Case 2 solutions.

The percentage residuals of Table 14 include the systematic discrepancies touched upon in the preceding section and evident in Table 12, but principally they must be attributed to the randomness of the spot-producing process. This randomness was emphasized in the first paper. Pending further study, it may be estimated as amounting to at least 10 per cent; it does not exceed 16 per cent. That is to say, given the best possible fit of equation (1) to a given outburst, altogether free from systematic error, the observed annual spot numbers may be expected to show an average discrepancy, regardless of sign, from the computed ones of at least 10 per cent of the observed number.

[4] Paper I, p. 391.

[5] *Ibid.*, p. 402.

TABLE 15

AUXILIARY TABLE: EQUATIONS (9) AND (35)

a	$\phi(a)$	$a\phi(a)$	$(a+1)\phi(a)$	$a\phi(a)/a$
1.0	0.3679	0.3679	0.7358	1.394
1.2	.3403	0.4084	0.7487	1.459
1.4	.3179	0.4451	0.7630	1.514
1.6	.2996	0.4794	0.7790	1.572
1.8	.2841	0.5114	0.7955	1.629
2.0	.2707	0.5414	0.8121	1.681
2.2	.2591	0.5700	0.8291	1.727
2.4	.2488	0.5971	0.8459	1.772
2.6	.2397	0.6232	0.8629	1.817
2.8	.2315	0.6482	0.8797	1.863
3.0	.2240	0.6720	0.8960	1.904
3.2	.2174	0.6957	0.9131	1.949
3.4	.2112	0.7181	0.9293	1.989
3.6	.2055	0.7398	0.9453	2.027
3.8	.2003	0.7611	0.9614	2.068
4.0	.1954	0.7816	0.9770	2.101
4.2	.1910	0.8022	0.9932	2.139
4.4	.1867	0.8215	1.0082	2.179
4.6	.1828	0.8409	1.0237	2.213
4.8	.1789	0.8587	1.0376	2.248
5.0	.1755	0.8775	1.0530	2.285
5.2	.1722	0.8954	1.0676	2.320
5.4	.1691	0.9131	1.0822	2.353
5.6	.1662	0.9307	1.0969	2.396
5.8	.1632	0.9466	1.1098	2.415
6.0	.1608	0.9648	1.1256	2.449
6.2	.1581	0.9802	1.1383	2.482
6.4	.1557	0.9965	1.1522	2.510
6.6	.1533	1.0118	1.1651	2.542
6.8	.1511	1.0275	1.1786	2.575
7.0	.1490	1.0430	1.1920	2.608
7.2	.1469	1.0577	1.2046	2.631
7.4	.1450	1.0730	1.2180	2.656
7.6	.1431	1.0876	1.2307	2.685
7.8	.1414	1.1029	1.2443	2.761
8.0	.1396	1.1168	1.2564	2.744
8.2	.1379	1.1308	1.2687	2.772
8.4	.1364	1.1458	1.2822	2.795
8.6	.1347	1.1584	1.2931	2.818
8.8	.1333	1.1730	1.3063	2.847
9.0	.1316	1.1844	1.3160	2.868
9.5	.1283	1.2189	1.3472	2.937
10.0	.1251	1.2510	1.3761	3.000
10.5	.1222	1.2831	1.4053	3.062
11.0	.1194	1.3134	1.4328	3.120
11.5	.1168	1.3432	1.4600	3.175
12.0	.1145	1.3740	1.4885	3.241
12.5	.1121	1.4013	1.5134	3.289
13.0	.1098	1.4274	1.5372	3.343
13.5	.1078	1.4553	1.5631	3.392
14.0	.1059	1.4826	1.5885	3.448
14.5	.1043	1.5124	1.6167	3.509
15.0	0.1025	1.5375	1.6400	3.559

This point of view, taken in connection with the systematic differences of Table 8 between the times of maximum, v', computed in Case 2 solutions, and the Zurich "observed" values, v, suggests that not the former but the latter ought to be adjusted.

The Zurich values are obtained from the smoothed monthly spot numbers. The method of smoothing has been to take a moving chain average. The month for which the smoothed number is required has weight 2 assigned to its observed spot number, as do the five immediately preceding and succeeding months. The sixth month before and after is assigned weight 1. This system has the advantage of leading in every case to a unique, or nearly enough unique, maximum in the smoothed monthly numbers of a given cycle. It does not have, presumably, any deep-seated justification.

To smooth a ragged curve is a statistically indeterminate problem unless an equation for the underlying trend is available. The Case 2 solutions themselves offer a method of smoothing, and for the present it seems that the question of whether it is not the superior method can be considered an open one.

In the first paper it was concluded that equation (1) could not be the finally satisfactory representation of the underlying trend of sunspot variation because with it the computed centroid, w', can never precede the computed time of maximum, v'. In cycles 1, 5, 7, 12, and 16 the observed w was earlier than the "observed" (i.e., from Zurich smoothing) v. The admittedly incomplete discussion of the present section tends to remove this objection. A detailed examination of the monthly spot numbers will be required to settle the matter. We have already started such an examination for several cycles,[6] and the general validity of equation (1) seems not to be ruled out.

XVI. FITTING MONTHLY NUMBERS; FURTHER AUXILIARY TABLES

Write, as in Pearson's tables,[7]

$$I(x, p) = \frac{\Gamma_x(p + 1)}{\Gamma(p + 1)} = I(u, p),$$

[6] In considering this question of the smoothing of the monthly numbers the cooperation of Mr. Hans A. A. Panofsky during a few weeks spent in Princeton has been very useful.

[7] *Tables of the Incomplete Gamma Function*, ed. Karl Pearson, London, 1922.

where

$$\Gamma_x(p+1) = \int_0^x x^a e^{-x} dx ,$$

and

$$u = \frac{x}{\sqrt{p+1}} .$$

Putting θ for $r - s$, define "incomplete zero, first, and second moments" as

$$m_0 = \int_0^\theta R d\theta = F \int \theta^a e^{-b\theta} d\theta , \tag{23}$$

$$m_1 = \int_0^\theta \theta R d\theta = F \int \theta^{a+1} e^{-b\theta} d\theta , \tag{24}$$

$$m_2 = \int_0^\theta \theta^2 R d\theta = F \int \theta^{a+2} e^{-b\theta} d\theta . \tag{25}$$

Substituting $x = b\theta$, with θ running from 0 to na/b, or x from 0 to na, n being an arbitrary number, it is easy to show that

$$m_0 = \frac{F}{b^{a+1}} \Gamma(a+1) I(u_0, a) , \tag{26}$$

$$m_1 = \frac{F}{b^{a+2}} \Gamma(a+2) I(u_1, a+1) , \tag{27}$$

$$m_2 = \frac{F}{b^{a+3}} \Gamma(a+3) I(u_2, a+2) , \tag{28}$$

where

$$u_0 = \frac{na}{\sqrt{a+1}} , \qquad u_1 = \frac{na}{\sqrt{a+2}} , \qquad u_2 = \frac{na}{\sqrt{a+3}} . \tag{29}$$

Consider now the two ratios

$$G = \frac{m_1}{\theta m_0} , \tag{30}$$

$$H = \frac{m_2}{\theta^2 m_0} , \tag{31}$$

with $\theta = na/b$. Then, remembering that

$$\Gamma(a+2) = (a+1)\Gamma(a+1)\,,$$
$$\Gamma(a+3) = (a+2)\Gamma(a+2)\,,$$

we have

$$G = \frac{(a+1)}{na} \cdot \frac{I(u_1, a+1)}{I(u_0, a)}\,, \tag{32}$$

$$H = \frac{(a+1)(a+2)}{n^2a^2} \cdot \frac{I(u_2, a+2)}{I(u_0, a)}\,. \tag{33}$$

When n is 1, θ runs from 0 to a/b, which is the position of the maximum of (1). G and H then become functions of a only and, as such, have been computed in Table 16. The third decimal may be slightly in error, because of interpolation and smoothing; but the values should be accurate enough for practical purposes, as applied to spot numbers.

In connection with these computations, values of

$$\alpha = I\left(\frac{a}{\sqrt{a+1}}\,, a\right), \tag{34}$$

in addition to those of Table 11, were necessary. These are presented in Table 15.

This table also extends Table 4 and adds values of $a\phi/\alpha$; which is another function of a. It is useful in connection with the relationships between m_0 (when n is 1), $v - s$ (which is a/b),[8] V (the maximum Wolf number), and M_0 (which then is m_0/α). From Paper I

$$V = M_0 b\phi\,. \tag{8}$$

Therefore,

$$V = \frac{m_0}{v-s} \cdot \frac{a\phi}{\alpha}\,. \tag{35}$$

In working with monthly numbers it is perhaps well to keep the year as unit of time and divide by 12 the values of m_0 obtained from summing monthly numbers. Values of the ratios G and H are independent of the unit of time.

[8] Paper I, eq. (3).

TABLE 16

AUXILIARY TABLE: EQUATIONS (30) AND (31)

a	G	H	a	a	G	H	a
1.0			0.264	5.7	0.756	0.599	
1.2			.280	5.8			0.392
1.3	0.628	0.446		5.9	.759	.603	
1.4			.294	6.0			.394
1.5	.640	.460		6.1	.762	.606	
1.6			.305	6.2			.395
1.7	.651	.473		6.3	.765	.609	
1.8			.314	6.4			.397
1.9	.660	.484		6.5	.768	.613	
2.0			.322	6.6			.398
2.1	.668	.494		6.7	.771	.617	
2.2			.330	6.8			.399
2.3	.676	.503		6.9	.774	.621	
2.4			.337	7.0			.400
2.5	.683	.512		7.1	.776	.625	
2.6			.343	7.2			.402
2.7	.690	.521		7.3	.778	.629	
2.8			.348	7.4			.404
2.9	.696	.529		7.5	.779	.632	
3.0			.353	7.6			.405
3.1	.702	.536		7.7	.780	.635	
3.2			.357	7.8			.406
3.3	.707	.542		7.9	.782	.638	
3.4			.361	8.0			.407
3.5	.711	.548		8.1	.783	.640	
3.6			.365	8.2			.408
3.7	.715	.553		8.3	.785	.641	
3.8			.368	8.4			.410
3.9	.719	.558		8.5	.787	.642	
4.0			.372	8.6			.411
4.1	.724	.563		8.7	.789	.644	
4.2			.375	8.8			.412
4.3	.728	.568		8.9	.790	.646	
4.4			.377	9.0	.791	.648	.413
4.5	.732	.573		9.5	.795	.654	.415
4.6			.380	10.0	.798	.661	.417
4.7	.737	.578		10.5	.802	.666	.419
4.8			.382	11.0	.806	.671	.421
4.9	.742	.583		11.5	.809	.675	.423
5.0			.384	12.0	.812	.680	.424
5.1	.746	.587		12.5	.816	.685	.426
5.2			.386	13.0	.819	.689	.427
5.3	.750	.591		13.5	.822	.693	.429
5.4			.388	14.0	.825	.697	.430
5.5	0.753	0.595		14.5	.827	.701	.431
5.6			0.390	15.0	0.829	0.705	0.432

Using these new tables, we worked out a tentative fit for the present incomplete cycle 17 and published, by that means, a prediction of its remaining course.[9] Pending further detailed studies, which we hope to make, of the monthly numbers in general, this fit is only tentative, because trial and error entered into it to some extent. It was not a Case 2 solution—obviously that case does not apply to an incompleted cycle. Nor was equation (10) of Paper I relied upon to give the value of s.

The method was to assume values of s and v and then to take the sum of the observed monthly numbers between these values—that is, to find m_0, with n assumed equal to 1. Similarly, to sum m_1 and m_2. These observed values had to be corrected for the overlap of the preceding cycle, 16; but in percentage this correction was significant only for m_0. An assumed value for V, together with those taken for m_0 and $v - s$, then gave a by equation (35), through $a\phi/\alpha$ in Table 15. Then G and H from Table 16 through equations (30) and (31), with θ equal to the trial $v - s$, gave values of m_1 and m_2. In the correct solution these ought to compare closely with the corrected values obtained from the observed monthly numbers.

Ideally, this results in overdetermination, as comparison of the computed and observed values of either m_1 or m_2 suffice theoretically to fix the curve. In practice the determination is not sharp; and it is useful to compute, by equation (19) of Paper I, the whole course of the theoretical curve for comparison with the run of observed sunspot numbers. Values of F were obtained from equation (18), taking b as $a/(v - s)$ and M_0 as m_0/a.

Waldmeier[10] had published a condensed prediction in 1936, presumably employing his graphical method.

We hope to continue these studies, paying particular attention to the monthly numbers. The principal conclusion to date is that equation (1)—especially in view of its elegant available tabulations through the gamma and incomplete gamma functions—is a remarkably satisfactory and useful mathematical form for dealing

[9] *Phys. Rev.*, **55**, 1102, 1939.

[10] *A.N.*, **259**, 267, 1936.

with sunspot cycles.[11] The objection to it which was emphasized in Paper I has—at least pending further investigation—lost its force, as explained in Section XV above.

Detailed examination of the dying-out of the low-latitude spots at the end of a cycle would be interesting. The term $e^{-b\theta}$ should be predominant there. Published "butterfly diagrams" are of little help in this connection, because it is not long, apparently, after the start of a new outburst before some of the new spots begin to appear rather near the solar equator—overlapping the spots of the fading outburst in latitude as well as in time. Where data are available, in recent years, the first appearance of high latitude spots, as well as the reversal of polarity, should fix the value of s, the time of start of a new cycle. The exact determination of this quantity would be the most desirable improvement in the present study.

PRINCETON UNIVERSITY OBSERVATORY
July 1939

[11] *Note added in proof.*—W. Gleissberg (*Zs. f. Ap.*, **18**, 199, 1939) recently applied a different form. It likewise involves four parameters and is frankly empirical. The representation is broken in two, before and after maximum. The four parameters are the height and time of maximum and the times, during ascent and descent, respectively, when half-maximum is passed. For completed cycles these quantities are readily determined, but the method is useless for predicting the remaining course of a half-completed cycle. The end of the descent is arbitrarily cut off. This form gives excellent representations, and the fit for a completed cycle is easily made. But the comparison of the values of O − C with ours in Table 12 above is weakened by Gleissberg's replacement of the Zurich observed annual numbers with numbers smoothed according to an arbitrary three-year formula. And the early cycles, 1–6, are rejected.

With respect to our prediction of the remaining course of the present cycle, the average of the observed monthly numbers January–September, 1939, was 97.6, as compared with 93.5 predicted. We had selected 1937.9 as the earliest advisable date for maximum, giving especial weight to the still earlier Zürich determination of 1937.4. It is possible that a later value of maximum will be indicated by the decrement of spot-numbers from now on.

Finally it ought to be noted that Mr. Eggleston is a member of the class of 1942 in Princeton University.

THE MOTION OF ERUPTIVE PROMINENCES

R. G. GIOVANELLI

ABSTRACT

A theory is suggested for the motion of such eruptive prominences as are associated with solar eruptions, according to which the constant velocities are maintained by radiation pressure of *La* and changes in velocity may originate in magnetic fields. The *La* line emitted by a single flocculus is shown to be strongly reversed. The total effect produced by several flocculi with different *La* widths is equivalent to that of an *La* contour with several maxima and minima. Provided the intensities are of the right order, to each hump in the contour there corresponds one stable velocity.

If the prominence is electrically charged, on moving into a horizontal magnetic field it experiences a force which accelerates it along a horizontal direction, but the radiation exerts sufficient pressure to maintain an essentially constant vertical velocity. On moving into a field of the opposite direction, the prominence is deflected toward the vertical with an increased velocity and may again be subjected to a further radiation pressure, thus giving rise to an increase in velocity.

The laws of motion of eruptive prominences have been studied by many investigators in the past few years, but no explanation has thus far received general acceptance. The laws as given by Pettit[1] are as follows:

1. The speed is uniform, except that at intervals it increases suddenly.

2. The speed following such a change is usually a small integral multiple of the value preceding the change.

The second law has been challenged on several occasions; and, at the present, its validity seems doubtful. The first law, on the other hand, is accepted generally; thus, any theory of prominence motion must provide not only for a constant velocity but also for sudden increases in this velocity.

Besides this law, several generalizations have been made about the motion of eruptive prominences. Among these are: (*a*) The motions are often at considerable angles to the radius of the sun.[2] (*b*) At the same time as a change in velocity there is a change in the direction of the motion.[3] (*c*) The changes in velocity are not always the same for all parts of a prominence or exactly in the same direc-

[1] *Ap. J.*, **84**, 319, 1936. [2] McMath and Pettit, *Ap. J.*, **88**, 254, 1938.

[3] Waldmeier, *Zs. f. Ap.*, **15**, 299, 1938.

tion.[2] (*d*) One part of a prominence may change its velocity while another part continues unchanged.[2]

It has recently been found[4] that approximately 20 per cent of the eruptions eject eruptive prominences, and also that, while the chance of an eruption ejecting a prominence is independent of its area and intensity, the velocity of such a prominence bears a relation to the intensity, and hence the width, of $H\alpha$. Since the width of $H\alpha$ is most probably related to the width of $L\alpha$, this might well be taken to indicate that these prominences are expelled by the light-pressure of $L\alpha$. On such a hypothesis the width of $L\alpha$ in an eruption, expressed in velocity units, has been found to be approximately six times that of $H\alpha$. Since $H\alpha$ has a minimum half-width of about 1 A, $L\alpha$ will also have a minimum half-width of about 1 A.

Below is advanced a theory for the motion of eruptive prominences in which it is suggested that the constant velocities of the prominence are due to light-pressure, while the sudden changes may be originated by variations in the magnetic field. Although not yet directly applicable to all eruptive prominences, all the known facts receive an explanation when the prominence is of the type expelled from eruptions.

It is necessary first to determine the shape of the $L\alpha$ contour during an eruption. The emission from an isothermal column of the chromosphere is given[5] by

$$I_\nu = (1 - e^{-a_\nu N_0}) P_\nu ,$$

where a_ν is the atomic absorption coefficient for radiation of frequency ν, N_0 is the number of atoms in the column, and P_ν is the Planckian function, to be evaluated at the effective temperature of the eruption.

The emission line given by the foregoing formula will thus be flat topped and will be of intensity P_ν over a half-width $\Delta\nu$, where $a_0 N_0 > 1$, approximately.

Now, a_ν has been given by Weisskopf,[6] and for $L\alpha$ this reduces to

$$a_\nu = \frac{2\pi\epsilon^4\nu^2}{m^2c^4(\Delta\nu)^2} \cdot \frac{g_1}{g_2} \cdot f_{21}^2 ,$$

[4] Giovanelli, *Ap. J.*, in press.

[5] Menzel, *Lick Obs. Pub.*, XVII, 241, 1931.

[6] *Observatory*, **56**, 291, 1933.

where ϵ is the electronic charge; m is the mass of the electron; c is the velocity of light; f_{21}, the oscillator strength, equals 0.416; and g_1/g_2 is the ratio of statistical weights of states 1 and 2. Putting $g_1/g_2 = 0.25$, then $a_\nu = (1 \cdot 32 \times 10^5)/(\Delta\nu)^2$.

N_0 may be estimated as follows: The density of 2-quantum hydrogen atoms at a height x above the base of the chromosphere is given by $n = n_0 e^{-ax}$, where $n_0 = 1 \cdot 3 \times 10^4$ atoms per cubic centimeter and $a = 10^{-8}$ per centimeter, approximately.[7] The depth of the average eruption may be taken as 10^9 cm. Under normal conditions there are approximately n/a 2-quantum atoms in a column of this depth above a region of density n, corresponding to $(n/a)e^{c_2/\lambda T}$ 1-quantum atoms, where T may be assumed to be 6000°. Assuming the total number of atoms to remain unchanged during an eruption, there will thus be $4 \cdot 67 \times 10^{20}$ 1-quantum atoms in such a column if the base of the eruption is placed at the base of the chromosphere. We may thus evaluate $\Delta\nu$ and obtain the result

$$\Delta\nu = 7.85 \times 10^{12} .$$

Thus, the half-width of $L\alpha$ will be about 3.8 A, of the same order as the values estimated from prominence velocities.

The maximum intensity of the foregoing line will be P_ν; i.e., it will equal black-body intensity at a temperature T. Unsöld[8] has shown that the ratio μ of light force to gravitation is

$$\mu = \frac{2\pi^2\epsilon^2 hf}{rmc\lambda^3 Mg} \cdot e^{-c_2/\lambda T} ,$$

where r is the ratio of black-body intensity to line intensity; M is the mass of the atom supported; g is the solar gravitation; f, the oscillator strength, equals 0.416; and λ is the wave length of the line.

Putting $\mu = 1$ and $r = 1$, the temperature is found to be 7600°. However, Unsöld's formula applies only to emission from an infinite plane. The solid angle subtended at a prominence by a flocculus will be considerably less than 2π, and so a greater temperature than

[7] Cillié and Menzel, *Harvard Circ.*, No. 410, 1935.

[8] *Physik der Sternatmosphären*, p. 423, Berlin, 1938.

7600° will be required to support the prominence. This may be compared with eclipse observations of the normal excitation temperatures of the Balmer lines in the chromosphere,[7] which indicate that these lie within the limits of 9,100°–16,900°. Although effective temperatures between the 2- and higher-quantum states cannot be applied to the 1- and 2-quantum states, yet this indicates that excitation temperatures of such an order are not unreasonable. Thus, it would seem that light-pressure may be expected to be of sufficient intensity to support the prominence against gravitation.

The foregoing theory of the emission lines has assumed a constant temperature throughout. It is not probable, however, that the temperature should remain constant to the outermost layers of the eruption. Suppose, for illustration, that the effective temperature drops from 9000° at the base of the eruption to 6000° at the top, then the intensity at the center of the line, which comes mainly from the outermost parts of the eruption, will correspond to an effective temperature of 6000°, while the effective temperature of the outer parts of the line will remain essentially unchanged; i.e., the intensity of the emission at the center of the line will be 1/700 of that at the edge. It is seen that the width of an *La* line depends solely on the total number of atoms in a column of unit cross-section down to the base of the eruption. The lower the base of the eruption, the wider will be the line. The intensity in the wings of the line corresponds to black-body radiation at the effective temperature of the base of the eruption, while at the center of the line the intensity corresponds to black-body radiation at the temperature of the uppermost layers of the eruption.

Suppose that two eruptive flocculi, or even different parts of the same flocculus, differ considerably as to the temperature distribution and depth of atoms involved. Then the contours of the lines emitted from the surfaces of the two flocculi may be given by curves *I* and *II* of Figure 1. Since there will probably be non-eruptive bright flocculi in the neighborhood, these may also give rise to an emission line *III*, which will not be so strongly reversed, since such large differences of temperature will not be possible.

The intensity of the radiation falling on the prominence is proportional to the intensity emitted by the flocculus and to the solid

angle subtended by the flocculus at the prominence. We suppose that contours *I*, *II*, and *III*, shown in Figure 1, have been multiplied by the solid angles which they, respectively, subtend at the prominence. The total intensity of radiation falling on the prominence, given by the broken curve in Figure 1, is obtained by adding the contributions from each flocculus. The resultant contour exhibits an irregular top, with several maxima and minima. Such a line as this can be used to explain how different constant velocities may be maintained in an eruptive prominence.

Let the *La* intensity necessary to support the prominence against gravity be represented by the line *XY* (Fig. 1). Then only those velocities corresponding to the positions where *XY* cuts the contour

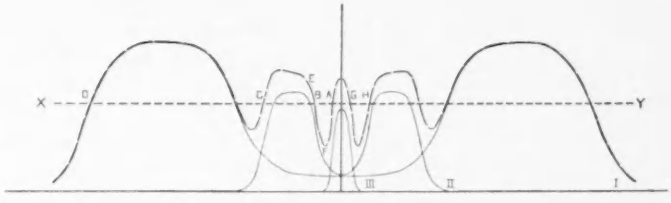

FIG. 1.—*La* contours. The continuous curves *I*, *II*, and *III* represent the *La* contours coming from flocculi of different depths and excitation temperatures. The broken curve represents the effective contour, as regards pressure of radiation on a prominence. The line *XY* represents the intensity required to balance gravitation.

can be maintained. Of these, only the positions *A*, *C*, and *D* will be stable for upward velocities. Thus, if a prominence, by some means, acquires a velocity corresponding to *E*, it will be accelerated to a velocity *C*. A velocity *F* would decrease to *A*. A velocity *B*, although constant, would be unstable, and a slight variation would give rise to either an acceleration or a retardation. Moreover, it can be seen that different parts of a prominence may possess different velocities corresponding to various parts of the contour. It is interesting to note that, if the slopes of the humps in the contour are steep, then the decrease in intensity of radiation with distance will not be of great influence on the velocity.

Any downward motion will also be of constant velocity. Positions such as *G* and *I* would be unstable, while velocities such as *H* would be stable, and constant velocities downward could be maintained.

It now remains to show how a velocity A can suddenly increase sufficiently to move it past B. There are several ways in which this may be done.

An increase in intensity might take place in one of the contours which contribute to the resultant contour: if this were to raise the minimum at F above the line XY, then the prominence would rapidly acquire the velocity C.

An increase in velocity can also be produced by a change in direction of magnetic fields. McCrea[9] has considered the resistance of one gas moving through another and has concluded that no large separation can take place in a prominence. Thus, neutral and ionized atoms will move together. Consider a prominence, mass M, charge E, originally moving vertically with velocity V in a horizontal field of strength H. The prominence experiences a force at right angles to its direction of motion, of strength HEV. This produces a continually increasing horizontal velocity and, as the direction of motion becomes inclined to the radius, a decrease in the vertical velocity. However, if the sides of the La contour are steep, so that a small decrease in velocity produces a large increase in radiation pressure, then this decrease is negligible, and the vertical velocity remains essentially constant. Under these circumstances the horizontal velocity at a time t becomes

$$\int_0^t \frac{EV}{M} \cdot H \, dt \, .$$

If the field becomes small, or the lines of force become parallel to the direction of motion, then the horizontal velocity becomes constant, while the vertical velocity always retains its original value, V. If the prominence now moves into a region where the magnetic field is reversed in direction, its direction of motion will be deflected toward the vertical; and if this takes place sufficiently rapidly, the vertical velocity will be approximately the same as the total velocity before the change. If from a velocity A this changes to one greater than B (Fig. 1), it will be increased automatically by radiation pressure, and a new velocity, C, will be produced.

[9] *M.N.*, **95**, 509, 1935.

It must be realized that in the neighborhood of spot groups the magnetic fields will probably be complex, and such variations as those described above will be possible. Even neglecting these, the complex magnetic fields set up by the movements of charges on other parts of the prominence will probably be sufficient to cause these variations.

To determine the magnitude of the magnetic field required to produce such a change, suppose that the change in direction is produced in about 60 seconds, compatible with Pettit's observations. The average downward acceleration, gravity *minus* light-pressure, will probably not exceed $\frac{1}{2}g$, and in this time a decrease in velocity of less than 8 km/sec will take place. This may be neglected in comparison with the velocities normally found in prominences.

The force HEV at right angles to the direction of motion, produced by the magnetic field, would cause the prominence to move in the arc of a circle of radius r where

$$r = \frac{MV}{HE}.$$

If we take the change of direction necessary as one radian, then the time required to produce this change, i.e., 60 seconds, is

$$\frac{r}{V} = \frac{M}{HE}.$$

Thus,

$$H = \frac{M}{E \cdot 60}.$$

Assuming the net charge on the prominence to be one ion per thousand atoms, then $H = 1.6 \times 10^{-3}$ gauss. Such small fields as this cannot be regarded as unlikely, whether the origin be sunspots or moving charges. It thus appears that the foregoing combination of light-pressure and magnetic field variations may be used to explain the motion of eruptive prominences ejected by eruptions. The generalizations outlined earlier can be satisfied; and, indeed, a suggestion may be put forward about the second of Pettit's laws, from which it would seem that, on the whole, as the velocity increases,

the increase in velocity is correspondingly greater. But this is what might be expected from a contour such as has been drawn in Figure 1. If, say, the reversal covers half the width of the line, then the maximum in *II* must lie less than halfway out toward the end of the maximum in *I;* and thus successive increases in velocity will be correspondingly greater.

When an attempt is made to apply the foregoing theory to eruptive prominences not associated with eruptions, the difficulty arises that we are not justified in assuming a high excitation temperature for *Lα* under such prominences. That, at times, eruptions have been observed when and after violent movements have taken place in dark flocculi on the disk[10] suggests that perhaps here, too, some mechanism similar to that described above may be operating.

It is a pleasure to acknowledge my indebtedness to Dr. C. W. Allen for the interesting discussions which we have had and for the many suggestions he has made during the preparation of this paper.

COMMONWEALTH SOLAR OBSERVATORY
CANBERRA, AUSTRALIA
July 1939

[10] Newton, *M.N.*, **95**, 650, 1935.

CH BANDS IN COMET SPECTRA

J. DUFAY

ABSTRACT

The intensity distribution in the λ 4300 and λ 3900 bands of *CH* is calculated according to the method of Swings and Nicolet, which has been slightly modified. A comparison with measurements of objective-prism spectra of four recent comets confirms the presence of the λ 4300 band. That of the λ 3900 band seems also established, in spite of the disturbing proximity of the strong λ 3883 cyanogen band. Many radiations not considered in the two *CH* bands are also found. Finally, the possibility of detecting the Raffety band in comets is briefly discussed.

1. Using old observations of bright comets by Wright, Baldet, Bobrovnikoff, and others, M. Nicolet[1] showed that the presence of the $A^2\Delta \rightarrow X^2\Pi$ band of *CH*, near λ 4300, was very probable. Observations of recent comets made at the Lyon Observatory by M. Bloch, J. Ellsworth, J. Gauzit, and myself proved this conclusion beyond any doubt and established definitively the presence of hydrogen in comets.[2]

In a more recent paper P. Swings and M. Nicolet[3] carefully studied the intensity distribution in the bands of cometary spectra and applied their theoretical considerations to the violet *CN* system and to the 4300 band of *CH*. Microphotometer tracings of the spectrograms taken at Lyon reveal much more detail than the old observations, and it is interesting to compare the results of the theory with new available observational data, for the $B^2\Sigma \rightarrow X^2\Pi$ as well as for the $A^2\Delta \rightarrow X^2\Pi$ band.

2. *Calculation of the intensity distribution in the* $A^2\Delta \rightarrow X^2\Pi$ *and* $B^2\Sigma \rightarrow X^2\Pi$ *bands.*—In the case of the *CH* bands the fundamental assumption of the theory is that the distribution of the molecules on rotational levels corresponds to the nuclear temperature $T_1 = 300 \cdot r^{-1/2}$ (r being the distance from the comet to the sun, in as-

[1] *Zs. f. Ap.*, **15**, 154, 1938; *Liége Pub.*, No. 237.

[2] Dufay, *C.R.*, **206**, 1550, 1938; *Bull. Soc. Française Phys.*, No. 406, p. 93, 1937.

[3] *Ap. J.*, **88**, 173, 1938; *Liége Pub.*, No. 244.

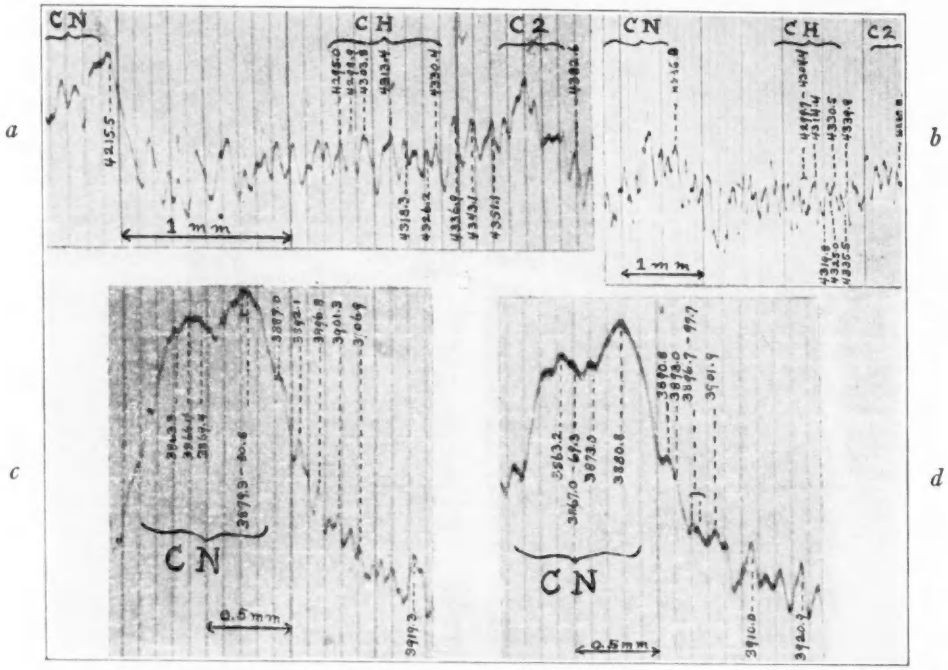

FIG. 1.—Microphotometer tracings of (*a*) Comet Peltier and (*b*), (*c*), (*d*) Comet Finsler

tronomical units). It is, therefore, possible to calculate the relative intensity of each rotational line by the classical formula

$$I = i \exp \frac{-E}{kT_1}, \qquad (1)$$

in which i denotes the so-called "intensity factor," k Boltzmann's constant, and E the rotational energy.

Apparently Swings and Nicolet used as E the rotational energy in the upper state. It seems, however, that the lifetime of the molecules in the excited state is not long enough to permit thermal equilibrium to be established. I assume, therefore, that equilibrium exists only in the lower state, and formula (1) leads me to calculate the intensity of the lines in the absorption process, i representing the intensity factor of the absorption line and E the rotational energy in the lower state.

The molecule can usually move to a given upper level in different ways (R and P branches, for instance). The intensities $I_1, I_2, \ldots$, of the corresponding absorption lines are calculated by formula (1), using appropriate values for the intensity factors $i_1, i_2, \ldots$. From this level the molecule can jump again to different lower levels. Let $i_1', i_2', \ldots$, be the intensity factors of the corresponding emission lines. The intensities of these lines may be expressed by

$$I_1' = \frac{i_1'(I_1 + I_2 + \ldots)}{i_1 + i_2 + \ldots}, \qquad I_2' = \frac{i_2'(I_1 + I_2 + \ldots)}{i_1 + i_2 + \ldots}.$$

If we consider, for instance, the upper level $K' = 0$, T_1' $(\frac{1}{2})$, in the $B^2\Sigma$ state, the molecules arising from the $X^2\Pi$ state give rise, in the absorption process, to the two transitions

$$P_1(1) : T_1''(\tfrac{1}{2}) \rightarrow T_1'(\tfrac{1}{2}), \qquad \text{with} \qquad i_1 = \tfrac{4}{3},$$
$$^PQ_{1,2}(1) : T_2''(\tfrac{1}{2}) \rightarrow T_1'(\tfrac{1}{2}), \qquad \text{with} \qquad i_2 = \tfrac{2}{3}.$$

We have, therefore, $i_1 + i_2 = 2$.

Assuming $T_1 = 333^\circ$ K, the values of $\exp(-E/kT_1)$ for the two

initial states $T_1''(\frac{1}{2})$ and $T_2''(\frac{1}{2})$ are, respectively, 0.911 and 0.985. Then the intensities of the absorption lines are

$$P_1(1) : I_1 = \tfrac{4}{3} \times 0.911 = 1.215 ,$$
$$^{P}Q_{1.2}(1) : I_2 = \tfrac{2}{3} \times 0.985 = 0.657 ,$$

and $I_1 + I_2 = 1.882$.

From this upper level, the same two transitions $P_1(1)$ and $^{P}Q_{1.2}(1)$ take place in the re-emission process with the same intensity factors, so that the final intensities of the two emission lines become

$$\lambda = 3892.8 , \qquad P_1(1) : I_1' = \tfrac{4}{3} \times \frac{1.882}{2} = 1.255 ,$$

$$\lambda = 3890.1 , \qquad ^{P}Q_{1.2}(1) : I_1' = \tfrac{2}{3} \times \frac{1.882}{2} = 0.627 .$$

The preceding case is the simplest possible illustration of the $B^2\Sigma \rightarrow X^2\Pi$ system. Four transitions must be considered in connection with the $K' = 1$, $T_1'(1\frac{1}{2})$, level; five in the $K' = 2$, $T_1'(2\frac{1}{2})$ level —namely, $P_1(3)$, $^{P}Q_{1.2}(3)$, $Q_1(2)$, $^{Q}R_{12}(2)$, and $R_1(1)$. But, with the increasing values of the rotational quantum number, the intensity factors of the satellite branches decrease and rapidly vanish, so that these branches can be disregarded for $K \geqslant 4$. Only three transitions remain for each upper level, the rotational quantum number of which exceeds 4, corresponding to the main branches P_1, Q_1, and R_1 (or P_2, Q_2, and R_2).

I have calculated, according to the preceding method, the intensity of each rotational line up to $K = 7$ for the two bands $A^2\Delta \rightarrow X^2\Pi$ and $B^2\Sigma \rightarrow X^2\Pi$, assuming that the nuclear temperature corresponds to the distance to the sun $r = 0.8$ astronomical unit (mean distance of the Comet Finsler during the observations). Thus, $T_1 = 300 \times 0.8^{-1/2} = 333^{\circ}$ K. The results of these somewhat laborious calculations differ very slightly from the simpler calculation taken, according to formula (1), on the less correct assumption that the molecule reaches thermal equilibrium in the upper level. The shape of the curve $I = f(K)$ is slightly more flattened when the long method is used, but the difference in intensity distribution is quite inappre-

ciable, considering the precision of the observations. This effect results from the fact that the moment of inertia of the molecule has about the same value in the $B^2\Sigma$, $A^2\Delta$, and $X^2\Pi$ states (the same fact happens in the case of the violet *CN* band). But the procedure here developed seems to be the most reliable when the transition is accompanied by a notable change in the moment of inertia.

3. *Graphical construction.*—In order to compare the theoretical with the observational distribution, Swings and Nicolet represent each rotational line by a rectangle, the height of which is proportional to the theoretical intensity I of the line. The plates considered are slit spectra. Let Δ be the width, in angstrom units, of the image of the slit on the plate; it is convenient to give the width Δ to the representative rectangles.

But the Lyon spectrograms are taken with a prismatic camera. In this case, monochromatic images of the nuclear radiations near λ 4300 are starlike points. Each radiation should be rigorously represented by a curve, the shape of which reproduces the intensity distribution in the photographic image. But graphical constructions based upon this consideration are quite impracticable; and, after trials, I have decided to represent each radiation by an isosceles triangle of height I, the base Δ of which is determined by the resolving-power of the spectrograph. This procedure seems to be a reasonable compromise and has the advantage of removing the high "chimneys" produced by two rectangles slightly superposed one upon another, which, however, do not conform to reality. The width Δ adopted for the bases of the triangles are 4 A in the λ 4300 region and 2 A in the λ 3900 region.

The diagrams thus obtained for the two *CH* bands are shown in Figures 2 and 3. A comparison with the diagram published by Swings and Nicolet shows no marked discrepancies, in spite of the different treatments.

4. *Observational data.*—Two prismatic cameras were used at the Lyon Observatory for the observation of cometary spectra. The first (*A*) consists of a 60° prism of dense flint and a camera lens 30 cm in focal length, of relative aperture $f/7$, giving a linear dispersion about 60 A/mm near λ 4300 and 40 A/mm near λ 3900. The second (*B*) consists of a 60° prism of ordinary flint glass and a camera lens 21 cm

in focal length, of relative aperture $f/3.5$, giving a linear dispersion of about 130 A/mm near λ 4300 and 90 A/mm near λ 3900.

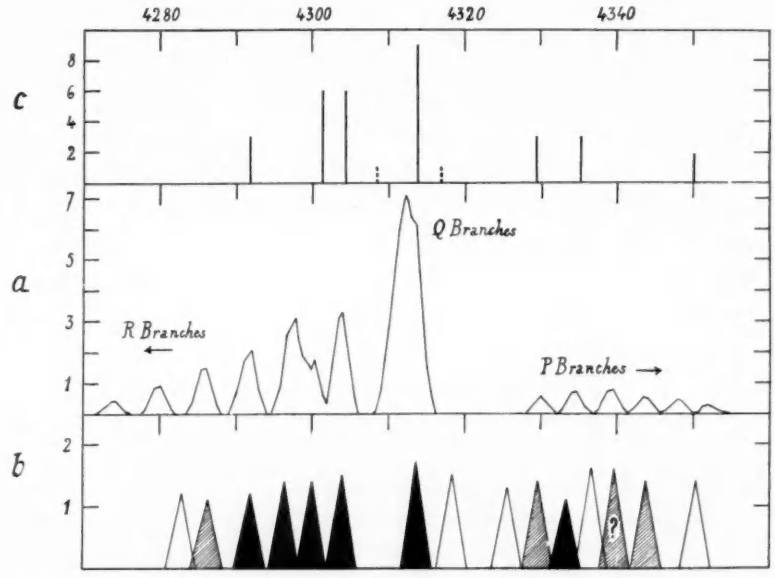

FIG. 2.—Band $A^2\Delta \rightarrow X^2\Pi$. The abscissas are wave lengths in angstrom units; the ordinates, intensities on arbitrary scales. (*a*) Intensity distribution calculated with $T = 333°$ K; (*b*) radiations measured on Lyon plates; (*c*) radiations of the nucleus according to Baldet.

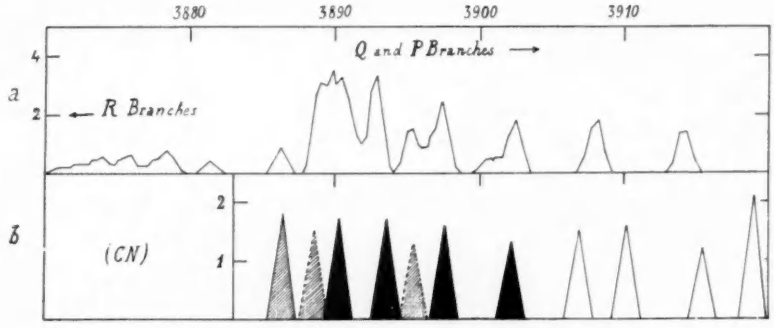

FIG. 3.—Band $B^2\Sigma \rightarrow X^2\Pi$. The abscissas are wave lengths in angstrom units; the ordinates, intensities on arbitrary scales. (*a*) Intensity distribution calculated with $T = 333°$ K; (*b*) radiations measured on Lyon plates.

The number of plates of each comet measured are listed in Table 1, in which r denotes the mean distance from the comet to the sun dur-

ing the observations. Two stellar comparison spectra were placed alongside the spectrum of the comet (except in the case of Comet Peltier). Several microphotometer tracings of each plate were taken under different conditions (different heights and widths of the analyzing slit); the abscissas of all the maxima were measured, but only the maxima present on tracings of almost all the plates were used. In this manner, accidental errors due to the grain of the plates seem to be reasonably eliminated. Moreover, all the spectrograms of Comet Finsler and the six best spectrograms of Comet Peltier were directly studied with a measuring machine, and the two sets of measures

TABLE 1

LIST OF PLATES

	Comet				
r (A.U.)	Peltier 1936*a*	Whipple 1937*b*	Finsler 1937*f*	Encke 1937*h*	Total
	1.1	1.8	0.8	0.76	
A	6	.....	5	.....	11
B	3	3	6	3	15
Total	.....	.....	.....	.....	26

were found, on the whole, to be in satisfactory agreement. In Tables 2 and 3 the wave lengths of the radiations which have been directly seen with the measuring microscope, as well as on the records, are marked with asterisks. The others are from the records alone.

5. *Band* $A^2\Delta \rightarrow X^2\Pi$ *near* λ *4300.*—Two records of the λ 4300 region of the spectra of Comet Peltier and Comet Finsler are shown in Fig. 1, *a* and *b*. In Table 2 all the wave lengths measured, from λ 4280 to λ 4355 are listed separately for each comet and for each dispersion (*A* and *B*). The weighted mean wave lengths adopted for the different radiations are represented in the lower part of Figure 1 by individual triangles. The heights of these are proportional to the mean intensity estimated on an arbitrary scale. This scale, however, appears much too smooth, and the intensity estimates are thus of low weight.

All the predicted maxima belonging to the *R* and *Q* branches really occur in cometary spectra and are represented by black triangles. The radiation λ 4314, corresponding to the *Q* branches, is the most intense in the spectral range considered. Triangles covered with lines represent radiations perhaps belonging to the band, but their intensity is too high. Mulliken[4] has pointed out that in the laboratory,

TABLE 2

WAVE LENGTHS IN THE λ 4300 REGION

☌ PELTIER		☌ WHIPPLE	☌ FINSLER		☌ ENCKE	ADOPTED	
A	*B*	*B*	*A*	*B*	*B*	λ	*i*
4283.5	.....	4284.1	4283.0	4282.0*	4282.3	4282.9	1.2
4286.7*	4285.0*	.....	4287.5	4285.9*	4286.9	4286.3	1.1
4292.8*	4292.0	.....	4292.6*	4291.5*	4290.3	4291.8	1.2
4295.9*	4296.7	4296.1	4296.8*	4296.6*	4297.5	4296.4	1.4
4299.4*	4300.0	4298.6	4300.0*	4300.3*	4299.7	4300.0	1.4
4303.8*	4302.9*	4302.2	4303.5*	4304.0*	4302.8?	4303.9	1.5
.....	.....	.....	4305.8	.....	4306.5	.....	.....
4309.7	.....	.....	.....	4308.3*	.....	.....	.....
4314.1*	4313.6*	4314.6	4313.9*	4312.4*	4314.0	4313.6	1.7
.....	4316.0	.....	.....	.....	.....	.....	.....
4320.0	4319.1*	4319.9	4318.1*	4317.7*	4317.1	4318.4	1.5
.....	.....	.....	4322.4*	4322.1	.....	.....	.....
4325.9*	4324.3	4325.6	4325.9	4325.5*	4325.2	4325.5	1.3
4329.5	4328.0?	4330.1	4329.9*	4329.2?	4329.4	4329.6	1.4
4333.2	4333.3	.....	4333.9	4333.5*	4333.8	4333.3	1.1
4336.2*	.....	4336.5	4337.7*	4336.5*	4336.5	4336.7	1.6
4339.5*	.....	.....	.....	4340 0?*	4339.7	4339.7?	1.6?
4343.5*	.....	.....	4344.5*	4343.6*	4344.7	4343.8	1.4
.....	4346.9*	4346.1?	4348.4	.....	.....	.....	.....
4350.8	4350.4	4350.2	4351.3*	4351.3*	4350.0?	4350.4	1.4
.....	.....	.....	4354.5*	.....	.....	.....	.....

also, the intensity of the *P* branches exceeds the theoretical intensity.

The presence of radiations foreign to the band is clearly seen; they are represented by open triangles. Several of these radiations may belong to the faint band of *CH* superposed on the λ 4300 band and interpreted as the 1 → 1 band of the same system. Particularly the line λ 4325, always present in laboratory spectra, seems to consist of the *Q* branches of the 1 → 1 band. Whether the λ 4318 line

[4] *Phys. Rev.*, **30**, 804, 1927.

belongs to the Vegard-Kaplan system of $N^2(1 \rightarrow 13)$ remains questionable.

In the upper part of Figure 1 the radiations found by Baldet[5] in the spectra of cometary nuclei are represented by straight lines (broken lines correspond to doubtful radiations, according to Baldet). They agree well with the most intense radiations here measured.

6. *Band* $B^2\Sigma \rightarrow X^2\Pi$ *near* λ *3900.*—It is difficult to observe a rather faint band near λ 3900, especially on objective-prism spectra, be-

TABLE 3

WAVE LENGTHS IN THE λ 3900 REGION

Peltier		Whipple	Finsler		Encke	Adopted	
A	*B*	*B*	*A*	*B*	*B*	λ	*i*
3886.9	3886.6*	3886.0	3887.1*	3886.0*	3885.7	3886.4	1.8
.....	3888.9	.....	3888.7*	.....	.....	3888.6?	1.5
3890.2*	3890.8	3889.9	3890.1	3890.3*	3890.7	3890.3	1.7
3894.1	3892.9	3894.2	3893.1	3893.9?*	3893.7	3893.6	1.7
3895.2	.....	.....	3895.1?	3896.0	.....	3895.5	1.3
3897.3*	3897.5*	3897.1?	3897.0	3898.3*	.....	3897.6	1.6
3899.8	.....	.....	3899.5	.....	.....	.....	.....
3902.3	3902.7	33902.0	3901.1*	3902.6*	3902.1	3902.2	1.3
3904.4?	.....	.....	3904.3	.....	.....	.....	.....
3907.1?*	3906.3*	3906.2	3907.1?	3907.0*	.....	3906.9	1.5
3909.1	3910.7	3910.1?	3909.9	3911.2?	.....	3910.2	1.6
3912.3	3919.3*	.....	3913.5	.....	.....	.....	.....
3915.5?*	.....	3915.5?	3915.5?	3915.8	.....	3915.5	1.2
.....	3917.5*	.....	3917.4	.....	.....	.....	.....
3918.9*	.....	3920.5	3919.3	3918.8	3919.2	3919.0	2.1

cause of the proximity of the strongest band of *CN*, λ 3883, which extends far into the coma. The presence of the $B^2\Sigma \rightarrow X^2\Pi$ band has, therefore, never been established.

Microphotometer records, however, disclose a number of faint maxima along the descending branch of the cyanogen band toward the red (see, for instance, in Fig. 1, *c* and *d*, two records of Comet Finsler). Their wave lengths have been measured in the same way as in the λ 4300 region, and the results are given in Table 3. The reality of most of these maxima is unquestionable; several are directly seen with the microscope.

[5] *Ann. Obs. Meudon*, **7**, 58, 1926.

In the lower part of Figure 3, individual triangles represent the adopted mean wave lengths. All the maxima predicted along the *Q* and *P* branches are present (black triangles), but the maxima along the *R* branches are hidden by the *CN* band. In addition, we find again radiations possibly belonging to the band and radiations not belonging to the *CH* band (white triangles).

The identification of the *CH* band may be slightly disturbed by the possible presence of other bands, namely: (*a*) the $8 \rightarrow 1$ band of CO^+, with the four heads λλ 3888.5, 3890.5, 3908.0, and 3909.9;[6] (*b*) the $10 \rightarrow 10$ tail band of *CN*, the presence of which will be discussed in a future paper in connection with the general structure of *CN* bands; (*c*) the $0 \rightarrow 11$ band of the Vegard-Kaplan system of N^2, near λ 3889. Finally, the radiation λ 3915.5 is perhaps the $0 \rightarrow 0$ band of the negative system of N^{2+}.[7]

The presence of the λ 3900 band of *CH* seems, however, to be well established by the radiations λλ 3893.6, 3895.5, 3897.6, and 3902.2.

Most of the radiations of Table 3 were, until now, unknown in cometary spectra. In his first list of nuclear lines Baldet[8] gives only the λ 3910.9 radiation; λ 3890 and λ 3906.3 appear in his list of "weak, rare or doubtful radiations."

7. *Possible presence of the Raffety band near λ 4050.*—The well-known group of cometary radiations near λ 4050 has been tentatively identified with the Raffety band. Baldet[9] showed, however, that (*a*) certain lines of the Raffety band do not occur in comets and (*b*) certain radiations of the λ 4050 group were absent in the Raffety band. Consequently, he concluded that the proposed identification was inconsistent.

Now, according to Grenat,[10] who analyzed the band on high-dispersion spectra, the Raffety band belongs to the same system as the λ 3900 band. It is presumably the band of the $B^2\Sigma \rightarrow X^2\Pi$ system. We can, therefore, expect for the Raffety band, if present in comets, an intensity distribution about similar to that of the λ 3900 band.

[6] Dufay, Bloch, and Ellsworth, *C.R.*, **204**, 663, 1937.

[7] Dufay, *C.R.*, **204**, 744, 1937.

[8] *Loc. cit.*

[9] *C.R.*, **192**, 1531, 1931.

[10] *C.R.*, **192**, 1553, 1931.

The absence in cometary spectra of certain lines of the band is, thus, not contradictory if these lines correspond to high rotational levels, and the argument advanced by Baldet against the presence of the Raffety band in comets seems no longer quite convincing. In fact, the lines of low rotational levels, especially in the *Q* and *P* branches, agree well with cometary radiations, so that it is not possible to confirm the absence of the Raffety band in cometary spectra.

However, our present investigation emphasizes the second argument of Baldet. It is quite certain that many radiations of the λ 4050 group do not belong to the Raffety band and thus remain unidentified. A detailed study of this spectral region will be presented in a future paper.

8. *Conclusions.*—It appears from the preceding analysis that the $A^2\Delta \rightarrow X^2\Pi$ band of *CH*, and very probably the $B^2\Sigma \rightarrow X^2\Pi$ band, are present in cometary spectra. Moreover, the theory of Swings and Nicolet furnishes a suitable working hypothesis for the intensity distribution in these bands. However, in the case of *CH* the intensity distribution is rather insensitive to temperature variations. Thus, a temperature decrease of about 100° does not considerably alter the intensity-curve; the intensity decreases naturally more rapidly with increasing values of the rotational quantum number, but its maximum is hardly displaced by one unit along the *K*-axis. No notable difference has been found, therefore, between the maxima in the *CH* bands in Comet Finsler ($r = 0.8$ astronomical unit, $T_1 = 333°$) and in Comet Whipple ($r = 1.8$ astronomical units, $T_1 = 223°$). On the contrary, the intensity distribution in the *CN* bands differs considerably in these two comets.[11] This fact results from the higher values of the rotational energy, *E*, in the *CH* molecules than in the *CN* molecules. The study of the intensity distribution in the *CN* bands should, therefore, give a better test of the theory.

The mechanism suggested by Wurm[12] to explain the intensity distribution in the bands presumably takes place. His recent objection[13] to the theory of Swings and Nicolet, involving the existence of a dilution factor, is more effective in the case of *CN* than in the

[11] Dufay, *C.R.*, **206**, 1948, 1938.

[12] *Zs. f. Ap.*, **15**, 115, 1938.

[13] *Ap. J.*, **89**, 318, 1939.

case of *CH*, because the *CN* molecules, having a higher energy of dissociation, move much farther away from the nucleus. On objective-prism spectra the radiations attributed to the λ 4300 band of *CH* are indeed localized close to the nucleus, even closer than the nuclear radiations near λ 4050. Thus, in the case of the *CH* bands it seems probable that the dilution factor does not play an important role.

I am indebted to my collaborators, Miss M. Bloch and Dr. J. Gauzit, for valuable assistance in measuring the plates and tracings. My thanks are also due to Professor P. Swings for several valuable discussions.

Observatoire de Lyon
April 1939

ON THE PHYSICAL SIGNIFICANCE OF THE M – S DIFFERENTIATION

KARL WURM

ABSTRACT

The relative prominence of the *TiO* and *ZrO* bands in spectral classes M and S is explained on the basis of different atmospheric conditions. S stars have a lower total atmospheric density than M stars of the same temperature. For a given temperature, T, the upper limit of the total density, ν, in S-star atmospheres, is given by

$$\nu = \rho \frac{\mu^{-1}}{1 - \mu^{-1}} K_{TiO}(T),$$

where $K_{TiO}(T) = \nu_{Ti}\nu_{O}/\nu_{TiO}$ designates the dissociation constant of the *TiO* molecule, ρ the abundance ratio of hydrogen to oxygen, and μ the abundance ratio of titanium to zirconium. The low values of ν for S stars indicate that they are supergiants.

1. The differentiation between stars of class M and class S is based chiefly on the relative intensity of the bands of the two related oxides, *TiO* and *ZrO*. If *TiO* is predominant, the stars are classified as M, whereas objects showing *ZrO* more strongly than *TiO* are generally designated as S stars. However, the existence of stars in which the strength in both bands is nearly equal makes it impossible to draw a sharp distinction between the two classes. S stars differ also from M stars by a slightly higher intensity of the enhanced lines of *Ba* and *Sr*.[1] Both types show strong absorption lines of neutral *Ti*, whereas the neutral *Zr* lines are strong in S but very weak, or absent, in M.[2] M and S stars doubtless cover the same temperature interval. Low-dispersion spectra over the wave-length region from λ 3000 to λ 9000 show a striking similarity in the intensity distribution of the continuous radiation for both types.[3] Pettit and Nicholson[4] observed radiometrically a number of late-type variables, among which there are three of type S. They show no characteristic peculiarities, compared with the others. The minimum temperatures of two of the three S stars are among the lowest observed thus far, namely, 1600°.

S stars are relatively rare, compared with those of class M. In re-

[1] P. W. Merrill, *Ap. J.*, **56**, 457, 1922; *Pop. Astr.*, **37**, 444, 1929.

[2] Merrill, *Ap. J.*, **63**, 13, 1926.

[3] R. Wildt, *Ap. J.*, **84**, 303, 1936.

[4] *Ap. J.*, **78**, 320, 1933.

gard to their position in the spectral sequence, they are supposed to form—aside from the classes M and R to N—a third division of the giant branch. No S dwarfs have been found. Recent investigations of the dissociative equilibrium have shown that the branching into "oxygen stars" of class M and "carbon stars" of classes R to N is caused primarily by an alteration of the abundance ratio of oxygen and carbon.[5] In the case of the M to S differentiation, it is not evident whether we have to deal with a similar phenomenon or only with a difference in atmospheric conditions. It is the purpose of the following considerations to show that the second assumption is the more probable one and that the observational facts can be explained without requiring a difference in the relative abundance of *Ti* and *Zr*.

2. Because of a higher intensity of the atomic lines of *Ti* in stellar spectra, compared with those of *Zr*, *Ti* is supposed to be more abundant than *Zr* by a factor of about 10 to 100. A precise value has not yet been established. We shall assume an abundance ratio, $\mu = 10$, for the two elements. It will be shown later that the essential results are consistent with either a higher or a lower value of μ.

Since no other compounds than the oxides of the two elements are known to exist in stellar atmospheres, we have good reason to assume that the total number of *Ti* and *Zr* atoms, ν', bound or free, per cubic centimeter, is given by

$$\nu'_{Ti} = \nu_{Ti} + \nu_{TiO}\,; \qquad \nu'_{Zr} = \nu_{Zr} + \nu_{ZrO}\,, \tag{1}$$

respectively, where the ν's designate the densities of the particles indicated by the indices. Because of the low ionization in late-type stars, we shall disregard completely the ionized particles.[6] It will also be permissible for our discussion to consider the densities ν and ν', as well as the temperature T, as uniform throughout the whole atmosphere, since we are mainly concerned with the properties of the dissociative equilibrium between the molecules and atoms present.

[5] Y. Cambresier and L. Rosenfeld, *M.N.*, **93**, 710, 1933; H. N. Russell, *Ap. J.*, **79**, 317, 1934.

[6] The degree of ionization will be the same for both elements, since they have practically the same ionization energy. As we are interested only in the relative values ν_{Ti}/ν_{Zr}, a higher ionization would not influence our considerations.

The relative intensity I_{TiO}/I_{ZrO} of the *TiO* and *ZrO* bands will be considered equal to the ratio of the molecular densities ν_{TiO}/ν_{ZrO}:

$$\frac{I_{TiO}}{I_{ZrO}} = \frac{\nu_{TiO}}{\nu_{ZrO}} = R\,. \tag{2}$$

We shall now show that, independent of the presence of other constituents forming oxides, the ratio, R, for a given temperature depends only on the partial density, ν_O, of free oxygen and on the values of $K_{TiO}(T)$ and $K_{ZrO}(T)$, the equilibrium constants of the two molecules.

In equilibrium we have

$$\frac{\nu_{Ti}\nu_O}{\nu_{TiO}} = K_{TiO}(T)\,; \qquad \frac{\nu_{Zr}\nu_O}{\nu_{ZrO}} = K_{ZrO}(T)\,. \tag{3}$$

As is well known, the equilibrium constants $K_{xy}(T)$ can be represented approximately by[7]

$$K_{xy}(T) = \frac{p_x \cdot p_y}{p_{xy} \cdot hr^2}\left(\frac{M_{xy} \cdot kT}{8\pi}\right)^{1/2} e^{-D_{xy}/kT}(1 - e^{-h\omega/kT})\,, \tag{4}$$

where k, T, and h have the usual meaning. The p's designate the statistical weights of the ground electronic states; D_{xy} is equal to the dissociation energy; ω gives the frequency of the lowest vibrational state; M_{xy} is the harmonic mass,

$$M_{xy} = \frac{m_x \cdot m_y}{m_x + m_y}\,;$$

and r is the nuclear separation.

From (3) we can easily derive

$$\nu_{TiO} = \nu'_{Ti}\frac{\nu_O}{K_{TiO} + \nu_O}\,; \qquad \nu_{ZrO} = \nu'_{Zr}\frac{\nu_O}{K_{ZrO} + \nu_O}\,. \tag{5}$$

Forming the ratio ν_{TiO}/ν_{ZrO}, we find

$$R(T, \nu_O) = \mu\frac{K_{ZrO} + \nu_O}{K_{TiO} + \nu_O}\,. \tag{6}$$

[7] xy stands for any diatomic molecule.

Values of K_{TiO} and K_{ZrO} are listed in Table 1. For D_{TiO} and D_{ZrO} the values 5.5 and 6.5 volts have been chosen.[8]

TABLE 1

T	K_{TiO}	K_{ZrO}	T	K_{TiO}	K_{ZrO}
1400°	$1.2 \cdot 10^{5}$	$3.4 \cdot 10^{1}$	2800°	$6.9 \cdot 10^{14}$	$9.7 \cdot 10^{12}$
1500	$1.3 \cdot 10^{6}$	$5.2 \cdot 10^{2}$	3000	$2.9 \cdot 10^{15}$	$6.4 \cdot 10^{13}$
1600	$2.5 \cdot 10^{7}$	$1.8 \cdot 10^{4}$	3200	$1.0 \cdot 10^{16}$	$2.9 \cdot 10^{14}$
1800	$2.2 \cdot 10^{9}$	$3.5 \cdot 10^{6}$	3400	$3.5 \cdot 10^{16}$	$1.1 \cdot 10^{15}$
2000	$7.4 \cdot 10^{10}$	$2.2 \cdot 10^{8}$	3500	$5.5 \cdot 10^{16}$	$2.2 \cdot 10^{15}$
2200	$1.3 \cdot 10^{12}$	$7.2 \cdot 10^{9}$	3600	$8.9 \cdot 10^{16}$	$3.6 \cdot 10^{15}$
2400	$1.6 \cdot 10^{13}$	$1.3 \cdot 10^{11}$	3800	$2.5 \cdot 10^{17}$	$1.1 \cdot 10^{16}$
2500	$4.2 \cdot 10^{13}$	$4.2 \cdot 10^{11}$	4000	$5.2 \cdot 10^{17}$	$2.4 \cdot 10^{16}$
2600	$1.2 \cdot 10^{14}$	$1.5 \cdot 10^{12}$			

Equation (6) shows that at constant temperature R decreases with decreasing ν_0 until ν_0 becomes small in comparison with K_{ZrO}. For all values of $\nu_0 \ll K_{ZrO}$, R remains constant and equal to

$$R_{\min}(T, \nu_0) = \frac{\mu K_{ZrO}}{K_{TiO}} . \tag{7}$$

Table 1 shows that K_{ZrO}/K_{TiO} decreases rapidly with decreasing temperature, roughly as $e^{-\Delta D/kT}$, where ΔD is equal to $D_{ZrO} - D_{TiO}$. The *ZrO* bands can become especially strong relative to the *TiO* bands for lower temperatures, but we have always the necessary condition that $\nu_0 \ll K_{ZrO}$, in order to reach the value $R_{\min}$ of equation (7).

The maximum value of R is reached when $\nu_0 \gg K_{TiO}$,

$$R_{\max}(T, \nu_0) = \mu , \tag{8}$$

and is the same for all temperatures. Figure 1 gives a representation of log R for a set of values of ν_0.

The ratios

$$\frac{\nu_{TiO}}{\nu'_{Ti}} = a_{TiO} , \qquad \frac{\nu_{ZrO}}{\nu'_{Zr}} = a_{ZrO} \qquad (a \leqq 1) , \tag{9}$$

[8] The reasons for the preference of these values are discussed in sec. 3.

for a given temperature always decrease with decreasing R. From equations (5) it can be seen that for any temperature

$$a_{ZrO} \geqq a_{TiO}\,, \tag{10}$$

as is evident from the higher dissociation energy of ZrO. The relative concentration of the free and bound atoms is given by

$$\frac{\nu_{Ti}}{\nu_{TiO}} = \frac{1 - a_{TiO}}{a_{TiO}}\,, \qquad \frac{\nu_{Zr}}{\nu_{ZrO}} = \frac{1 - a_{ZrO}}{a_{ZrO}}\,. \tag{11}$$

Hence, the intensity of the atomic lines, compared with the intensity of the corresponding bands, increases with decreasing R. From

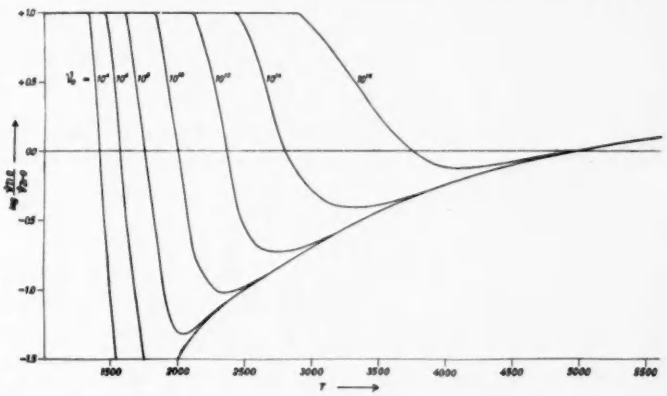

FIG. 1.—The logarithm of the ratio of the abundance of TiO to ZrO is given as a function of temperature, T, and number of atoms of free oxygen, ν_0. Stars of type S will be found below the line $\log \nu_{TiO}/\nu_{ZrO} = 0.0$.

equations (9), (10), and (11) the behavior of the Ti and Zr lines in class M ($R > 1$) and class S ($R < 1$), as previously mentioned, can be easily understood.

For S stars we have the condition

$$\mu \frac{a_{TiO}}{a_{ZrO}} < 1\,, \tag{12}$$

or

$$a_{TiO} < \mu^{-1}\,. \tag{13}$$

From equation (13) it follows that

$$\nu_O < \frac{\mu^{-1}}{1 - \mu^{-1}} K_{TiO}(T) . \tag{14}$$

Equation (14) gives the upper limit of ν_O for stars of class S with a given temperature. The numerical values of $K_{TiO}(T)$ in Table 1 show that low-temperature S stars demand extremely low partial densities of free oxygen. The critical value of ν_O decreases rapidly with falling temperature and is roughly proportional to $e^{-D_{TiO}/kT}$.

Thus far we have obtained only a relationship between R and the partial density ν_O. The connection between R and the total density, in which we are chiefly interested, represents a more complicated problem. Its general formulation can hardly be expected at present because it demands a rather accurate knowledge of the chemical composition of M-type atmospheres. However, our approximate knowledge of the relative abundance of a number of elements is sufficient to show that S stars have not only a lower ν_O but also a lower total density than M stars of the same temperature.

Furthermore, we shall see that ν_O in equation (14) can be replaced by ν'_H/ρ, where ν'_H designates the total density of hydrogen and ρ the ratio of the abundance of hydrogen and oxygen.

The value of ν_O will be equal to

$$\nu_O = \nu'_O - (2\nu_{O_2} + \nu_{OH} + \nu_{NO} + \nu_{CO} + \dots .) , \tag{15}$$

where ν_{O_2}, ν_{OH}, ... , designate the partial densities of the oxides indicated by the subscripts. Replacing the molecular concentrations by

$$\frac{\nu_O^2}{K_{O_2}} , \frac{\nu_O \cdot \nu_H}{K_{OH}} , \dots . ,$$

we have

$$\nu'_O = \nu_O \left(1 + \frac{2\nu_O}{K_{O_2}} + \frac{\nu_H}{K_{OH}} + \frac{\nu_N}{K_{NO}} + \frac{\nu_C}{K_{CO}} + \dots .\right) . \tag{16a}$$

Similar equations exist for the other constituents, such as H, N, C, ... :

$$\left.\begin{aligned} \nu'_H &= \nu_H \left(1 + \frac{2\nu_H}{K_{H_2}} + \frac{\nu_O}{K_{OH}} + \ldots.\right), \\ \nu'_N &= \nu_N \left(1 + \frac{2\nu_N}{K_{N_2}} + \frac{\nu_O}{K_{NO}} + \ldots.\right), \\ \nu'_C &= \nu_C \left(1 + \frac{2\nu_C}{K_{C_2}} + \frac{\nu_O}{K_{CO}} + \ldots.\right). \end{aligned}\right\} \tag{16b}$$

The determination of ν_O involves the evaluation of the simultaneous quadratic equations (16). The total density would be given by

$$\nu_{\text{tot}} = \nu_H + \nu_O + \nu_N + \ldots. + \nu_{H_2} + \nu_{O_2} + \nu_{OH} + \ldots.. \tag{17}$$

For reasons previously mentioned we shall not try to compute ν_O on the basis of (16) but shall show that, with a given chemical composition in stellar atmospheres, condition (14) excludes a strong formation of oxides. Therefore, ν_O must be of the same order as ν'_O for $R < 1$.

Since there is an excess of oxygen in "oxygen stars," compared with nitrogen and carbon, the formation of NO and CO cannot influence the partial density of free oxygen in so far as the order of magnitude is concerned. Equation (16*a*), therefore, reduces to

$$\nu'_O = \nu_O \left(1 + \frac{2\nu_O}{K_{O_2}} + \frac{\nu_H}{K_{OH}}\right). \tag{18}$$

To show that the second and the third members in the parentheses are of the order of 1 or smaller (if $R < 1$), we proceed as follows:

Since TiO is more tightly bound than O_2 (5.5, compared with 5.1, volts), we have $K_{O_2} > K_{TiO}$ for all values of T. Replacing K_{TiO} in (14) by $K_{O_2} \cdot K$, we find

$$\frac{2\nu_O}{K_{O_2}} < \frac{2\mu^{-1}}{1 - \mu^{-1}} K \leqq \frac{2\mu^{-1}}{1 - \mu^{-1}} e^{-\Delta D/kT}, \tag{19}$$

where $\Delta D = 0.4$ volts. Hence,

$$\frac{2\nu_O}{K_{O_2}} \ll 1 . \tag{20}$$

The value of ν_H/K_{OH} depends essentially on the relative abundance, ρ, of hydrogen to oxygen. We shall determine the upper limit of ρ which we can allow in order to keep ν_H/K_{OH} of the order of 1. Since $\nu'_H = \nu_H + 2\nu_{H_2}$ is always larger than ν_H, the value of ν_H/K_{OH} will always be smaller than unity if

$$\nu'_H \leqq K_{OH} . \tag{21}$$

Because of the excessive abundance of hydrogen, ν'_H can be regarded as roughly equal to the total density.

In the second column of Table 2 the values of K_{OH} are tabulated for $T = 1500°$, $2000°$, and $3000°$. The third column of the table gives the upper limits, ν^e_O, of ν_O according to (14); the fourth, the ratios $\rho^e = K_{OH}/\nu^e_O$. From the preceding considerations it follows that ν_O in (14) is identical with ν'_O as long as the ratio K_{OH}/ν^e_O is larger than or equal to the actual abundance factor $\rho = \nu'_H/\nu'_O$.

TABLE 2

T	K_{OH}	$\nu^e_O = \frac{\mu^{-1}}{1-\mu^{-1}} K_{TiO}$	$\rho^e = K_{OH}/\nu^e_O$
1500°	$8 \cdot 10^9$	$1.3 \cdot 10^5$	$6 \cdot 10^4$
2000	$4 \cdot 10^{13}$	$7.4 \cdot 10^9$	$5.5 \cdot 10^3$
3000	$1 \cdot 10^{17}$	$3.0 \cdot 10^{14}$	$3.3 \cdot 10^2$

There is no doubt that the value of ρ in stellar atmospheres is smaller than the smallest value of ρ^e in Table 2.[9]

Replacing ν_O in equations (14) and (6) by ν'_H/ρ $(=\nu'_O)$, we have

$$\nu'_H < \rho \frac{\mu^{-1}}{1-\mu^{-1}} K_{TiO}(T) , \tag{22}$$

$$R(T, \nu'_H) = \mu \frac{K_{ZrO} + \nu'_H/\rho}{K_{TiO} + \nu'_H/\rho} , \tag{23}$$

for all values of $R < 1$.

[9] The dependence of ρ^e on the assumed values of μ and D_{TiO} is discussed later.

Summarizing, we have the following results:

a) S stars have a lower total density than M stars of the same temperature. The upper limit of the total density in S is given by (22).

b) In comparing two S stars of the same temperature but having different values of R, the star with the lower value of R has also the lower total density.

c) In comparing two S stars of different temperatures but having equal values of R, the star with the lower temperature has also the lower total density.

d) The values of K_{TiO} in Table 1, which give approximately the upper limit of the total density ν'_H, indicate that S stars, especially for $T < 2500$, must be supergiants. This explains the nonexistence of S dwarfs and the general scarcity of S types.[10]

The relation between R and the total density in M stars cannot be determined at the present time. It is rather certain that there exists for each temperature a density range within which R decreases with increasing total density. The application of equation (23) to type M is in no way justified. An exception can possibly be made for the first subdivision M1, in which the general dissociation is still high, making ν_O approximately equal to ν'_O.

3. In this section we shall briefly discuss how far our results depend on the adopted values of D_{TiO} and D_{ZrO} and the abundance factor μ, the accuracies of which are still uncertain.

It is evident that all conclusions are based on an actual higher value of D_{ZrO} than that of D_{TiO}. Exact figures of the dissociation energies of *TiO* and *ZrO* are not yet known. The values ordinarily used are those derived by the Birge-Sponer approximation method, which gives 6.5 and 7.5 volts, respectively. The values 5.5 and 6.5 volts, assumed in the present paper, lie perhaps closer to the real ones than do 6.5 and 7.5. Experience has shown that the Birge-Sponer method generally gives values which are too high by about 10 to 20 per cent. Our conclusions would be invalidated only—in so far as the influence of D_{TiO} is concerned—if the real value of D_{TiO} is

[10] Merrill, *Ap. J.*, **65**, 25, 1927, from his study of S-type spectra, came to the conclusion that the general appearance of a typical S-type spectrum points to high luminosity and low density.

appreciably smaller than the dissociation energy of O_2, which is equal to 5.1 volts. ΔD in equation (19) would then become negative and $2\nu_O/K_{O_2}$ eventually large, compared with unity. However, a smaller value of D_{TiO} than 5.1 volts is highly improbable.

The assumed value for $D_{ZrO} - D_{TiO}$ (= 1 volt) is probably somewhat too large. A smaller ΔD influences the results only to the extent that the minima in Figure 1 become less deep (see eq. [7]) and are shifted to lower T.

The abundance factor used, $\mu = 10$, may be too small. A larger ratio affects, qualitatively, the values of the minima in Figure 1 in the same way as does a smaller ΔD.

The author is indebted to Dr. G. P. Kuiper and, especially, to Dr. P. W. Merrill for several valuable discussions.

YERKES OBSERVATORY
April 1939

SPECTRAL TYPES OF STARS OF THE NORTH POLAR SEQUENCE*

PHILIP C. KEENAN

ABSTRACT

The spectral types of the stars of the North Polar Sequence brighter than photographic magnitude 11.2 were determined from spectrograms having a dispersion of 160 A/mm. The new types average from one to two subdivisions later than the earlier estimates available from various sources.

If full use is to be made of the well-determined magnitudes and colors which are available for the stars of the North Polar Sequence, particularly in connection with studies of interstellar absorption, it is important that, over as wide a range of magnitudes as possible, the spectral types should all be estimated from spectrograms of the same dispersion in order to avoid systematic errors depending upon apparent magnitude.

For the purpose of providing such a homogeneous set of types, spectrograms of all stars of the Polar Sequence down to the eleventh photographic magnitude were taken at the McDonald Observatory during the summer of 1939. The observations were made with the Cassegrain quartz spectrograph on the 82-inch reflector, using an f/2 Schmidt camera giving a scale of 160 A/mm at $H\gamma$. This instrument is well adapted to observations near the pole, since the spectrograph can be rotated to permit trailing of the image along the slit by means of the declination slow-motion motor. Agfa Super Pan Press films were employed for all except a few of the faintest stars, for which the exposures were made on Agfa Super Plenachrome Press films because of their greater speed in the blue region of the spectrum.

The estimates of spectral type were made by direct comparison with spectra of the accompanying list of standard stars taken with the same dispersion.

88 Herculis	B8	α Cygni	cA2
β Orionis	cB8	β Arietis	A5
α Lyrae	A0	ϵ Cephei	F0

* *Contributions from the McDonald Observatory, University of Texas*, No. 15.

θ Cygni	F4 V	η Serpentis	G9 IV
β Delphini	F4 III	η Cephei	G9 IV–V
Polaris	F7 Ib	δ Draconis	K0 III
γ Cygni	F8 Ib	θ Herculis	K0 II
β Draconis	F9 I	Arcturus	K1 III
μ Herculis	G5 V	ϵ Pegasi	K1 I
η Herculis	G6 III	η Persei A	K2 I
ϵ Draconis	G7 III	γ Sagittae	K5 III
σ Draconis	G8 V	α Orionis	M1 I

The system of classification is that of the bright stars of the *Henry Draper Catalogue* for classes earlier than F0 and follows

TABLE 1

Star	Pgp	Spectral Type			C_r	C_i
		McDonald	Harvard Mt. W.	Schwassmann		
1S	2.58	(cF7)	cF7	F8	+0.49	+0.30
1	4.34	A2	A0	.....	+0.00	−0.04
2	5.16	B9	A0	.....	−0.08	−0.08
3	5.73	F0 III	A2	.....	+0.18	+0.08
4	5.94	A3p	A3	.....	+0.13	+0.07
5	6.49	A5	A2	A1p	+0.00	+0.01
2S	6.57	F2 III	F0	.....	+0.20	+0.13
3S	6.72	F4 V	F0	.....	+0.31	+0.15
1R	6.72	K5–M0:III	M2	d:K8	+1.59	+1.08
6	7.20	A3	A0	A2	+0.07	+0.02
7	7.45	B9	B8	B9	−0.19	−0.05
2R	7.99	M1:III:	M4	.....	+1.57	+0.99
8	8.42	F4 III	.....	F2	+0.17	+0.16
9	9.07	F2 III	.....	F0	+0.09	.....
3R	8.98	K2 III:	gK2	d:K2	+1.38	+0.98
10	9.23	A9	.....	A5p	+0.10	.....
4R	9.31	G9 III	.....	.....	+0.90	+0.77
11	9.87	F0 V	.....	F2	+0.20	.....
12	10.16	A7	.....	A3	+0.29	.....
5R	10.28	K3:III	.....	gK5	+1.55	+1.07
4S	10.39	F5 III	.....	d:G0	+0.49	+0.29
13	10.59	A7	.....	A3	+0.20	.....
6R	10.58	G9 III	.....	d:G8	+1.26	+0.79
14	10.93	F2	.....	F2	+0.41	.....
7R	11.03	G8 IV	.....	d:G7	+1.12	.....
5S	11.13	G8 III	.....	d:G4	+1.05	.....

Morgan's revised subdivisions and luminosity classes[1] for the later types. For three of the stars, NPS 2, 3, and 4, the classification was

[1] *Ap. J.*, **87**, 460, 1938.

checked on spectra taken at the Yerkes Observatory with a dispersion of 120 A/mm at $H\gamma$, but no changes from the estimates on the small-scale films were found necessary.

In Table 1 the spectral types given in the third column are based on at least two satisfactory spectra for each star. The Roman nu-

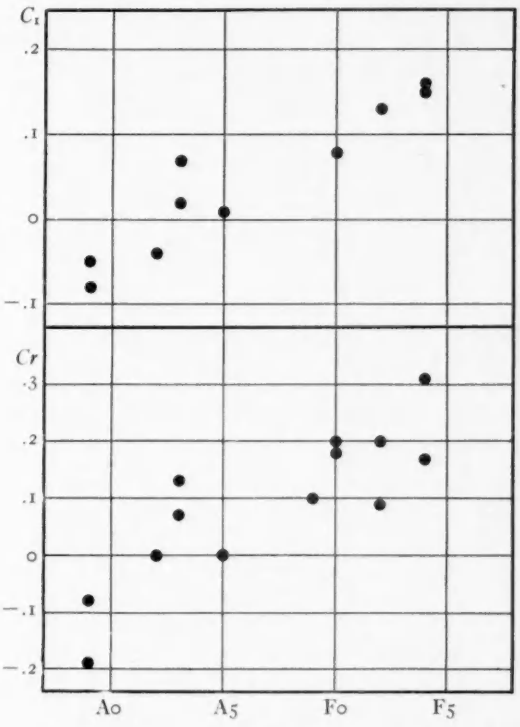

FIG. 1.—Photoelectric colors (C_1) and photographic colors (Cr) plotted against spectral type. The most discrepant star at A3 is NPS 4, in which the metallic lines are unusually strong in comparison to the Balmer series.

merals indicate the luminosity class for types later than F0. For comparison, the fourth column shows the type determined at either Harvard or Mount Wilson, as given by Seares,[2] and the fifth column contains Schwassmann's estimates based on objective-prism spectrograms.[3]

[2] *Ap. J.*, **87**, 257, Table 5, 1938.

[3] *Bergedorfer Spektral-Durchmusterung*, **1**.

The sixth and seventh columns show, respectively, the international color indices determined photographically by Seares[4] and the photoelectric colors obtained by Stebbins and Whitford during the summer of 1939 on their C_1 scale.[5] The spectrum-color relations of the brighter, early-type stars for these two sets of data are shown in Figure 1, where the photoelectric measures have been plotted on a scale 1.5 times greater than that of the international colors, in order that the diagrams for the two systems will be comparable.

The mean absolute values indicated for the colors by the diagrams should not be taken too seriously as indicators of the amount of selective absorption at the pole, since the number of stars is small and there exists uncertainty as to the zero points of the color scales for unreddened stars. The significant result of the redetermination of spectral types is the fact that the new types average 2.2 subdivisions later, between B9 and K5, than the earlier Harvard–Mount Wilson estimates and 1.1 subdivisions later than the slitless estimates, corresponding to a reduction of about 0.05 mag in the international color excess at the north pole, whatever may be the absolute amount of this excess.

It is a pleasure to acknowledge the co-operation of Dr. W. W. Morgan, who suggested the investigation, and of Dr. D. M. Popper, who helped greatly in securing the observations.

McDonald Observatory
and
Yerkes Observatory
October 1939

[4] *Op. cit.*, Table 3, col. 4.

[5] These are current values, which Professor Stebbins has kindly given me permission to include in the table, and may be subject to slight revision.

MAGNITUDES AND COLORS OF STARS OF LARGE PROPER MOTION*

CARL K. SEYFERT

ABSTRACT

Photographic and photovisual magnitudes on the International System have been determined for 144 stars, mostly of proper motion larger than 0".3 per year, from focal plates taken with two 3-inch Ross cameras. For 91 additional proper-motion stars photovisual magnitudes have been determined from extrafocal plates taken with a 5.7-inch camera with ultraviolet optics. A simplified photometer built for the purpose of measuring these latter plates is described.

Faint stars of large proper motion are important because they form a homogeneous group of dwarf stars in close proximity to the sun. A co-operative program for the study of these stars has been carried out by the author in collaboration with Dr. G. P. Kuiper, of the Yerkes Observatory, with the assistance of Miss Mary R. Calvert. The purpose of the writer's part of this joint investigation has been the determination of magnitudes and colors on the International System of a number of these stars.

Three cameras have been employed in this investigation: two 3-inch Ross cameras (focal length 21 inches), one corrected for photographic or blue light, the other for photovisual light; and a 5.7-inch camera (focal length 32 inches) constructed of ultraviolet glass (hereafter called the "UV camera"). The Ross camera plates were exposed simultaneously for the determination of colors, whereas the UV camera was used only for the determination of photovisual magnitudes.

Yellow-sensitive plates (Eastman 1-G emulsion) were exposed in the Ross photovisual camera and the UV camera. An optical-glass yellow filter was placed over the objective of the former, and the latter camera was equipped with a yellow-glass filter placed about 1 inch in front of the emulsion. Blue-sensitive plates (Eastman 1-O emulsion) were used in the Ross photographic camera without filter. Since the two Ross cameras were exposed simultaneously, the aperture of the photographic camera was diaphragmed down to $1\frac{1}{2}$ inches

* *Contributions from the McDonald Observatory, University of Texas*, No. 16.

in order to make the limiting magnitudes of the two cameras approximately equal.

Each Ross camera plate contains three exposures of equal length, two of a region containing one or more stars of large proper motion and a single exposure of the North Polar Sequence. A few of the UV camera plates were also taken in this manner, though for the majority the exposure on the pole was made on a separate plate and developed in the same bath with the plate containing the proper-motion star or stars. An examination of the multiple-image Ross plates revealed no systematic difference in the strength of the images depending on the order in which they were exposed.

The Ross camera plates were taken at the best focus and were measured with the aid of a graduated scale of star images. This measuring-device has a step interval of about 0.5 mag., and the diameter of each star was estimated to the nearest tenth of a single step interval.

The UV camera plates were taken approximately 1 mm out of focus and were measured in a physical photometer designed by the author with the assistance of Dr. C. T. Elvey, of the McDonald Observatory, and constructed by Mr. Arch Garner, engineer of the 82-inch reflector. The author gratefully acknowledges the assistance of both of these men in this work. A short description of this instrument is presented in the following paragraphs.

The photometer is of the null type, built up largely of $1\frac{1}{4}$-inch black iron pipe and pipe fittings, and employs two inexpensive photovoltaic cells which do not require any amplification of the current. The optical design is presented schematically in Figure 1. The light source (*a*) is a 50-candle-power automobile headlight lamp which is focused by means of a simple lens of focal length 2 inches (*b*) on the 32-mm microscope objective (*d*). A small interchangeable diaphragm (*c*) is focused by the microscope objective on the photographic plate (*e*). The diverging beam then passes through another simple lens (*f*), which produces a spot of light about $\frac{3}{4}$ inch in diameter on the sensitive element of the photovoltaic cell (*g*). The light path through the right-hand side of the photometer is similar, except that a movable photographic wedge (*h*) is situated at the position corresponding to the photographic plate. In addition, the mi-

croscope objective is omitted on the wedge side of the photometer in order to obtain a large beam falling on the wedge so that small irregularities in the wedge will be averaged out.

The photographic plate rests horizontally, emulsion down, in a light metal frame, which permits the plate to be moved about on the flat table top. The metal frame holds the emulsion of the plate about $\frac{1}{16}$ inch above the table top, and plate and frame are moved by hand to place the star to be measured centrally in the beam of light. The plate is viewed by means of a binocular microscope which is mounted above the plate at an angle of 20° to the vertical. Since the beam

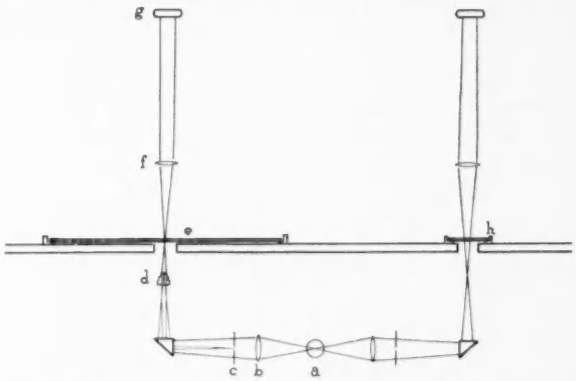

FIG. 1.—Schematic diagram of the physical photometer of the McDonald Observatory.

is focused on the emulsion, no parallax difficulties are encountered when centering the star image in the beam.

The photovoltaic cells and a galvanometer are connected in series in such a way that the currents from the two cells are opposing each other. Hence, when the amount of light falling on the two cells is equal, no current is registered by the galvanometer.

The method of measurement is as follows: The image of the star to be measured is placed centrally in the beam, and the wedge is moved until the galvanometer reads zero. The position of the wedge is then read by means of a millimeter scale mounted beside it. The fog background near each star is measured in a similar manner; and for plates which show evidence of variable fog, the clear reading near each star is kept constant by means of a second wedge placed

in the optical system just below the primary wedge. Magnitudes are determined in the usual manner by drawing a calibration-curve for the stars of known magnitude (i.e., wedge-reading against magnitude) and by using this curve for converting the wedge-readings of other stars to magnitudes. In spite of the fact that the plate must be moved by hand instead of by mechanical means, the measurement is very fast, and the errors of measurement amount to only 2 or 3 per cent.

Special plates were taken with all three cameras to determine the correction for distance from the center of the plate. This correction, depending on the density of the image as well as on the distance from the plate center, was found and applied to all the measures.

The correction to the measures depending on the color of the star was determined from a large number of plates of the North Polar Sequence. The correction was small and was found also to be a function of the density of the image. This correction, when applied, reduced all the magnitudes—photographic and photovisual—to the International System. In addition, appropriate corrections for extinction were applied for plates which were not taken at the same altitude as that of the pole.

Many of the stars in the following tables were measured on two or more plates, and the photovisual magnitudes in a number of cases have been measured from plates taken with both the Ross and the UV cameras. Intercomparisions of measures from pairs of plates yielded a mean error of a single magnitude determination of ± 0.10 mag.

Table 1 lists the magnitudes and colors of the stars, which have been determined principally from the Ross camera plates. For 25 of these stars additional photovisual measures were available from UV camera plates and have been incorporated in the mean photovisual measures given. Photovisual magnitudes determined solely from UV camera plates, and for which no photographic magnitudes have been determined, are given in Table 2.

Preliminary magnitudes and spectral types for 9 white stars of large proper motion have been published earlier by Dr. Kuiper and the present author.[1] For 8 of these stars, magnitudes and colors, improved by the addition of more data, are listed in Table 1.

[1] *Ap. J.*, **87**, 78, 1938.

TABLE 1

PHOTOGRAPHIC AND PHOTOVISUAL MAGNITUDES OF STARS OF LARGE PROPER MOTION

STAR	R.A. 1900	Decl. 1900	m_{pg}	m_{pv}	C.I.	μ
+45°4408AB	0^h00^m4	+45°16′	9.70	8.07	$+1^m63$	0″.86
+36°57	0 21.6	+36 44	9.98	9.47	0.51	0.47
+70°35	0 34.3	+70 29	10.29	9.92	0.37	0.34
+71°31*	0 37.2	+71 38	10.36	10.15	0.21	0.35
+38°125	0 46.9	+38 58	10.57	9.76	0.81	0.37
Ross 318	0 55.1	+71 09	11.54	10.05	1.49	1.78
+63°137	1 00.4	+63 24	10.40	8.96	1.44	1.55
−16°214	1 12.6	−16 01	10.80	9.69	1.11	0.58
−13°245	1 17.3	−12 40	11.08	10.03	1.05	0.43
+82°38	1 22.8	+82 20	10.06	9.05	1.01	0.30
+30°228	1 23.1	+31 06	10.03	9.02	1.01	0.39
+63°224	1 35.7	+63 23	8.93	7.92	1.01	0.05
+63°229	1 36.8	+63 20	9.32	8.11	1.21	0.70
+72°94*	1 38.9	+72 58	10.20	10.06	0.14	0.30
+57°383	1 39.2	+57 22	9.53	9.21	0.32	0.36
+68°138	1 50.8	+68 32	9.79	9.18	0.61	0.35
+71°145	2 21.4	+71 44	9.60	8.97	0.63	0.33
+ 4°415	2 29.4	+ 5 01	10.71	9.99	0.72	0.69
+33°529	2 45.8	+34 00	10.86	9.58	1.28	1.37
+49°787	2 46.0	+49 40	10.97	10.49	0.48	0.30
Ross 364	2 49.1	+55 02	11.79	10.41	1.38	0.87
+49°873	3 06.0	+50 05	11.05	9.80	1.25	0.31
− 6°637	3 11.1	− 6 13	11.20	10.26	0.94	0.38
+33°622	3 13.5	+33 14	10.40:	9.63	0.77:	0.70
+52°683	3 14.5	+53 08	9.70	8.73	0.97	0.32
− 5°642	3 20.1	− 5 42	9.15	7.99	1.16	0.82
− 6°727	3 37.0	− 6 17	10.87:	10.05	0.82:	0.44
− 7°699	3 49.7	− 7 08	10.41	8.92	1.49	0.53
+32°719	3 59.7	+32 42	10.93	9.95	0.98	1.08
− 7°781†	4 10.7	− 7 49	9.21	9.20	0.01	4.06
+32°1398	6 39.6	+32 39	9.74	8.83	0.91	0.52
+ 7°1457	6 43.3	+ 7 45	8.28	7.89	0.39	0.32
Wolf 294	6 48.4	+33 24	11.66:	9.79	1.87:	0.87
+ 1°1600	6 51.4	+ 1 18	8.21:	7.43	0.78:	0.57
− 0°1520	6 53.5	− 0 20	9.50:	8.88	0.62:	0.72
+31°1742	6 56.2	+31 43	10.93	9.93	1.00	0.37
−26°4750	7 36.7	−26 07	9.25	8.60	0.65	0.47
−29°4973	7 44.8	−30 01	8.06	7.30	0.76	0.38
−24°6144	7 50.0	−25 03	11.26	9.52	1.74	0.44
+13°1870	8 09.1	+13 19	10.11	8.76	1.35	0.46
+ 9°1912	8 09.2	+ 9 32	9.32	8.78	0.54	0.50
+71°482AB	8 46.0	+71 11	9.41	8.12	1.29	1.39
+77°361	9 06.3	+77 40	11.37	10.14	1.23	1.14
+81°297	9 14.0	+81 01	10.59	9.46	1.13	0.46
+76°351	9 16.2	+76 22	10.37	9.12	1.25	0.35
−12°2889	9 20.3	−12 32	10.73	9.59	1.14	0.93
+77°374	9 25.1	+77 01	11.06	9.85	1.21	0.24
−12°2918	9 26.5	−13 03	12.00:	10.22	1.78:	0.76
Ross 889	9 35.6	+ 1 28	10.85	10.61	+0.24	0.54

* Subdwarf (*Ap. J.*, **87**, 78, 1938). † 40 Eridani BC.

TABLE 1—*Continued*

Star	R.A. 1900	Decl. 1900	m_{pg}	m_{pv}	C.I.	μ
Ross 434	9^h36^m6	+76°31′	12.05	10.79	+1m26	0″95
+70°578	9 40.3	+70 14	10.87	9.59	1.28	0.33
+29°2091	10 41.9	+28 57	10.67	10.43	0.24	0.95
+31°2240A	11 05.6	+31 00	9.42	8.25	1.17	0.62
+31°2240B	11 05.6	+31 00	11 25:	9.82	1.43:	0.62
+36°2165	11 07.3	+36 17	10.19	9.84	0.35	0.52
+36°2193	11 25.1	+36 24	10.45	9.86	0.59	0.43
+40°2442	11 31.3	+39 45	11.47	10.25	1.22	0.60
+ 5°2529	11 36.6	+ 5 42	11.09	9.72	1.37	0.52
+ 5°2546	11 45.0	+ 5 28	10.19	8.94	1.25	0.38
+14°2453	11 51.8	+13 56	10.79	9.80	0.99	0.35
+ 6°2536	11 55.2	+ 5 55	9.00	8.37	0.63	0.37
+15°2410	12 00.8	+15 13	10.88	10.23	0.65	0.47
− 4°3208	12 02.2	− 5 10	10.42	10.10	0.32	0.54
+13°2493	12 02.4	+13 36	10.64	9.61	1.03	0.33
+14°2481	12 07.0	+13 50	10.49	10.37	0.12	0.43
− 5°3450	12 07.3	− 5 48	10.98	10.24	0.74	0.36
+11°2439	12 08.1	+11 24	8.17	7.62	0.55	0.59
− 3°3258	12 12.0	− 3 42	11.01	10.20	0.81	0.37
+78°428	12 32.6	+78 06	10.01	9.17	0.84	0.38
+73°566	12 38.3	+73 30	9.73	9.44	0.29	0.30
+ 0°2989	12 45.6	− 0 13	10.01	8.46	1.55	0.39
− 1°2754	12 55.2	− 2 10	10.97	9.83	1.14	0.74
+69°681	12 55.2	+69 19	8.55	8.08	0.47	0.39
− 6°3742	13 03.2	− 6 47	9.09	8.45	0.64	0.38
+67°775	13 06.1	+67 01	11.35	10.81	0.54	0.16
+68°714	13 07.0	+68 02	9.94	8.97	0.97	0.75
+74°526	13 08.8	+74 23	9.86	9.34	0.52	0.33
− 7°3646	13 29.5	− 7 50	10.61	9.29	1.32	0.58
+75°511	13 33.2	+75 00	11.10	9.79	1.31	0.43
− 3°3508	13 35.0	− 3 42	11.17	9.72	1.45	0.58
− 8°3624	13 38.4	− 8 58	10.49	9.52	0.97	0.39
− 6°3907	13 51.5	− 6 49	10.35	9.26	1.09	0.37
−16°3969	14 50.7	−17 04	10.41	10.11	0.30	0.35
−16°3974	14 52.8	−17 08	10.89	10.44	0.45	0.36
−11°3865	14 57.1	−12 01	10.74	10.24	0.50	0.37
+75°551	15 02.1	+75 39	10.60	9.52	1.08	0.32
+65°1033	15 03.2	+65 12	9.86	9.18	0.68	0.27
+65°1050	15 20.5	+65 33	10.65	10.27	0.38	0.15
+77°584	15 22.8	+77 29	9.78	8.87	0.91	0.38
+74°618	15 26.5	+74 50	10.45	9.32	1.13	0.24
+67°910	15 38.3	+67 08	10.46	10.37	0.09	0.39
+46°2115	15 45.8	+46 06	9.68	9.23	0.45	0.31
+74°634	15 49.8	+74 43	10.36	9.09	1.27	0.32
+64°1102	15 55.2	+64 05	10.21	9.51	0.70	0.27
+65°1092	15 56.7	+65 41	9.80	9.03	0.77	0.25
+42°2667	15 59.9	+42 32	10.18	10.01	0.17	0.48
+68°861	16 03.1	+68 48	10.37	10.14	0.23	0.28
+44°2555	16 10.4	+44 42	10.86	9.66	1.20	0.34
+67°935	16 16.5	+67 29	9.97	8.74	1.23	0.50
+68°946	17 37.0	+68 26	10.68	9.15	1.53	1.33
+71°851	17 40.1	+71 22	10.09	9.16	0.93	0.33
+70°950	17 42.7	+70 30	10.63	9.66	+0.97	0.21

TABLE 1—*Continued*

Star	R.A. 1900	Decl. 1900	m_{pg}	m_{pv}	C.I.	μ
+72°803	17h43m0	+72°27′	8.05	7.38	+0m67	0″.32
+68°986	18 16.6	+68 35	10.95	10.26	0.69	0.44
+ 8°3689	18 21.4	+ 8 44	8.39	7.82	0.57	0.51
+ 8°3692	18 21.6	+ 8 34	9.00	8.30	0.70	0.51
−11°4672	18 27.9	−11 42	11.23	10.31	0.92	0.41
+13°3683	18 28.7	+13 03	11.00	10.63	0.37	0.33
+45°2743	18 32.4	+45 39	11.35	10.21	1.14	0.56
+42°3123	18 34.9	+42 35	9.00	8.19	0.81	0.30
+ 7°3814	18 38.2	+ 7 37	10.63	9.67	0.96	0.30
+ 7°3815	18 38.3	+ 7 37	9.32	8.54	0.78	0.30
+10°3665	18 43.8	+10 39	8.98	7.74	1.24	0.46
+11°3045	18 47.8	+11 06	11.20	10.33	0.87	0.39
− 5°4811	18 50.6	− 5 52	7.99	7.28	0.71	0.59
− 4°4636	18 51.1	− 4 32	10 78	10.24	0.54	0.42
− 9°5030	19 06.1	− 9 43	10.74	9.74	1.00	0.37
− 0°3676	19 08.2	− 0 45	9.31	9.01	0.30	0.53
+42°3607	20 05.6	+42 34	10.35	9.96	0.39	0.30
+45°3091	20 08.9	+45 59	9.60	8.89	0.71	0.50
+31°4054	20 18.4	+32 00	9.19	8.38	0.81	0.32
+32°3853	20 28.0	+32 40	10.50:	9.86:	0.64:	0.42
+52°2815	20 47.6	+52 31	11.19	9.61	1.58	0.54
+61°2068	20 51.3	+61 48	10.00	8.87	1.13	0.77
+54°2461	20 57.9	+54 55	10.35	10.16	0.19	.....
+45°3371	20 59.1	+45 29	8.30	7.22	1.08	0.40
+61°2153	21 30.3	+61 33	10.43	9.34	1.09	0.36
+62°1971	21 40.4	+62 43	10.52	9.46	1.06	0.32
+ 9°4055	21 56.0	+ 9 28	11.20	10.69	0.51	0.51
+53°2788	22 03.4	+53 41	9.57	9.10	0.47	0.42
+17°4708	22 06.7	+17 36	9.65	9.27	0.38	0.56
+56°2783‡	22 24.4	+57 12	11.27	9.57	1.70	0.87
+48°3755	22 27.6	+49 11	10.32	9.48	0.84	0.41
+53°2911	22 28.7	+53 16	11.33	10.28	1.05	1.58
+ 9°5076	22 33.6	+10 03	9.96	9.36	0.60	0.57
−13°6235	22 34.2	−13 08	8.35	7.74	0.61	0.31
+59°2723	23 21.9	+60 04	10.60	10.48	0.12	0.40
−17°6709	23 27.6	−17 23	10.07	8.54	1.53	0.35
−18°6342	23 31.5	−17 47	10.26	9.33	0.93	0.44
+58°2074	23 51.1	+59 12	8.02	7.45	0.57	0.50
+45°4378	23 53.5	+46 10	11.08	9.52	1.56	0.64
+49°4301	23 54.6	+49 34	10.65	9.68	0.97	0.59
Ross 309	23 59.2	+57 31	11.10	10.35	0.75	0.48
+45°4408F	23 59.9	+45 14	11.68	9.87	+1.81	0.86

‡ Krüger 60, AB.

TABLE 2

PHOTOVISUAL MAGNITUDES OF STARS OF LARGE PROPER MOTION DETERMINED WITH THE 5.7-INCH UV CAMERA

Star	R.A. 1900	Decl. 1900	m_{pv}	μ
+62°194	0h59m0	+63°11′	8.34	0″.32
− 9°256	1 14.0	− 9 27	8.87:	0.53
+66°191	2 06.4	+66 16	7.60	0.12
+67°191	2 07.5	+67 13	7.07	0.60
Ross 345	3 07.4	+51 59	10.13	0.48
+51°722	3 14.7	+51 59	9.02	0.42
+43°699	3 16.8	+43 36	8.73	0.37
+41°678	3 18.5	+41 46	9.27	0.31
+43°744	3 25.2	+43 20	8.38	0.30
+41°727	3 32.1	+42 04	9.10	0.40
+25°613	3 40.3	+25 54	9.51	0.43
+28°593	3 43.3	+28 20	8.43	0.34
+34°796	3 56.5	+35 02	8.48	2.21
Ross 587	4 02.2	+33 22	10.19	0.74
+21°607	4 08.6	+22 06	9.07:	0.54
+20°802	4 35.5	+20 43	7.95	0.35
+18°683	4 37.0	+18 48	9.93:	1.27
+63°537	4 41.1	+63 10	9.91:	0.30
+19°815	4 49.8	+19 51	7.80:	0.37
+44°1078	4 54.9	+44 54	10.19:	0.32
+52°911	4 55.0	+53 03	9.81	1.96
+24°726	4 55.5	+24 30	8.07	0.44
+13°778	4 56.5	+13 57	8.19	0.41
+40°1166	4 58.5	+40 07	9.64	0.31
+55°960	5 00.2	+55 19	9.18	0.37
+14°831	5 01.0	+14 19	7.89	0.39
+16°715	5 05.1	+16 19	8.55	0.31
+41°1107	5 05.2	+41 21	8.80	0.43
+44°1142	5 07.8	+44 26	10.38	0.65
+19°872	5 08.3	+19 46	9.42:	0.35
+54°886	5 15.0	+54 43	9.59	0.40
− 3°1123	5 26.4	− 3 42	8.03	2.22
+ 2°1041	5 37.5	+ 2 39	8.72	0.54
+ 2°1085	5 49.3	+ 2 08	8.86	0.66
+19°1185	5 57.3	+19 23	9.17	0.93
+26°1067	5 59.7	+26 24	9.44	0.42
+17°1145	6 04.2	+17 57	8.46	0.30
+47°1276	6 09.2	+47 07	9.27	0.52
+44°1408	6 09.6	+44 45	9.32	0.41
+48°1446	6 43.6	+48 10	10.06	0.33
+47°1355	6 44.1	+47 30	8.98	0.83
−14°1750	7 06.2	−14 16	10.10	0.62
Ross 425a	7 16.5	+ 0 47	10.77	0.36
−15°1776	7 16.6	−15 10	9.70	0.53
−12°1914	7 16.7	−12 28	10.07	0.53
+73°380	7 23.8	+73 29	8.63	0.32
+31°1684	7 47.2	+30 55	8.27	1.96
− 1°1883	7 49.5	− 1 09	7.42	0.31
+57°1128	8 08.1	+57 24	7.64:	0.39
+54°1216	8 11.7	+54 25	9.47:	0.64

TABLE 2—*Continued*

Star	R.A. 1900	Decl. 1900	m_{pv}	μ
−15°2546	8^h36^m2	−15° 59′	9.58	0″.63
+10°1857	8 37.3	+ 9 55	9.50	0.67
+ 7°2031	8 43.1	+ 6 51	10.45	0.53
Ross 683	8 45.1	+ 8 00	11.43	0.51
− 3°2525	8 54.1	− 3 37	9.81	0.74
+73°447	9 00.2	+73 50	9.75	0.31
+21°2033	9 23.1	+21 09	9.44	0.39
+23°2121	9 31.5	+23 09	9.36	0.33
Ross 85	9 35.8	+13 40	10.74:	0.90
+22°2118	9 36.7	+22 12	9.75	0.42
+44°1910	9 43.2	+44 46	10.63	0.21
+14°2151*	9 43.5	+14 14	8.42	0.83
+69°558	10 00.7	+68 56	8.85	0.31
Ross 892	10 22.3	+ 1 55	11.04	0.38
+ 1°2447	10 23.8	+ 1 22	9.73	0.98
Ross 109	11 21.6	+60 07	11.40:	0.55
AC+77°4245	11 26.0	+77 12	11.31:	0.60
+26°2251	11 39.5	+26 07	10.67	0.52
+51°1696	11 41.4	+51 28	9.58	1.00
+38°2285	11 47.2	+38 26	6.45	7.05
+66°748	12 05.6	+66 13	8.73	0.31
+10°2519	13 06.4	+10 09	8.65	0.56
Ross 484	13 13.9	− 2 34	10.96	0.70
+34°2476*	13 54.8	+34 23	10.17	0.54
Ross 838	13 56.8	+ 9 25	11.62	0.88
−21°4009*	14 54.2	−21 36	8.54	0.75
+ 9°3001	15 03.0	+ 9 16	8.34	0.53
−15°4041	15 04.7	−15 59	9.43	3.67
−15°4042	15 04.7	−15 54	9.09	3.67
+40°2862	15 08.4	+40 20	9.35	0.31
−14°4209†	15 22.9	−14 24	9.60	....
+13°2985	15 37.6	+13 16	9.75	0.32
−10°4149*	15 37.7	−10 36	7.23	1.18
+ 5°3113	15 50.1	+ 5 22	8.52	0.32
+ 7°3125	16 11.1	+ 7 37	8.45	0.50
− 3°3968	16 29.5	− 4 00	9.31	0.73
Ross 643	16 40.1	+ 6 14	10.65:	0.35
+25°3173	16 54.1	+25 55	9.61	0.52
Ross 539	17 52.9	+ 4 08	10.21	0.36
+ 4°3561‡	17 52.9	+ 4 25	9.44	10.30
+ 4°3562	17 53.5	+ 4 28	9.68	0.05

* Subdwarf. † ADS 9655; π (dyn) = 0″.020. ‡ Barnard's star.

In a subsequent note Dr. Kuiper and the writer will publish the relation between the spectral types obtained by Kuiper and the colors derived here.

McDonald Observatory
September 20, 1939

THE SPECTRUM OF 25 ORIONIS, 1933–1939

HELEN W. DODSON

ABSTRACT

During 1933–1938 the hydrogen lines showed equal emission components and no variations in velocity. Throughout this interval the emission lines steadily increased in width. In 1938–1939 the violet component became stronger than the red, velocities increased, and emission widths diminished.

A previously reported[1] investigation of the spectrum of 25 Orionis[2] indicated that from 1915 to 1933 there had been cyclic variations, with decreasing period and amplitude, in the velocities of the central absorption and emission lines of hydrogen and in the ratio of the red and violet components of the emission lines. Further estimates

JD	Velocity (Km/Sec)				Emission Ratio, log V/R		Width of Emission Lines in Angstroms		Velocity Represented by Edges of Emission Lines (Km/Sec)				Number of Plates
	Central Absorption		Emission						$H\beta$		$H\gamma$		
	$H\beta$	$H\gamma$	$H\beta$	$H\gamma$	$H\beta$	$H\gamma$	$H\beta$	$H\gamma$	Red	Violet	Red	Violet	
2427412...	+27	+29	+29	+25	−0.02	−0.02	5.7	5.5	+205	−146	+214	−164	6
7789...	26	23	24	23	− .06	− .04	6.3	5.7	216	170	223	174	7
8188...	20	24	17	25	− .01	+ .01	6.4	6.6	217	179	251	220	9
8557...	22	26	28	15	− .04	− .01	6.6	7.4	233	188	270	240	5
8923...	51	16	44	26	+ .02	.00	8.3	7.6	307	202	289	236	3
9243...	+50	+45	+49	+33	+0.11	+0.15	7.6	6.2	+280	−187	+264	−164	3

by McLaughlin[3] of the emission ratio, V/R, during 1933–1937 indicated that the conspicuous changes in the relative intensity of the emission components had ceased and that the red and violet components of the emission lines had been practically equal throughout this later interval.

The data for the present study have been obtained from 33 one-prism spectrograms taken at the University of Michigan Observatory between 1933 and 1939 (JD 7345–9339). Velocities were de-

[1] *Ap. J.*, **84**, 180, 1936.

[2] HD 35439; BD+1°1005; α 5^h19^m6; δ +1°45′ (1900); visual magnitude, 4.73; spectral class, B3p.

[3] *Ap. J.*, **85**, 185, 1937.

termined from the central absorption lines and from the means of the outer edges of the two emission components for both $H\beta$ and $H\gamma$. Measures were also made of the velocities represented by the outer edges of the emission lines, total widths of the emission lines, and the ratio of the intensity of the red and violet emission components. Normal places formed from the individual plate measures are given in the accompanying table, and the results are shown graphically by the black dots in the right-hand portion of Figure 1.

The curves of the diagram indicate that for the 2000-day interval, JD 7000–9000, when the emission components were practically equal, there were no marked changes in the average values of either the absorption or the emission velocities. The measures of individual spectrograms showed the same wide scatter about the average values that had been found during the period of cyclic variations.[4] The spectrograms for the winter of 1938–1939 gave the first evidence of a real change in the ratio of the emission components. The violet component became stronger than the red; and on the last spectrogram secured, it is estimated as one and one-half times more intense than the red component. It is possible that the "resumption of variation in the spectrum of 25 Orionis" suggested by McLaughlin[5] is taking place. This view is further indicated by the accompanying increase in both the absorption and emission velocities from an average value of about +24 km/sec to almost double that figure for JD 9243.

During the interval of constant velocities and equal emission components the $H\beta$ and $H\gamma$ emission lines continually increased in width to maximum breadths of 8.3 A and 7.6 A, respectively, for JD 8923, the date which just precedes the suggested resumption of variations in velocity and emission ratio. The emission widths at this time were considerably greater than at any previous time for which the star had been studied, and this excessive width could not have been caused by a mere spreading of the photographic image, because there was no conspicuous increase in the emission intensity. Throughout the times of cyclic variation there had been maxima of emission width at both maximum and minimum velocity (data for JD 5400 not comparable).[6] The velocities represented by the sepa-

[4] *Ibid.*, **84**, 184, 1936. [5] *Ibid.*, **85**, 193, 1937. [6] *Ibid.*, **84**, 187, 1936.

rate edges of these lines (see the last four curves of Figure 1) indicate that this was caused by the flaring-out of the weaker of the two emission components. However, the maximum in emission width at JD 8923 resulted from a simultaneous spreading-outward of *both* of the emission components. As the violet component became stronger and the velocities increased in value at JD 9243, the emission became narrower.

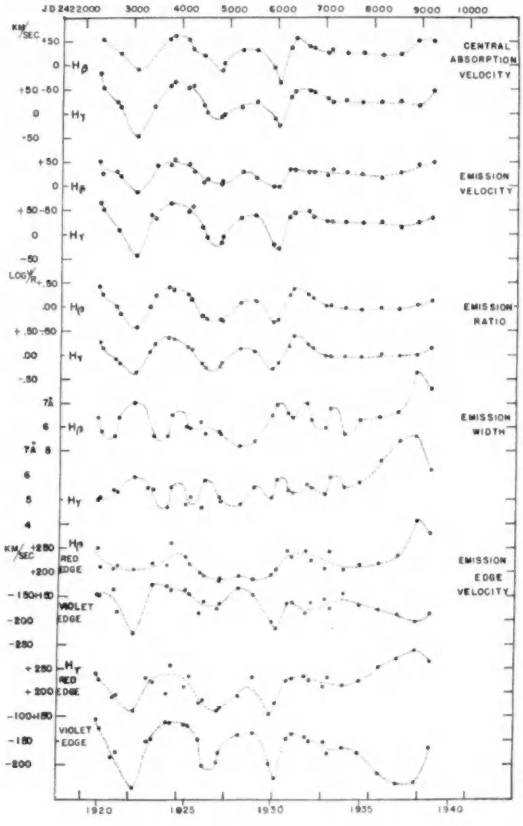

FIG. 1

It is difficult to suggest a physical interpretation for the phenomena. They do not seem to fit into the model previously described for 25 Orionis.[7] It is interesting to note, however, that immediately preceding the commencement of variations in velocity and emission ratio in γ Cassiopeiae,[8] about JD 7000, there was a corresponding conspicuous increase in the width of the emission lines, followed by a sudden decrease.

WHITIN OBSERVATORY
WELLESLEY, MASSACHUSETTS
October 1, 1939

[7] *Ibid.*, p. 200.

[8] *Ibid.*, **83**, 499, 1936.